UNIVERSITA' DEGLI STUDI DI VERONA

Department of Neurosciences, Biomedicine and Movement Sciences

PHD SCHOOL OF LIFE AND HEALTH SCIENCES

Doctoral program in Neuroscience, Psychological and Psychiatric

Sciences, and Movement Sciences

CYCLE XXXV/2019

EXTRACELLULAR VESICLES FROM ADIPOSE MESENCHYMAL STEM CELLS: A THERAPEUTIC STRATEGY FOR NEURODEGENERATIVE DISEASES

S.S.D. BIO/17

Coordinator: Prof. Rimondini Michela

Tutor: Prof. Mariotti Raffaella

PhD candidate: Dr. Virla Federica

6

7

ABSTRACT

Neurodegenerative diseases are fatal disorders of the central nervous system which currently lack effective treatments. The application of adipose-derived mesenchymal stem cells (ASCs) represents a new promising approach for treating these incurable disorders. Growing evidence suggest that the therapeutic effects of ASCs are due to the secretion of neurotrophic molecules through extracellular vesicles (EVs). The EVs produced by ASCs (ASC-EVs) have valuable innate properties deriving from parental cells and could be exploited as cell-free treatments for many neurological diseases. The aim of this PhD project was to evaluate the therapeutic effect of ASC-EVs in different *in vivo* and *in vitro* models of neurodegeneration, with a particular focus on Amyotrophic Lateral Sclerosis (ALS) and Spinal Muscular Atrophy (SMA).

SMA is an autosomal-recessive neuromuscular disease caused by the mutation or deletion of the survival motor neuron 1 (*SMN1*) gene. In this study, ASC-EVs were administered via intracerebroventricular injections in SMNΔ7 mice, a severe SMA model. The results showed positive effects of ASC-EVs on the disease progression, with improved motor performance and a significant delay in spinal motor neurons (MNs) degeneration of treated animals. ASC-EVs could also reduce the apoptotic activation and modulate the neuroinflammation with an observed decreased glial activation in lumbar spinal cord, while at peripheral level ASC-EVs could only partially limit the muscular atrophy and fibers denervation.

ALS is a fatal neurodegenerative disease characterized by progressive degeneration of MNs. Here, we tested the potential therapeutic effect of ASC-EVs on a murine model commonly used to study ALS, the SOD1(G93A) transgenic mouse. We compared the effect of two different routes of ASC-EVs administration: intravenous and intranasal (i.n.). Our results demonstrated that repeated administration of ASC-EVs improved the motor performance, protected lumbar MNs, the neuromuscular junctions and muscle, and decreased the glial cells activation in treated SOD1(G93A) mice. Furthermore, we compared different concentration and frequencies of administration of ASC-EVs injected intranasally in order to individuate the correct administration regimen to obtain the more significant therapeutic effect.

Moreover, we use an *in vitro* model of epithelial RPMI 2650 cells to investigate the mechanisms used by ASC-EVs to overcome biological barriers encountered once

administered in the human body. The neuroprotective effect of ASC-EVs was also evaluated on both damaged *in vitro* MN and neuron cells (NSC-34 and SH-SY5Y cells respectively) after their passage through the epithelial cellular layer. The results showed that ASC-EVs neuroprotective effects observed in previous studies were maintained after their passage through the epithelial barrier as well, with a rescue of the neuronal cells viability after oxidative stress. In addition, a strategy for EVs labelling has been set up to detect and confirm their capability of migration and internalization by injured cells.
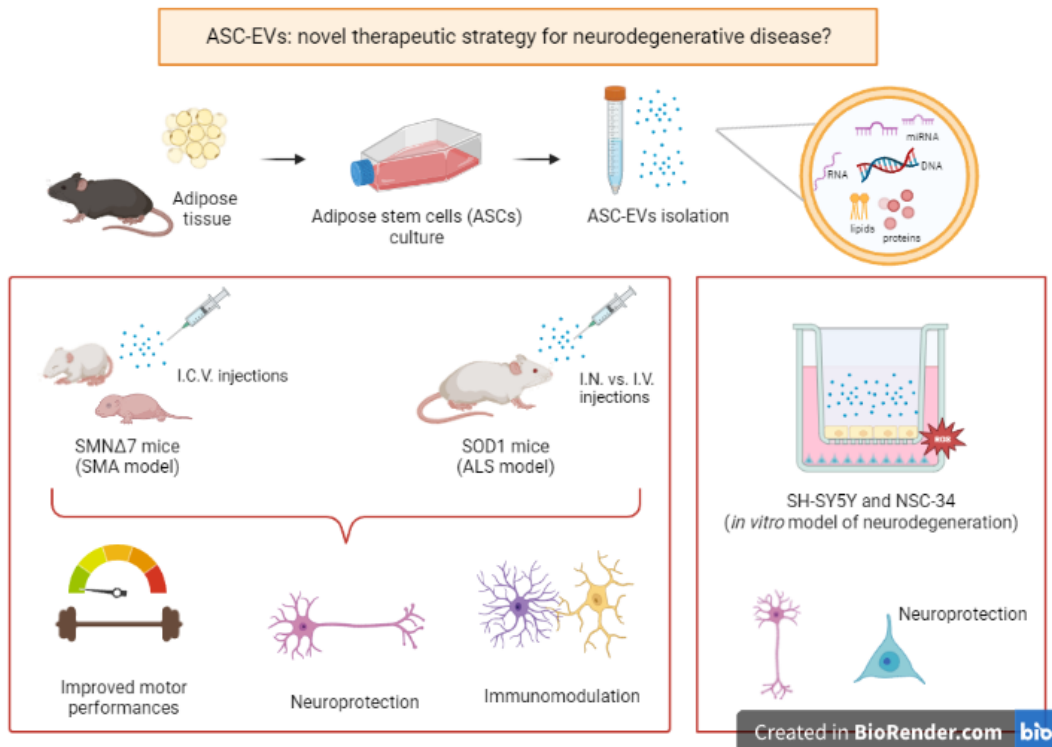
1. NEURODEGENERATIVE DISEASES

Neurodegenerative diseases are a group of multifactorial debilitating disorders; among the more relevant Alzheimer's disease (AD), Parkinson's disease (PD), Huntington's disease (HD) and Amyotrophic Lateral Sclerosis (ALS). Considering the huge number of people suffering from neurological disorders, including brain tumors, epilepsy, neurodegenerative disorders, multiple sclerosis and chronic neuropathic pain, they are one of the most threatening public health issues and with the elongation of life expectancy in several countries, the predominance of this kind of diseases is estimated to increase [1].

Even though these disorders emerge from different pathological backgrounds and in most cases are considered multifactorial, neurodegenerative diseases can share several common traits, like abnormal protein dynamics with defective protein degradation and aggregation, free radical generation and oxidative stress, impaired bioenergetics and mitochondrial dysfunctions, and neuroinflammatory processes [2]. These interconnected mechanisms lead to cell death with subsequent neurodegeneration. Neurodegeneration is characterized by progressive loss of neurons from the brain and/or spinal cord, which can lead to motor and/or non-motor dysfunctions based on the affected neuronal regions [3].

However, the pathogenic mechanisms remain still not fully understood and the failure to identify the precise causes of neuronal degeneration makes their treatment a critical unmet need in the current healthcare environment [4]. The available therapeutics aim to slow the progression of neurodegenerative diseases, relieve pain, improve symptoms and lengthen patients autonomy and functionality. Therefore, the treatment of these diseases represents one of the main challenges for the scientific community.

2. SPINAL MUSCULAR ATROPHY

2.1. *Characteristics and clinical manifestations*

Spinal Muscular Atrophy (SMA) is an autosomal recessive neuromuscular disease, characterized by the selective degeneration and loss of lower motor neurons (MNs) located in the spinal cord and in the brainstem [5]. The MNs are neuronal cells responsible of the innervation of voluntary muscle. The typical symptoms consist in hypotonia, muscular atrophy and weakness due to the denervation, till the final paralysis of the muscles of both upper and lower limbs as well as of the trunk [6].

With an incidence of about one case every 6,000-10,000 births [7, 8], SMA is one of the autosomal recessive disorders more frequent in humans [9, 10] and one of the most common causes of infant mortality [11].

Depending on the age of symptom onset and on the achieved motor milestones, five main phenotypes have been described [12] (Table 2.1). The more severe cases, with prenatal onset, and intrauterine death or with severe asphyxia at birth and early neonatal death fit into the more severe category SMA type 0 [13]. SMA type 1, also known as "non-sitter patients" and "Werdnig–Hoffman syndrome", is the most frequent one [14], occurring in the first six months of life and leading to death due to respiratory failure within two years. Patients show marked muscle weakness and hypotonia [15] that affect also the intercostal muscles resulting in paradoxical breathing, i.e. the inversion of chest movements during the act of inspiration and expiration compared to the normal condition; fasciculations are also reported as well as weakness of tongue muscles resulting in swallowing problems. SMA type 2, also classified as "sitter patients" is of intermediate severity and patients show the first symptoms between 6 and 18 months, leading to adolescent-adult death in the worst cases. They can sit without help at any point in their development but they are not able to walk freely or they lose the ability to walk. Furthermore, they often develop orthopedic complications, such as scoliosis, which may require surgery, due to lack of muscle support and intercostal muscle weakness that may lead to restrictive lung disease and respiratory insufficiency. In patients with SMA type 3, also known as "Kugelberg-Welander syndrome", the clinical manifestations can be quite heterogeneous: in general, patients exhibit the first symptoms after 18 months of life and the majority of them requires assistance due to the disease progression;

respiratory compromise can be mild or absent. SMA type 4, also known as "walkers patients" accounts for 5% of cases and is considered to be the mildest form of the disease [16]; onset occurs in the second or third decade of life, motor deficits are moderate and patients maintain the ability to walk independently for their whole life [17]. In addition to the main symptoms already described, patients with SMA can report other complications at the gastrointestinal system [18, 19], such as dysphagia, delayed gastric emptying and constipation [20]. In the more severe forms, cardiac alterations have also been observed which could arise following congenital anomalies during cardiogenesis [21, 22] or secondary to autonomic nervous system defects [23, 24]. Furthermore, both structural defects in heart development [25], arrhythmias and cardiomyopathies [26] are referred. As mentioned, orthopedic problems (such as scoliosis) are common [27], but contractures also occur [28] as well as a high fracture frequency [29]. On the contrary, in any SMA type cognitive alterations are reported [30, 31].

Type	Age of Onset	Maximal Motor Milestone	Motor Ability and Additional Features	Prognosis[c]
SMA 0	Before birth	None	Severe hypotonia; unable to sit or roll[a]	Respiratory insufficiency at birth; death within weeks
SMA I	2 weeks (Ia) 3 months (Ib) 6 months (Ic)	None	Severe hypotonia; unable to sit or roll[b]	Death/ventilation by 2 years
SMA II	6 to 18 months	Sitting	Proximal weakness; unable to walk independently	Survival into adulthood
SMA III	<3 years (IIIa) >3 years (IIIb) >12 years (IIIc)	Walking	May lose ability to walk	Normal life span
SMA IV	>30 years or 10 to 30 years	Normal	Mild motor Impairment	Normal life span

[a]Need for respiratory support at birth; contractures at birth, reduced fetal movements.
[b]Ia joint contractures present at birth; Ic may achieve head control.
[c]Prognosis varies with phenotype and supportive care interventions.

Table 2.1. Clinical classification and subtypes of Spinal Muscular Atrophy (From Farrar et al., 2017 [32]).

2.2. *Genetic basis of pathology*

Despite the great variability of phenotypic expression, SMA is due to well-known genetic causes. In 1995, *survival motor neuron gene* (*SMN*) was firstly described [15]: *SMN* is located on the 5q13 chromosome and due to duplication in the human

genome, the *SMN* locus contains two copies of the gene, *SMN1* (telomeric form) and *SMN2* (centromeric form). These two copies differ in five nucleotides; however, the only difference in the coding region involves a C to T transition in exon 7. Despite it is a silent mutation and does not modify the aminoacidic sequence, it is critical as it results in splicing defects [33, 34]. Indeed, *SMN1* encodes for the functional full length SMN (FL-SMN) protein of 38 kDa and 294 amino acids, expressed in all tissues, while *SMN2*, due to its alteration, for the majority of cases leads to the production of a truncated, unstable and not functional form of the protein, called SMNΔ7 that is quickly degraded [33, 35, 36]; only a small percentage of the pre-mRNA undergoes proper splicing and is translated into the FL-SMN (Figure 2.1) [15].
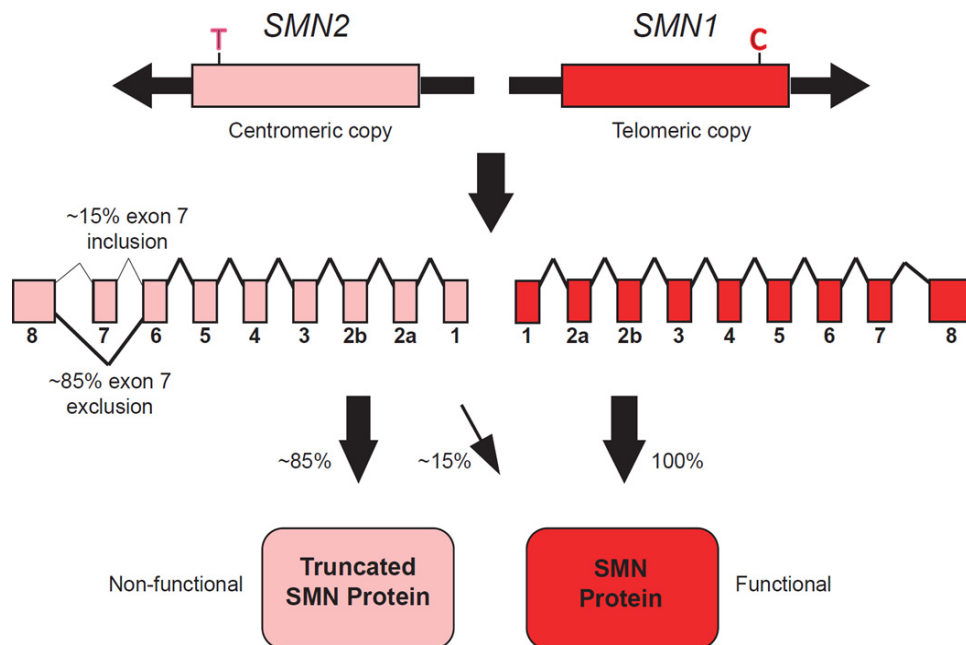
Figure 2.1. Schematic diagram of the human *SMN1* and *SMN2* genes. *SMN1* gene encode for the functional FL-SMN protein. The *SMN2* gene is also expressed, however the majority of the resultant *SMN2* pre-mRNA lacks exon 7 because of a C-to-T transition at position 6 of exon 7. The truncated SMN protein is unstable and non-functional. A small proportion of full-length mRNA containing exon 7 is produced by from the *SMN2* pre-mRNA, resulting in full-length SMN protein that is functional (From Kolb and Kissel, 2015 [16]).

Homozygous mutations or deletions in the *SMN1* gene have been observed in individuals with SMA: in these cases the entire production of FL-SMN depends on the *SMN2* centromeric copy of the gene, which, as already mentioned, is only able to produce a small percentage of the functional protein [15, 37]: the numbers of copies

of the *SMN2* gene are critical for determining the phenotype and the severity of the disease [38].

FL-SMN protein is expressed in all tissues (not only in neurons), in the cytoplasm and in the nucleus. It plays important roles in many different biological mechanisms, although some of them is not yet fully understood. The *SMN1* gene has been conserved from yeasts up to humans [39, 40], but the reasons that lead to the prelevant death of MNs among other cell populations, which is the key feature of SMA, are still unclear and are still being studied by the scientific community. However, the connection between the *SMN1* gene mutation and the MNs degeneration and loss was demonstrated in a study of MNs derived from induced pluripotent stem cells (iPSCs) from patients with SMA: low expression of the FL-SMN protein makes MNs more susceptible to cell death from toxic compounds, while an overexpression is protective [41]. Among other functions of SMN protein, one of the most important is its participation in different protein complexes involved in small nuclear ribonucleoproteins (snRNP) biogenesis that play a role in the regulation of protein homeostasis catalysing the removal of introns from the pre-mRNA molecules [42]. The snRNP complex consists of several subunits made up of uridine-rich small nuclear RNA (UsnRNA) and Sm proteins. UsnRNA molecules from the nucleus are transported to the cytoplasm to be assembly, and subsequently taken back to the nucleus, where they can perform their function. In the cytoplasm the FL-SMN protein forms a stable complex with another protein known as SIP1 to recruit Sm proteins and catalyse their transfer on UsnRNA molecules, allowing the biogenesis of mature subunits of the snRNP spliceosome. It is clear that defects in the snRNP due to a reduced concentration of the FL-SMN protein could be considered among the molecular causes of SMA [43, 44].

SMN expression is higher in the spinal cord and brain during development, while it declines in adulthood [45] to localize in particular in the dendrites and in motor neuron axons [46], suggesting an involvement of SMN in the neuronal growth and in the formation of the synaptic and axonal cytoskeleton [47]: indeed, in a zebrafish model in which *SMN1* expression was switched off, axonal defects have been observed [48].Therefore, in order to understand the complex mechanisms underlying the pathogenesis and progression of SMA, several *in vitro* and *in vivo* models were developed. To date, one of the most commonly used animal model is the transgenic

SMNΔ7 mouse model (SMN2+/+; SMNΔ7+/+; SMN−/−): it can summarize the main pathophysiological characteristics of SMA type 2, as it exhibits the first motor symptoms around the fifth postnatal day and has a life expectancy of approximately 14 days [49].

2.3. _Pathogenesis of SMA: cellular/molecular alterations_

The pathogenesis of SMA is certainly very complex and it also emerged that SMA is likely a non-cell autonomous disease in which several signalling pathways and molecular/cellular mechanisms are involved: understand these mechanisms is of great importance to identify new targets and therapeutic strategies, thus contributing to delay the onset and progression of the disease.

2.3.1. _Mechanisms of neuronal death_

As already said, SMA is a MNs disease: however, the scientific community is still trying to clarify the mechanisms involved that lead to the selective neuronal death following the lack of SMN protein. Apoptosis seems to be involved in the progressive neurodegeneration that characterizes SMA. Indeed, it has been observed that the cascades of the terminal c-Jun NH2 kinase ASK1/MKK4/7/JNK and MEKK1/MKK4/7/JNK are activated in the spinal cord of mice and SMA patients. The lack of SMN triggers the MAP kinase of the intracellular stress signalling cascade and induces the activation of the three isoforms of JNK (JNK1, 2 and 3); among these, in particular, JNK3 (which has a specific expression at the level of the nervous tissue) seems able to induce neurodegeneration. Indeed, in a JNK3 knock-out SMA model, the phenotype of the disease was milder, suggesting that JNK3 could represent an interesting therapeutic target [50]. Based on these findings, a study aims to slow down the disease progression in SMNΔ7 mice, using a peptide (D-JNKI1) capable of inhibiting JNK. The treatment induced several positive effects at the spinal and muscular level: indeed, a reduced expression of the active phosphorylated form of c-Jun (target of JNK) was observed and of the activated caspase 3 (apoptotic marker) as well. Analysing the quadriceps muscles, authors also observed a reduction of muscular atrophy and an improvement in the morphology of neuromuscular junctions (NMJs) in terms of maturation and size; finally, the inhibition of the

cascade of JNK also improved motor performances of animals, slowed down the body weight loss and increased the survival of treated animals [51].

Another intracellular signalling pathway involved in cell apoptosis mechanisms is the one of PI3K-Akt: indeed, it has been observed that its inhibition can induce cell death [52]. Akt, once phosphorylated, is able to inactivate two pro-apoptotic proteins, Bad and caspase 9 [53]. This signalling pathway has already been considered by some authors as a possible therapeutic target: indeed, its activation obtained for example by inhibition of Phosphatase and tensin homologue (PTEN), a molecule that negatively regulates the PI3K-Akt pathway, leads to a prolonged survival of SMA animals [54].

2.3.2.   The neuroinflammation

The term neuroinflammation describes the cellular and molecular processes that encompass the activation of microglia and astrocytes and the infiltration of peripheral immune cells; it is reported in the central nervous system (CNS) in a variety of pathological conditions, including neurodegenerative diseases such as SMA. Although it was initially thought that the neuroinflammation was a cellular event secondary to MNs loss and limited to damaged cells, today numerous evidence support the idea that it itself can compromise neuronal survival, inducing neurodegeneration and stimulating the progression of degenerative processes [55]. Although many pathological aspects regarding the inflammatory process of SMA have not been yet clarified, some studies conducted on others neurodegenerative diseases, such as ALS and PD, let us hypothesize some possible parallelisms; in particular that both astrocytes and microglia can be activated in a similar way, independently from the pathology considered [56].

Astrocytes are the most abundant cell population of the CNS, present in both white and grey matter; they have a star-shape morphology characterized by numerous processes that make contact with the surrounding blood vessels and adjacent neurons. Under physiological conditions, astrocytes are involved in the maintenance of neuronal functions [57] and they actively participate in the regulation and maintenance of synaptic activity [58]. Furthermore, they release proteins involved in the control of neuronal maturation and differentiation, such as neurotrophic factors

including neurotrophin-3 [59] or nerve growth factor [60]. In pathological conditions however, astrocytes become reactive and respond with an increase in proliferation and with both morphological and functional changes [61]: indeed, they produce pro-inflammatory cytokines which can trigger the apoptotic process (in particular through ERK1 and ERK2, members of the MAPK signaling pathway) and the consequent loss of MNs. No significant differences in astrocyte expression were reported between wild type (WT) and SMA mice in the first days of postnatal life, but the difference becomes significant around the postnatal day nine [62]. An evident astrogliosis was observed in the spinal cords of both SMA mouse models and patients, in the final stages of the disease [63]: the same authors observed that, after the restoration of SMN protein levels induced in astrocytes via a viral vector, the survival of SMA mice was significantly extended and the expression of pro-inflammatory cytokines was reduced as well.

Microglia as the resident macrophagic cells, represents the main form of the immune defence in the CNS: in a pathological condition microglial cells are activated and undergo a morphological transformation moving from a branched quiescent phenotype to an activated amoeboid phenotype capable of releasing inflammatory mediators [64]. The triggering event may be the presence in the CNS of pro-inflammatory cytokines and chemokines (such as interferon γ, tumor necrosis factor a, macrophage colony-stimulating factor) which may be produced by astrocytes: this suggests a possible mutual influence between the two cell populations [65].

In SMA, although the pathological role of microglial cells is not clear, the activation of this cell population has been observed in the early stages of the disease in the spinal cord of patients; similarly, in the SMNΔ7 mouse model, the increase in the expression of IBA1 (a specific marker of microglia) is significant from the early symptomatic stages up to the terminal stage of the disease [66].

2.3.3. Neuromuscular junctions

It is increasingly evident that SMA does not determine alterations only in the CNS, but that the reduction in SMN protein level affects also the peripheral districts [11, 67]; in particular, several studies have demonstrated that since the early stages of the

disease in mouse models of SMA morphological and functional alterations also affect NMJs [68, 69].

NMJs are specialized synapses of the peripheral nervous system that allow communication between motor nerve terminal and skeletal muscle fibers. In the mechanisms that lead to the innervation of muscles, through the development and maintenance of the NMJs, a large number of molecules are involved [70]. In the mouse, the development of NMJs begins around the 12th-14th embryonic day [71] and undergoes further structural modifications in the postnatal period: indeed, acetylcholine receptors are initially organized in small groups and subsequently assume the typical "pretzel-shape" [72] (Figure 2.2). Regarding the muscle innervation, all muscle fibers undergo an initial immature phase of poly-innervation, to then lose the exceeding axons and evolve into a mature phase of mono-innervation [73]. Pathological alterations of NMJs are found in both SMA animal models and patients, including immaturity, reduced size, fragmentation, denervation and accumulation of neurofilament (NF) [74]. Another distinctive pathological trait affecting NMJs concerns their prolonged poly-innervation, normally an indication of a still immature phase typical of the first stages of their maturation process; in SMA, on the other hand, the NMJs remain in the "poly-innervated" phase longer [69]. At the same time, muscle denervation is also observed, caused by the pathology progression [75]. Furthermore, accumulation of the NF at the NMJ level in skeletal muscles of SMA models has been associated to slowed axonal transport of components essential for plaque maturation and maintenance [76]. All these alterations affect skeletal muscles at different time points and affect proximal muscles earlier than the distal ones [68].
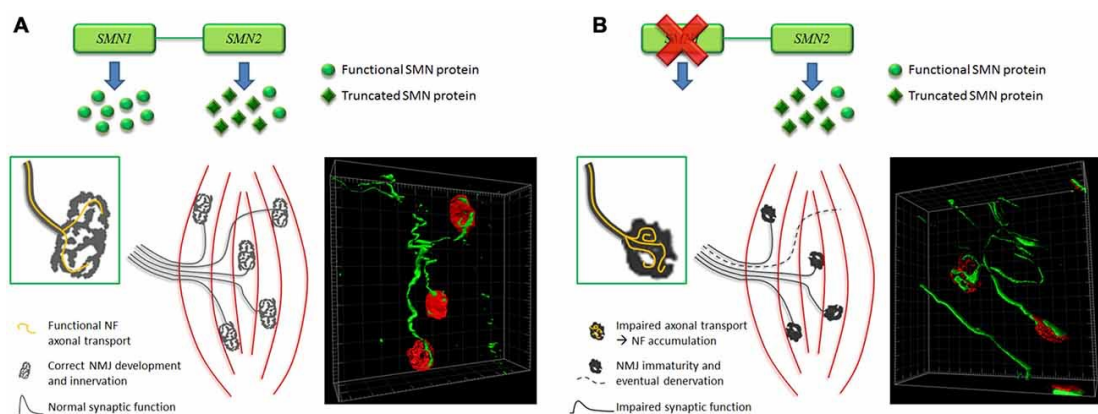
Figure 2.2. Abnormalities of the NMJs of the muscles of SMA animals. (A) Normally mature NMJs are characterized by a pretzel-like structure and functional synaptic activity; the reconstruction shows a situation of mono-innervation of the plaque (in red) by thin neurofilaments (in green). (B) In the case of SMA, the absence of the SMN protein generates small, immature plaques with abnormal synaptic activity; accumulation of neurofilament is also observed (in green) (From Boido and Vercelli, 2016 [70]).

2.4. *Therapeutic strategies: SMN-dependent strategies*

At the moment, an effective cure for SMA is absent. In recent years, thanks to the progress obtained from basic research studies and the development of cellular and animal models, various effective therapeutic strategies have been developed to significantly slow down the course of the disease. Currently, there are three SMN-dependent treatments approved by FDA and EMA.

Since manipulation of the splicing pattern of the *SMN2* gene can produce full-length, functional SMN protein, a recent therapeutic approach that target splicing regulatory elements and boost exon 7 inclusion has shown great success and was the first SMN-dependent therapy to achieve regulatory approval.

This is possible with the administration of antisense oligonucleotides (ASO): ASO are small sequences of synthetic nucleotides, complementary to exon 7 and for this reason able to bind to it inhibiting the splicing factors [77, 78]. After several efficacy evidence in cellular and animal experimental models and in several clinical trials [79], the ASO Nusinersen (Spinraza, Biogen) (Figure 2.3) was approved by FDA and EMA: the results of clinical studies have in fact demonstrated a good safety profile and encouraging efficacy data when administered, particularly in children with SMA type 1. However, ASO are not able to overcome the blood-brain barrier (BBB) and this requires an intrathecal administration of the treatment, with repeated lumbar injections [80], which are highly invasive.
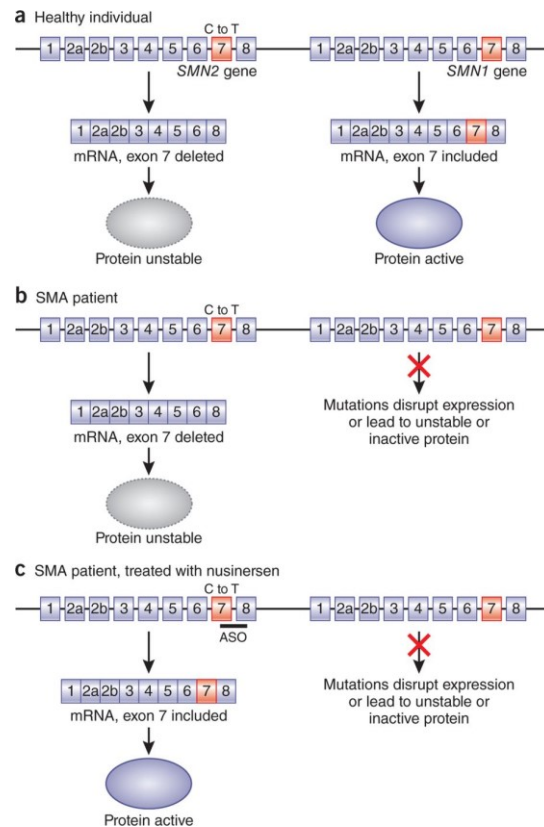
Figure 2.3. Nusinersen mechanism of action. (A) In a normal individual, the C-T transition in the *SMN2* gene results in the exclusion of exon 7 from the mRNA and the expression of an inactive protein. However, the functional *SMN1* gene produces the required amount of FL-SMN protein. (B) In a SMA patient the *SMN1* gene is mutated, and the production of the protein is reduced or deleted. *SMN2* encodes for the higher percentage for a truncated and unstable protein. (C) In treated SMA patients, Nusinersen binds to the pre-mRNA molecule favoring the inclusion of exon 7 in the mRNA molecule produced from *SMN2*; this increases the expression of the FL-SMN protein (From Corey, 2017 [81]).

A different class of small synthetic molecules, able as well to act upregulating the full-length *SMN2* transcripts, includes Risdiplam (Evrysdi, Roche). Its administration in both severe and mild mouse models of SMA significantly increased SMN protein levels, motor function and animal survival [82, 83]. Recently published results from the phase II/ III of a clinical trial determined improved efficacy for 7 of 17 infants that were able to sit independently after 12 months of oral treatment with Risdiplam [84].

A different strategy consists instead in gene therapy: since the cause of SMA is a monogenic defect, this pathology is a perfect candidate for gene replacement therapy [85]. Its overexpression, in addition to restoring the levels of SMN protein in MNs, also mitigates the defects at peripheral level of NMJs, such as the increase in their

size, the reduction of the accumulation of NF and the denervation [86, 87]. The relatively small *SMN1* cDNA can be successfully packed into a non-replicating self-complementary adeno-associated virus 9 vector (scAAV9) that can be systemically delivered. Thus, it can efficiently cross the BBB and transduce target cells in the spinal cord as well as reach the muscle or other peripheral tissues where the SMN protein is abundantly expressed. Experimental studies show that scAAV9 vector administered to puppies of mice affected by SMA with a single intravenous injection at post natal day 1, increased the expression of *SMN1* by 60% in MNs of the spinal cord, ensuring a recovery of muscle function and strength and an increased survival of the animals [88, 89]. These successes led to the initiation of a clinical trial of Onasemnogene abeparvovec (Zolgensma, Novartis): a recombinant scAAV9 viral vector encoding human SMN protein and administered with a single intravenous injection. In 2019 Zolgensma became the first gene therapy to be approved by FDA for the treatment of pediatric SMA patients; its safety information includes severe acute liver injury as the main risk; however, the recommended dose appeared to be well tolerated both short and long term in patients with SMA type I or II and presymptomatic SMA infants [90].

However, despite the important contribution of these approved drugs in the treatment of SMA some limitations and concerns still remain, such as patient inclusion criteria, invasiveness of the administration methods (regarding Nusinersen), the still unknown long-term effects, the possible treatment-related toxicity, and lastly the high cost of these therapies [91]. Moreover, SMN-dependent therapeutic approaches cannot be sufficient in completely arresting the disease progression, since they overlook the contribution of numerous other molecular and cellular pathways involved in the complex pathogenesis of SMA. It is therefore necessary to develop synergistic treatments, which combine therapeutic strategies aimed at increasing the concentration of SMN with therapies that affect non-SMN-dependent targets.

3. AMYOTROPHIC LATERAL SCLEROSIS

Amyotrophic Lateral Sclerosis (ALS), also known as Lou Gehrig's disease, is a fatal neurodegenerative disease of the human motor system, with an adult onset, characterized by progressive and irreversible degeneration upper motor neurons (UMNs) and/or lower motor neurons (LMNs) [92]. It was firstly described in 1869 by the French neurologist Charcot, who analysed post-mortem tissues of patients with muscle spasms. Charcot observed a decrease in MNs in the anterior horn of the spinal cord, as well as muscular atrophy (to which the term "Amyotrophic" refers to) and the presence of scars around the lateral tract of the spinal cord (Lateral Sclerosis), directly associated with cell death. However, despite several years from its discovery and many studies, ALS remains difficult to diagnose and with several associated mechanisms still poorly understood.

The incidence of ALS is approximately 1-2.6/100000 persons every year, whereas the prevalence is approximately 6/100000. The average age of onset of ALS is currently 58-60 years [93]. This pathology has accelerated progression if compared to other neurodegenerative diseases, leading to patient death within about 2–5 years after the onset of disease symptoms. ALS is more common in men than in women by a factor of 1.5. Traditionally, ALS has been classified in two clinical and pathologically similar forms: sporadic ALS (sALS, 90% of cases) or familial ALS (fALS, 10% of cases) [94].

3.1. *Clinical manifestation of ALS*

ALS is classified as a MN disease. The heterogeneity of ALS depends on the familial or sporadic occurrence, the sites of onset, the MNs population involved in the degeneration during the disease, with the possible extension to extra-motor nuclei. MNs are classified in two groups: UMNs located in the brain cortex and LMNs in brain stem and spinal cord; UMNs have axons projected from the primary motor cortex to the LMNs [95].

Most ALS patients have the spinal ALS phenotype and onset, with signs of UMNs and LMNs degeneration. The disease starts from a limb with focal weakness and asymmetrically spreads to other limbs; it may start both distally and proximally in the upper and lower limbs. Clinical evaluation reveals atrophy and fasciculations of the

muscles involved and usually absence of Babinski signs [96]. On the other hand, bulbar phenotype is caused by the degeneration on MNs in the bulbar region and begins with signs of bulbar muscles weakness through dysarthria, dysphagia and tongue fasciculations. The prognosis of bulbar ALS is more severe than the spinal one, with a mean survival of 2 years, correlated with problems of aspiration and deglutition of the affected patients [97].

The pathological condition caused by selective UMNs impairment is called Primary Lateral Sclerosis (PLS) and their involvement predominately induces muscle spasticity, brisk reflexes and Babinski signs. Whereas, Progressive Muscle Atrophy (PMA) predominantly involves LMNs degeneration and causes weakness, muscle twitching and muscle atrophy of the subjects [98].

The 15% of the ALS cases present also clinical features of frontotemporal dementia (FTD). FTD is characterized by the degeneration of frontal and anterior temporal lobes and clinically shows behavioural changes, impaired executive function, and language dysfunction. ALS and FTD are now considered to belong to the same spectrum due to the overlap in genetic and molecular mechanisms underlying both these neurodegenerative disorders [99] (Figure 3.1).
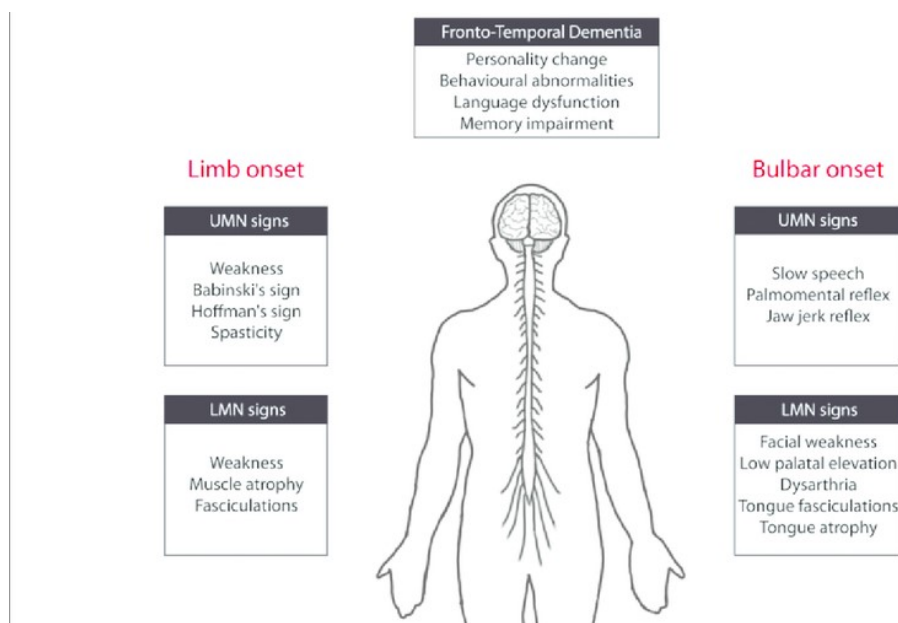
Figure 3.1. Clinical manifestation in ALS. The differently onset degeneration site and the different MNs population involvement in the degeneration produce a different clinical sign. Up to 15% of ALS patients may have symptoms of FTD (From Picher-Martel et al., 2016 [100]).

3.2. *Sporadic and familial ALS*

In sporadic cases of ALS, the occurrence of the disease is due to a gene-environment interaction. sALS has been associated with 'susceptible' genes, that may trigger the cascade of MNs degeneration interacting with environmental risk factors. Mutation in these genes may potentially contribute to increase the risk of the disease development only in conjunction with other genetic or environmental factors. Among the risk factors there are lifestyle, as smoking and dietary factors, and physical activity [101]. Moreover, environmental risk factors could potentially increase the risk of ALS onset. In particular, fertilizers, pesticides, smoking, radiation, atmospheric pollutants, heavy metals and aromatic solvents may be associated with the development of the disease [102].

The majority of ALS cases are sporadic, while the familial cases account only for the 10%; moreover, the fALS form is linked to genetic mutations and in the most affected cases has an autosomal dominant inheritance.

Among the mutations studied, at least 160 mutations have been observed in the gene encoding for Cu/Zn superoxide dismutase 1 protein (SOD1) [103]. In humans, the SOD enzyme is present in three forms: Cu/Zn SOD1 (SOD1), Mn SOD (SOD2) and SOD (SOD3). SOD1 is located in cytoplasm while SOD2 and SOD3 are distributed in the mitochondria and extracellular compartment respectively [104]. All three forms catalyse the dismutation of the superoxide anion in oxygen and hydrogen peroxide; therefore, SOD enzymes provide an important antioxidant defence in cells exposed to oxygen. SOD1 gene mutations can cause a dominant gain of function, resulting in an increase of SOD1 activity, with an excessive production of H_2O_2 , or in a dominant loss of function with a decrease in enzyme activity which results in insufficient degradation of ROS. The pathogenic mechanism underlying the neurodegenerative processes in MNs caused by SOD1 mutation are still debate and numerous hypothesis have been proposed [105].

Based on these evidence, several *in vivo* models overexpressing human SOD1 gene were created to reproduce the typical hallmark of ALS phenotype. A large number of SOD1 transgenic mice were created with different mutations, like G37R [106], G85R [107], A4V [108] and G93A that is the most common animal model used to study ALS. It develops first motor deficits at 80-90 days, it shows degeneration of MNs

and progressive hindlimb paralysis that lead to death of the animals at 120-130 days of life [109].

Mutations in the TARDBP gene, which encode for the TAR DNA-binding protein 43 (TDP-43), were also reported. Under physiological condition TDP-43 is located in the nucleus, but mutations on the corresponding gene are responsible for the protein aggregation in the cytoplasm of MNs in fALS [110]. In addition, this protein's loss of function impairs axonal transport, which is also associated with neurodegeneration [111].

Mutations in the FUS/TLS gene, which encodes for the RNA-binding protein, sarcoma fusion protein (FUS), can also be involved in the disease pathogenesis. This protein is normally located in the cell nucleus, but mutated forms are found in aberrant aggregation in the cytoplasm of MNs, causing their degeneration [112].

Finally, the repeated expansion of "GGGGCC" located in a non-coding region of the C9orf72 gene was associated with different forms of the disease. Currently in European populations, this mutation is known to be the most common inherited cause of fALS [113]. However, despite it is a highly conserved gene, its role in neural cells remains still unclear. Farg and colleagues demonstrated a possible role of C9orf72 protein in endosomal trafficking and autophagy in cells [114].

3.3. *Pathogenic mechanisms in ALS*

The cause of the MNs degeneration in ALS is complex and still unclear, and it is considered to be the result of the combination of environmental risk, genetic causes and many pathogenic cellular/molecular mechanisms, rather than one single causing factor [115]. Here, the main neurodegenerative processes that trigger the death of MNs are summarized (Figure 3.2).

Glutamate-induced excitotoxicity has been implicated in ALS pathogenesis. Glutamate is the main excitatory neurotransmitter in the CNS: through the binding with α-amino-3-hydroxyl-5-methyl-4-isoxazole-propionate (AMPA) or N-methyl-D-aspartate (NMDA) receptors, it depolarize the post-synaptic neurons. Excessive activation of these postsynaptic receptors by glutamate can induce neurodegeneration through activation of calcium-dependent enzymatic pathways [116]. Glutamate-induced excitotoxicity can also result in generation of free radicals,

which in turn can cause neurodegeneration by damaging intracellular organelles and upregulating proinflammatory mediators [117]. Spreux-Varoquaux and colleagues showed that increased concentration of glutamate is present in cerebrospinal fluid of ALS patients [118].

Mitochondria are the cellular organelles responsible for the cellular respiration and energetic production of the cells. Through the respiratory chain they reduce O_2 to product ATP, but they can also generate ROS, like superoxide anion O_2^-. In ALS patients and in the murine model SOD1(G93A), morphological alteration of mitochondria of MNs were observed [119]. These alterations may lead to ROS accumulation, inducing an irreversibly damage to MNs. Moreover, the alteration of the mitochondrial membrane permeability, determines the release of apoptotic proteins, contributing to the neurodegeneration. The aggregated SOD1 enzyme alter mitochondrial function increasing the production of ROS in rodent models of ALS [120].

Misfolded proteins tend to accumulate and to form inclusions in neurons, gaining toxic properties. The abundance of cytoplasmic inclusions could alter the capacity of chaperon proteins and ubiquitin proteasome to solve their normal function, altering the clearance of regulatory cellular factors and inducing neurodegeneration [121]. Before the discovery of the aggregation of the mutated nuclear proteins FUS and TDP-43 in the cytoplasmic region [110, 112], aberrant inclusions of mutated SOD1 were observed in ALS patients and in the transgenic murine models [122]. Other proteins have shown to improperly aggregate and to form inclusions like neurofilament proteins. In this regard the abnormal organization of NF cause an impairment of axonal transport and induce the degeneration of the MNs axons [123]. A common characteristic of ALS and other neurodegenerative diseases is the neuroinflammatory response, characterized by activated microglia, astrogliosis and infiltrated immune cells in the sites of neuronal injury. Astrocytes from sALS and fALS patients resulted to have a cytotoxic effect when co-cultured with MNs [124]. On the other hand, the selective expression of mutated SOD1 in microglia develop typical ALS traits in mouse [125], enhancing inflammatory processes in the spinal cord.
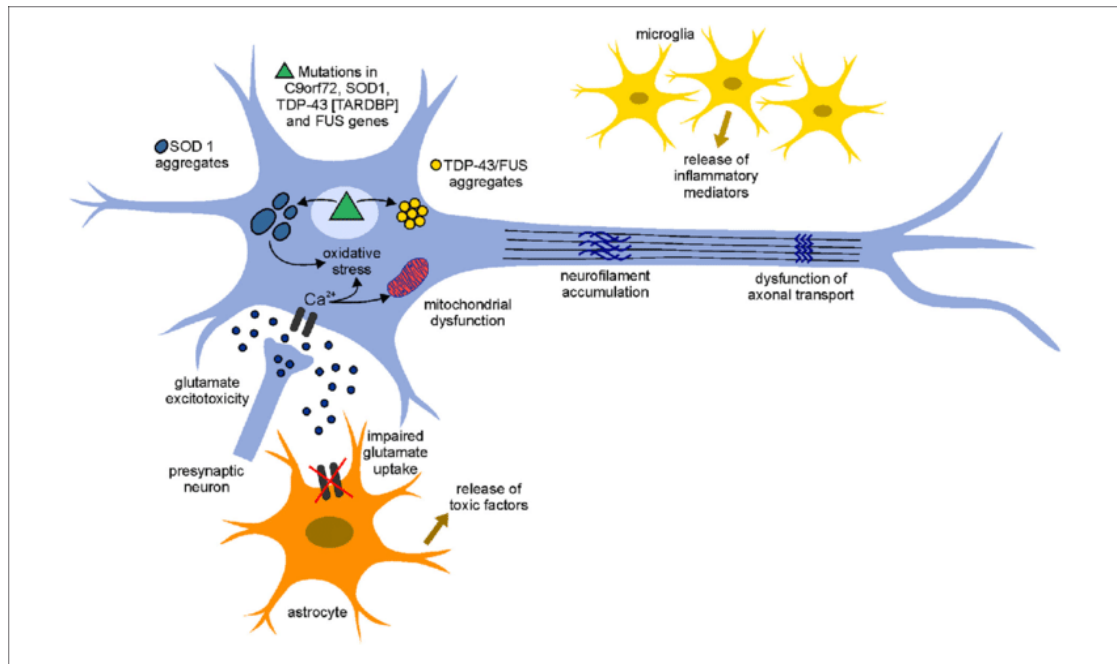
Figure 3.2. Pathogenetic mechanisms involved in ALS. The pathophysiological mechanism of the disease appears to be multifactorial and several mechanisms contribute to neurodegeneration. An increase of the neurotransmitter glutamate in the synaptic cleft leads to an increased influx of Ca^{2+} ions in the MNs causing neurodegeneration. Mutant misfolding proteins (such as SOD1, C9orf72, TDP-43 and FUS, NF) form intercellular aggregates and contribute to an increase of oxidative stress, to mitochondrial dysfunction and to dysfunction of axonal transport. Moreover, activated astrocyte and microglia release inflammatory mediators and toxic factors, contributing to neurotoxicity (From Bonafede and Mariotti, 2017 [115]).

3.4. *Therapeutic approaches in ALS*

Given the complexity of ALS pathogenesis, to date there is no effective treatment. Nevertheless, several therapeutic strategies have been proposed to mostly relieve symptoms and improve the quality of life of ALS patients. Currently, four compounds have been approved for clinical use: riluzole, edaravone,AMX0035 and Tofersen.

Riluzole was the first FDA-approved therapy in 1995. It acts reducing glutamate release from the presynaptic terminals by blocking voltage-gated sodium channels, and thus ameliorating excitotoxicity [126, 127]. However, it showed modest and controversial effects in modifying the disease progression: Riluzole did not ameliorate the motor function, tremor and pulmonary capacity and the initial trial results with a prolongation of patients life of approximately 3 months on average [128].

28

Edaravone (Radicava™), an antioxidant agent administered intravenously, is known to decrease the aggregation of mutated SOD1 in SOD1(G93A) murine model [129]. After a 6-month trial period there was evidence that it could slowed down disability progression early after disease onset. It is not yet known whether there is an effect on patients survival [130]. Edaravone was approved for the treatment of ALS by FDA in 2017.

The FDA approved AMX0035 (Relyvrio, Amylyx) for the treatment of ALS in 2022. AMX0035 is a combination of taurursodiol and sodium phenylbutyrate that is considered to mitigate mitochondrial dysfunction and endoplasmic reticulum stress. Moreover, ALS patients who received AMX0035 lived an average of 6.5 months longer than the comparison placebo group [131].

Finally, in April 2023 FDA approved Tofersen (Qualsody™, Biogen) for the treatment of ALS patients who have a mutation in the SOD1 gene, becoming the first approved treatment to target a genetic cause of ALS. Tofersen is an antisense oligonucleotide designed to bind to SOD1 mRNA to reduce the protein production: the results of the clinical study showed that participants treated with QALSODY experienced less decline from baseline, a reduction in plasma neurofilaments light chain (NfL, a biomarker of axonal injury and neurodegeneration) and in CSF SOD1 protein compared to the placebo group. Tofersen is administered intrathecally with three loading doses administered at 14-day intervals, followed by a maintenance dose every 28 days (reviewed in [132]).

However, these pharmacological strategies are directed against one or few altered mechanisms involved in ALS pathogenesis and in most cases their use has only a minimal impact on the disease course. For an efficient therapeutic approach, it could be helpful to counteract different pathogenetic mechanisms involved in the disease.

4. MESENCHYMAL STEM CELLS AND EXTRACELLULAR VESICLES IN NEURODEGENERATIVE DISEASES

4.1. *Stem cells therapy*

The use of stem cells was considered a potential strategy for the treatment of neurodegenerative disorders, including ALS and SMA. Stem cells are defined as undifferentiated totipotent or multipotent cells, capable of both self-renewal and differentiate into mature cells [133]. They can be classified into different types: embryonic stem cells (ESCs) are isolated from the inner cell mass of the blastocyst [134], they are pluripotent and therefore can give rise to all the different cell populations of the organism [135] including neurons [136]; however, the use of ESCs can result in the formation of teratomas following transplantation [137, 138], as well as raise ethical questions related to the use of embryonic cells [139]. Neural stem cells (NSCs) can be isolated from different regions of the CNS of mammalian embryos or adults [140]; another possibility is to use somatic cells that can be reprogrammed through the introduction of transcription factors, to obtain induced pluripotent stem cells (iPSC) [141].

Among the different types of stem cells used in the treatment of neurodegenerative diseases, mesenchymal stem cells (MSCs) seem to have aroused the highest interest as promising candidates [142]. MSCs can be obtained from bone marrow, dental tissue, umbilical cord, or adipose tissue [143]. The isolation of MSCs from adipose tissue can bring several advantages over the others: the procedure for the extraction of adipose-derived MSCs (ASCs) is easy and less invasive for the patient, the collected quantity of stem cells higher [144] and it allows autologous transplantation of ASCs, as well. Once isolated, ASCs have the ability to grow *in vitro* and have the potential to differentiate into different cell lineages [145] like osteoblasts, adipocytes, and chondrocytes *in vitro* [146]. Thanks to their characteristics, the efficacy of MSCs in neurological diseases was demonstrated in several preclinical studies. Indeed, they are able to home to damaged brain and to prevent from apoptosis, modulate the local immune system, promote proliferation and angiogenesis [147]. MSCs are also capable of releasing soluble molecules such as chemokines and anti-inflammatory cytokines, neurotrophic and neuroprotective factors (such as nerve growth factor, brain-derived neurotrophic factor, neurotrophin-3 and VEGF) and to express

immune-relevant receptors important for tissues [147-149]. They were also found to be able to stimulate regrowth axonal, preserving peripheral connections and NMJs maturation [150]. Regarding neuroinflammation, some authors also have demonstrated the ability of MSCs to influence the functions of microglia and astrocytes, shifting the microglia phenotype toward the neuroprotective one [151]. However, despite their therapeutic activity, the engraftment and differentiation of MSCs in CNS tissues, after their transplantation, results in a small percentage [152, 153]. These observations suggest that the ability of MSCs to modify the tissue microenvironment secreting soluble factors may contribute more significantly to the tissue repairing. Such action is achieved through a paracrine mechanism, that was first described in 2006 analysing the entire secretome released by MSCs, composed by a soluble fraction (mostly growth factors and cytokines) and a vesicular component, extracellular vesicles (EVs), which can transfer proteins, lipids, and genetic material to other cells [154-157].

4.2. *Extracellular vesicles*

EVs are membranous structures present in many biological fluids, including blood, CSF, urine, saliva and amniotic fluid, as well as in the conditioned medium of cell culture [158, 159]. It has been found that EVs play important roles in participating in intercellular communication via the transfer of membrane receptors, proteins, lipids and RNAs and also in cell maintenance and tumor progression [160, 161]. The function of small EVs depends on their interaction with other cells and on the ability to deliver their contents [162]. Thanks to their small size, which allows them to pass the BBB and deliver their cargo to the CNS, they attracted interest as a therapeutic tool for neurodegenerative diseases where the BBB represents one of the main obstacle to reach the injured area of CNS.

Initially EVs were commonly distinguished through a classification made on their size, content, release pathway and function: microvesicles (MVs) with an average size of 50-1000 nm and exosomes with a size of 30-100 nm in diameter. Furthermore, MVs are generated by the outward budding of the plasma membrane, while exosomes are intraluminal vesicles formed by the inward budding of endosomal membrane during maturation of multivesicular endosomes (MVEs) and secreted

upon fusion of MVEs with the cell surface [163-166] (Figure 4.1). However, this characterization of EVs based only on their size is considered limited since there isn't a method to optimally separate EVs into its component and in 2018 the International Society for Extracellular vesicles (ISEV) recommends the use of appropriate nomenclature for EVs, classifying them by univocal and more easily measurable characteristics (such as cell of origin, molecular markers, etc.), abandoning terms such as "exosomes" or "microvesicles" that were previously used and considering the generic term of "extracellular vesicles" [166-168].
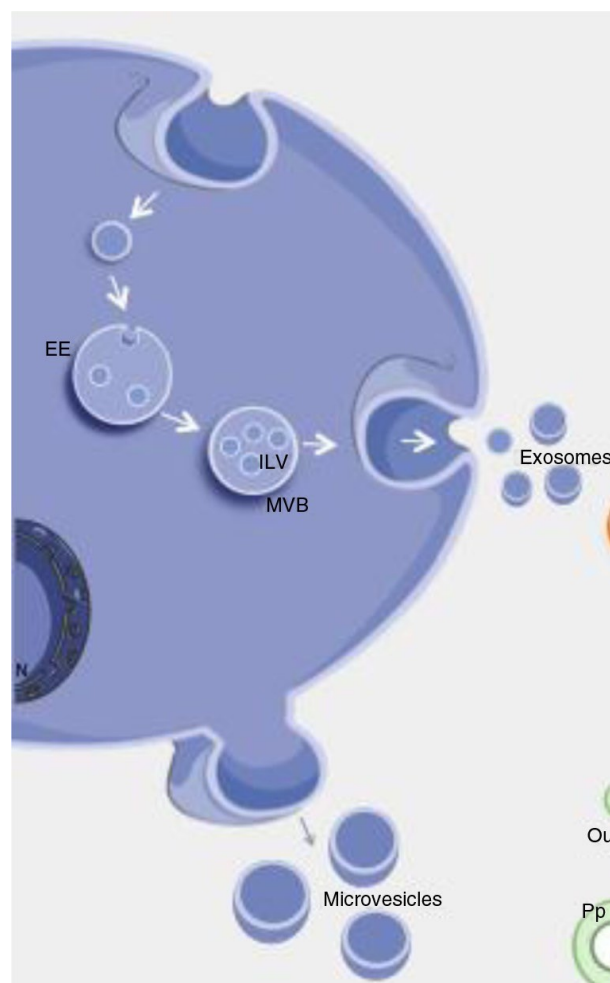
Figure 4.1. Biogenesis and release of extracellular vesicles. Extracellular vesicles can be broadly classified into 3 main classes: microvesicles that are produced by outward budding and fission of the plasma membrane; exosomes that are formed within the endosomal network and released upon fusion of multi-vesicular bodies with the plasma membrane. EE=early endosome; MVB=multi-vesicular body; ILV=intraluminal vesicles. (Adapted from Yanez-Mo et al., 2015 [169]).

In particular, MSCs are able to release a large number of EVs that, with their therapeutic power, could constitute an effective alternative to cell-therapy for neurodegenerative diseases. This is possible thanks to their content which can recapitulate the effect of their parental cells [170-172] with significant advantages due to a high safety profile, low immunogenicity and tumorgenicity [173]. Indeed, MSC-EVs contain many neurotrophic factors, immunomodulatory and anti-inflammatory molecules including transforming growth factor-β (TGF-β), and interleukin-10 (IL-10), which are involved in neurogenesis and neuroprotection and functional recovery [174-176]. Proteins involved in neural development and synaptogenesis, such as nestin, growth-associated protein 43 (GAP-43) and synaptophysin were also found in MSC-EVs [177]. Moreover, a specific signature of miRNAs related to MSC-EVS was reported, which was found to be implicated in promoting CNS recovery by modulating neurogenesis and stimulating axonal growth [178] (Figure 4.2). The composition of MSC-derived EVs is reported in several databases such as VESICLIPEDIA (http://microvesicles.org/) [179] or EXOCARTA (www.exocarta.org) [51]. The phenotype, number and function of MSC-EVs may vary depending on the source of MSCs [180, 181].
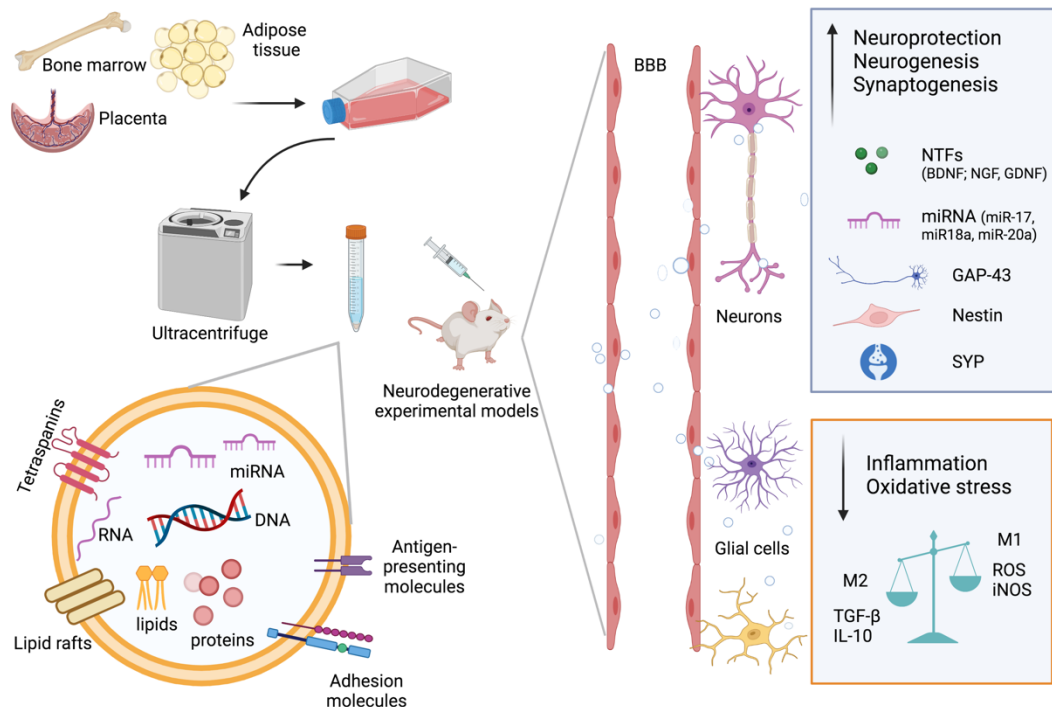
Figure 4.2. Extracellular vesicles from MSCs as a possible strategy for the treatment of neurodegenerative diseases. MSC-EVs derived from different cellular sources, can cross the blood–brain barrier and reach the affected cells. Here, EVs release neurotrophic factors,

miRNA, and anti-inflammatory molecules that mediate neuroprotection, neurogenesis, synaptogenesis, and decrease the neuroinflammation, contributing to functional recovery and a reduced neurodegeneration. BBB=blood–brain barrier; NTFs=neurotrophic factors; TGF-β=transforming growth factor-β; IL-10=interleukin-10; GAP-43=growth-associated protein-43; SYP=synaptophysin; ROS=reactive oxygen species; iNOS=inducible nitric oxide synthase; M1=pro-inflammatory M1-polarized microglia; M2=anti-inflammatory M2-polarized microglia. (From Turano et al., 2023 [182]).

4.3. *Therapeutic application of MSC-EVs*

Thanks to their small size, MSC-EVs are able to migrate to the target organ or the injured area in the CNS after infusion [183] and crossing the BBB, making them a suitable therapeutic agent for neurodegenerative diseases, as extensively reported in literature (Table 4.1).

Some typical hallmarks of AD are the accumulation of amyloid beta (Aβ) and the presence of neurofibrillary tangles and neuronal loss, correlated to a progressive decline in cognitive functions. Several therapeutic approaches have tried to reduce the Aβ burden in AD patients and in mouse models: the presence of high levels of Aβ-degrading enzymes in adipose MSC-derived EVs has been considered a useful strategy to regulate the level of Aβ accumulation in the brain [184]. Indeed, EVs isolated from human MSCs of the umbilical cord significantly boosted the expression of Aβ-degrading enzymes such as Neprilysin and Insulin degrading enzyme, reducing Aβ deposition in transgenic APP/PS1 mice [185]. Moreover, the presence of antioxidant enzymes, like the Catalase, in MSC-EVs protects hippocampal neurons from oxidative stress and synaptic damage [186].

The use of MSC-EVs was beneficial also against neuronal damage and synaptic dysfunction [187], pathological signs that manifest during the initial phase of AD and which are directly related to cognitive impairment. In this context, MSC-EVs have shown to promote neuroprotection [188] and stimulate neurogenesis [189].

A similar scenario is observed with PD, another highly common chronic neurodegenerative disease [190], characterized by the degeneration of dopaminergic neurons with the accumulation of α-synuclein protein in the intraneuronal structure and a consequent deficiency of dopamine production [191]. The use of MSC-EVs in this case turns out to be promising although still at an early stage. The delivery of MSC-EVs content in PD rat models showed an improvement of motor performance outcomes [192, 193]. MSC-EVs from different sources were able to promote

34

neuroprotection of 6-hydroxy-dopamine dopaminergic neurons from oxidative stress [194], reducing substantia nigra dopaminergic neuron loss and upregulating the dopamine levels in the striatum [195].

The beneficial traits of MSC-EVs have been observed also in other settings: EVs derived from ASCs promoted re-myelination after injury and neuroprotection of neurons and motor neuron-like cells, after peroxide treatment *in vitro* [196, 197], demonstrating their potential therapeutic application in several neurodegenerative diseases. In particular, MNs represent the principal target of motor-dysfunction such as ALS [115]. ASC-EVs have demonstrated the ability to regulate the aggregation of the pathological SOD1 protein restoring the levels of mitochondrial proteins in neurons from G93A mutated ALS mice [198] and in MN cultures, thanks to their antiapoptotic ability [199].

The regulation of ROS production is involved in different pathogenic mechanisms of neurodegenerative diseases and recently, the role of MSC-EVs in reducing oxidative and nitrosative damage has drawn much attention. Antioxidant effects have been observed in models of PD on different cell types including neurons and glial cells [200], as well as effects reported on brain ischemic injury [201]. The ability to act against mitochondrial dysfunction is also reported to be a possible strategy to counteract neurodegeneration [199, 202]. Furthermore, MSC-EVs are able to act as modulators of the inflammatory component, that plays a role among the pathological mechanism of neurodegeneration as well: indeed, inflammation (with the contribution of activated microglia and astrocytes) associated to chronic neurodegenerative diseases is not the trigger itself of such diseases, but it contributes and amplify their progress, the neuronal dysfunction and death [203]. MSC-EVs perform a strong anti-inflammatory effect in an AD mouse model, improving the number of M2-polarized macrophages. A reduction of inducible nitric oxide synthase (iNOS) was observed in ALS mice after MSC-EVs administration [187].

In light of this promising evidence, the use of MSC-EVs in the field of neurodegenerative diseases appears to be a possible innovative strategy for the treatment of still incurable diseases.

Table 4.1. Relevant preclinical studies on MSC-EVs in neurodegenerative experimental models (From Turano et al., 2023 [182]).

Disease	Source of EVs	Route of administration	Outcomes	References
AD	UMC	i.v.	Reduction of Aβ levels and improvement of cognitive functions	[185]
	BM (hypoxia-preconditioned)	i.v.	Reduction of Aβ levels, anti-inflammatory impact and improvements of learning and memory functions	[187]
	Not reported	ICV	Promotion of neurogenesis and improvement of cognitive function	[189]
	BM (cytokine-preconditioned)	i.n.	Stimulation of neuroprotection and inhibition of neuroinflammation	[204]
	BM	ICV	Reduction of Aβ burden and cognitive improvements	[205]
PD	BM	i.v.	Neuroprotection of dopaminergic neuron in substantia nigra and upregulation of thus dopamine levels in striatum	[195]
	DP	i.n.	Improvement of motor functions and normalization of tyrosine hydroxylase expression in the substantia nigra and striatum	[206]

	BM	i.n.	Reduction of α-syn aggregates and functional recovery	[207]
ALS	AT	i.v./i.n.	Neuroprotection of motor neurons, and neuromuscular junctions and improvement of motor performances	[208]
HD	AM (conditioned medium)	i.p.	Amelioration of motor functions	[209]
MS	AT	i.n.	Improvement of motor function, and attenuation of inflammation and demyelination	[210]
	Placenta	s.c.	Improvement of motor function and induction of myelin regeneration	[211]
	AT	i.v.	Reduction of demyelination in the spinal cord and immunomodulation	[212]

AD=Alzheimer's disease; PD=Parkinson's disease; HD=Huntington's disease; ALS=amyotrophic lateral sclerosis; MS=multiple sclerosis; UMC=umbilical cord; BM=bone marrow; DP=dental pulp; AT=adipose tissue; AM=amniotic membrane; i.v.=intravenous injection; i.n.=intranasal injection; ICV=intracerebralventricular injection; i.p.=intraperitoneal injection; s.c.=subcutaneous injection; Aβ=amyloid beta; α-syn=alpha-synuclein.

MSC-EV therapies proved to be safer and more easily accessible than cell therapy, despite the few clinical results already available [213, 214]. Several studies involving the use of EVs/exosomes are registered on https://beta.clinicaltrials.gov: the majority of them focuses on the analysis of EVs isolated from patient body fluids for diagnostic and prognostic purposes. Promising results have been confirmed in other diseases [215]. Worthy of mention is the clinical trial NCT03384433, which evaluated the injection of MSC-EVs overexpressing miR-124 for the treatment of ischemic

37

stroke. Currently, only two trials including MSC-EVs and chronic neurodegenerative diseases are registered: depression, anxiety, and dementias (NCT04202770) and Alzheimer's disease (NCT04388982). In the first one focused ultrasound was used to enhance the intravenous delivery of EVs from MSCs to the subgenual target for patients with refractory depression, the amygdala for patients with anxiety, and the hippocampus for patients with cognitive impairment. The second study evaluates the safety and efficacy of MSC-EVs in patients with mild to moderate dementia by repeated i.n. administration of MSC-EVs (at three different concentrations).

Although there are still few clinical studies currently registered, the interest in these therapies seems to be growing and thanks also to the promising results obtained from preclinical studies.

5. AIM OF STUDIES

Adipose mesenchymal stem cells (ASCs) represent a feasible and valid alternative to other sources of mesenchymal stem cells in the treatment of several neurological disorders. Currently, the scientific community brings a growing body of evidence indicating that ASCs exert their neuroprotective and immunomodulatory effects by a paracrine mechanism through the release of extracellular vesicles (EVs). Indeed, EVs are considered important mediators in intercellular communication as they can transfer their cargo (proteins, miRNAs and mRNAs) to nearby cells promoting nerve regeneration, neuronal protection, synaptic plasticity and remyelination in different pathophysiological contexts, recapitulating the effect of origin cells.

The overall aim of this PhD project was to evaluate the therapeutic effect of ASC-derived EVs (ASC-EVs) in different *in vivo* and *in vitro* models of neurodegeneration.

In particular, in experiment 1 and 2, we took into account two different murine models of neurodegenerative diseases to test the neuroprotective activity of ASC-EVs: Spinal Muscular Atrophy (SMA) and Amyotrophic Lateral Sclerosis (ALS) respectively. Indeed, despite these two disorders are caused by different pathogenic mechanisms and affect different targets, they share some pathological dysfunctions, they are both characterized by the progressive loss of motor neurons (MNs) in the spinal cord and brainstem that leads to a progressive motor decline.

As reported in experiment 1 of this thesis, ASC-EVs were injected in SMNΔ7 mice, a severe SMA model. With this setting, we aimed to evaluate the effects of ASC-EVs on animals disease progression and motor performance. Moreover, we evaluated the capability of ASC-EVs to reduce the apoptotic activation and modulate the neuroinflammation in lumbar spinal cord, counteracting the MNs degeneration. The activity of ASC-EVs at the peripheral level was also investigate, with particular regard to the muscular atrophy and fibers denervation of quadriceps and gastrocnemius muscles.

With the first part of experiment 2, we aimed to test the potential therapeutic effect of ASC-EVs on a murine model commonly used to study ALS, the SOD1(G93A)

transgenic mouse. To do this, we compare the effect of two different routes of ASC-EVs administration, intravenous (i.v.) and intranasal (i.n.), on the disease progression, on the modulation of the neurodegeneration and neuroinflammation at the central level and on the muscular preservation at the peripheral level.

Starting from this first part, we identified the i.n. route of administration as an optimal choice to deliver ASC-EVs in this particular animal model thanks to its low invasiveness and comparable efficacy to the i.v. route.

Thus, the second part of experiment 2 aimed to compare different doses and therapeutic frequencies of intranasally administered ASC-EVs to determine the more effective one, based on their correlated effect on the disease progression and on the neuroprotection of MNs in lumbar spinal cord.

Furthermore, an EVs-based therapy needs to take into account the obstacles (such as epithelia and endothelia) that vesicles encounter before reaching the target site and that can negatively affect their biodistribution and the effective therapeutic concentration.

In view of this, experiment 3 aimed to set up an *in vitro* model of epithelial barrier to acquire more information on the mechanisms used by EVs to pass the cellular barrier in the human body. Besides, we wanted to confirm their neuroprotective effect on an oxidative stress-induced model of both motor neuron (NSC-34) and neuron (SH-SY5Y) cells, even after their passage through the epithelium. Regarding the evaluation of the mechanisms by which EVs are able to cross the epithelium and reach the central nervous system, we set up a fluorescent labelling protocol to isolate and characterize labelled ASC-EVs and to evaluate their uptake by injured NSC-34 cells. This will pave the way for further studies in order to clarify ASC-EVs passage through biological barrier and their capture by injured cells in the central nervous system.

6. EXPERIMENT 1

EXTRACELLULAR VESICLES FROM ADIPOSE-DERIVED STEM CELLS: THERAPEUTIC EFFECT ON A MURINE MODEL OF SPINAL MUSCULAR ATROPHY

Manuscript in preparation for submission. Author contribution: Virla Federica[1], Scambi Ilaria[1], Turano Ermanna[1], Schiaffino Lorenzo[1], Mariotti Raffaella[1], Boido Marina[2]

[1]Department of Neuroscience, Biomedicine and Movement Sciences, University of Verona, Verona, Italy

[2]Neuroscience Institute Cavalieri Ottolenghi, Department of Neuroscience "Rita Levi Montalcini", University of Turin, Turin, Italy

6.1. INTRODUCTION

Spinal Muscular Atrophy (SMA) is an autosomal recessive neuromuscular disease, characterized by the selective degeneration and loss of lower motor neurons (MNs) [5]. The typical symptoms consist in hypotonia, muscular atrophy and weakness due to the denervation, till the final paralysis of the muscles of both upper and lower limbs as well as of the trunk [6].

Depending on the age of symptom onset and on the achieved motor milestones, five main phenotypes have been described, from the more severe type 0 SMA to the milder type IV [12]. Despite the great variability of phenotypic expression, SMA is due to well-known genetic causes; in particular, homozygous deletions or mutations of the survival motor neuron 1 (*SMN1*) telomeric gene, encoding for the functional full length SMN (FL-SMN) protein [15]. Humans also display a centromeric copy of the gene, *SMN2*; it differs from the *SMN1* copy for a C to T transition in exon 7 that results in splicing defects and that in most of cases leads to the production of a truncated, unstable and not functional form of the protein, called SMNΔ7 [34]. The numbers of copies of the *SMN2* gene are critical for determining the phenotype and the severity of the disease. Indeed, *SMN2* is able to produce the FL-SMN protein in low percentage, but not fully sufficiently to compensate the *SMN1* loss [38].

Currently, three SMN-dependent treatments have been approved by FDA and EMA: the antisense oligonucleotide Nusinersen (Spinraza, Biogen) and the small molecule Risdiplam (Evrysdi, Roche) are both splicing modifiers and act to boost the production of FL-SMN protein from *SMN2* gene. The third one is Onasemnogene abeparvovec (Zolgensma, Novartis) and use the viral vectors strategy to deliver a functional copy of the *SMN1* gene to SMA patients (reviewed in [91]).

Despite the important contribution of these approved drugs in the treatment of SMA, some limitations and concerns still remain, such as patient inclusion criteria, the still unknown long-term effects, the possible treatment-related toxicity, and lastly the high cost of these therapies. Moreover, although SMA is widely considered a MN disease, it has been confirmed that reduced levels of SMN can also affect different cells and tissues, other than motor neurons [216, 217]. It also emerged that SMA is likely a non-cell autonomous disease in which several signalling pathways and molecular/cellular mechanisms are involved [218]. Thus, the implementation and further development of SMN-independent therapies appears to be extremely relevant to enhance the beneficial effect of SMN-dependent strategies [12].

In this sense, a promising therapeutic option in neurodegenerative diseases is represented by mesenchymal stem cells (MSCs): indeed, they can be easily isolated from a variety of different tissues, they are able to migrate to damage tissues stimulating reparative and regenerative processes [142, 219, 220], as demonstrated in different disease models, such as spinal cord injury [221], experimental autoimmune encephalomyelitis [222] and amyotrophic lateral sclerosis (ALS) [153, 223, 224] murine models. Among MSCs, adipose-derived stem cells (ASCs) are accessible in large amount and could be easily used in autologous transplantation [115].

However, despite many advantages of MSCs-based therapy, various challenges limit their clinical application. Furthermore, it is well accepted that MSCs act through paracrine mechanisms by releasing their content in extracellular vesicles (EVs) [157, 225]. EVs are considered important mediators in intercellular communication as they can transfer their cargo, including proteins, miRNAs and mRNAs to nearby cells in several physiological and pathological conditions [162]. Furthermore, EVs maintain the neuroprotective role of their parental MSCs, as demonstrated by several groups [226, 227].

Giving the remarkable results obtained by our previous studies in *in vitro* and *in vivo* ALS models [196, 208], in the present study we evaluated whether ASCs-derived EVs (ASC-EVs) could exert their neuroprotective role also in SMNΔ7 mice, a largely used model of severe SMA. Here we demonstrated that intracerebroventricular (ICV) injections of ASC-EVs could delay lumbar MN degeneration, and in turn limit the neuromuscular junction (NMJ) degeneration/denervation and skeletal muscle atrophy ; we also observed a decrease in the glial activation in SMNΔ7 treated animals, compared to vehicle-treated mice. By inducing such neuroprotective and anti-inflammatory effects, the ASC-EV administration was also able to improve the motor performance of SMA pups.

Taken together, these results demonstrate the neuroprotective contribution of this non-cells strategy and pave the way for a synergic therapy in combination with SMN-dependent drugs, in order to enhance their beneficial effects for the treatment of SMA patients.

6.2. MATERIALS AND METHODS

6.2.1. ASCs Culture

Murine ASCs were isolated from inguinal adipose tissues of 8-12 week-old C57Bl6/J mice (n=5) (Charles River Laboratories, Sant'Angelo Lodigiano, Italy). Animals were housed in pathogen-free, climate-controlled facilities and were provided with food and water ad libitum according to current European Community laws. All mouse experiments were carried out in accordance with experimental guidelines approved by the University of Verona committee on animal research (Centro Interdipartimentale di Servizio alla Ricerca Sperimentale) and by the Italian Ministry of Health (protocol #642/2021-PR). The research complies with the commonly accepted "3Rs", minimizing the number of animals used and avoiding their suffering. The isolation of stromal vascular fraction was carried out as previously described [228]. Briefly, the extracellular matrix was incubated in Hank's Balanced Salt Solution (Life Technologies Italia, Milan, Italy) with collagenase type I (Life Technologies Italia, Milan, Italy) and bovine serum albumin (BSA, AppliChem Nova Chimica Srl, Milan, Italy), centrifuged, and suspended in NH4Cl. The fraction was centrifuged again and filtered through a 40 μm nylon mesh to remove cell debris. ASCs were cultured using DMEM, 10% FBS, 100 U/mL penicillin, and 100 μg/mL streptomycin (all from GIBCO Life Technologies, Milan, Italy) and incubated at 37°C/5% CO_2.

The immunophenotypic analysis of murine ASCs was performed using monoclonal antibodies specific for CD106, CD9, CD44, CD80, and CD138 and by the absence of hematopoietic and endothelial markers (as CD45, CD11c and CD31), as previously described [153].

6.2.2. ASC-EVs isolation and characterization

ASC-EVs were isolated from the culture medium of $1x10^7$ murine ASCs at 14-18 passages. The cells were cultured to confluence and 48 h of FBS deprivation was made to avoid any contamination of vesicles from serum. Then, cell culture supernatant was collected and EVs were obtained using Pure Exo Exosomes Isolation Kit (101Bio, Montain View, CA, USA), following the manufacturer's

protocol. The protein content of EVs was determined by Bicinchoninic Protein Assay (BCA method) using the manufacturer's protocol (Thermo ScientificTM, Milan, Italy BCATM Protein Assay).

To characterize ASC-EVs, their size distribution and concentration were measured by Nanoparticle Tracking Analysis (NTA) using a Nanosight NS300 (Malvern Instruments, UK). For the measurements, five video recordings with a duration of 1 minute were carried out for each sample. Camera level and the detection threshold were set in the acquisition and analysis, respectively, in order to achieve a concentration between 20 and 120 particles/frame. The NTA 3.4 software version was used to acquire and analyse the sample videos. The results are reported as the mean ± SEM of 5 measurements. For size determination, the data are reported as the statistical mode ± SEM of 5 measurements.

To perform electron microscopy ASC-EVs pellets were fixed in 2% glutaraldehyde in Sorensen buffer (pH 7.4) for 2 h, and then post-fixed in 1% osmium tetroxide (OsO4) in aqueous solution for 2 h. The sample was dehydrated in graded concentrations of acetone and embedded in Epon-Araldite mixture (Electron Microscopy Sciences, Fort Washington, PA, USA). The semithin sections (1 μm in thickness) were examined by light microscopy (Olympus BX51, Olympus Optical, Hamburg, Germany) and stained with toluidine blue. The ultrathin sections were cut at a 70 nm thickness, placed on Cu/Rh grids with Ultracut E (Reichert,Wien, Austria), and observed with transmission electron microscopy (TEM) using a Morgagni 268D electron microscope (Philips).

To confirm ASC-EVs isolation and purity the immunoblotting analysis was performed: ASC-EVs proteins were denatured, separated on 4%–12% polyacrylamide gels and transferred onto a nitrocellulose membrane. Antibodies against murine HSP70 (70 kDa, 1:100 HSP70 (K-20): sc-1060 Santa Cruz Biotechnology, DBA Italia Srl, Milan, Italy) and CD9 (25 kDa, 1:100 MM2/57, Millipore CBL-162) were used. After incubation with IgG HRP-conjugated secondary antibodies (Dako Agilent, Milan, Italy) the membranes were incubated with a chemiluminescent HRP substrate and detected with G:BOX F3 GeneSys (Syngene, Cambridge, UK). ASCs lysates were used as a positive control.
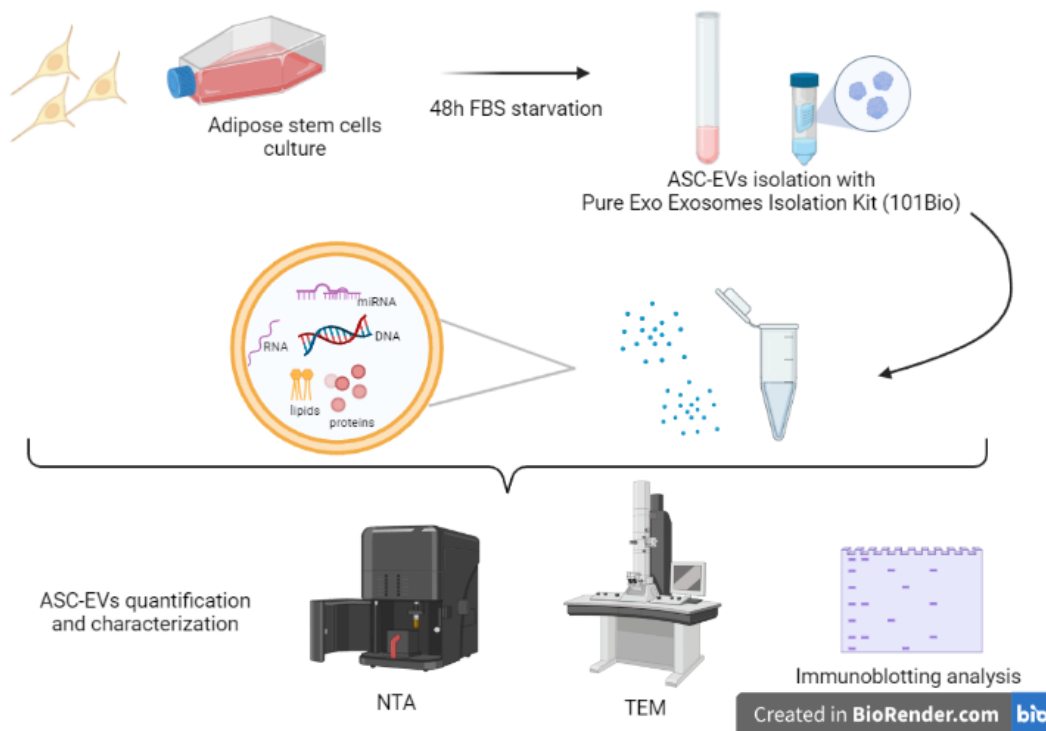
6.2.3. SMA animals

SMN2+/+; SMNΔ7+/+; SMN+/- mice (stock number 005025; Jackson Lab, Bar Harbor, ME, USA) were bred to obtain the experimental animals SMN-/- (SMA, as model of severe SMA) and SMN+/+ (WT) offspring. SMA and WT pups were left in the cage with the mother until the sacrifice at post-natal day 10 (P10). Pups of both sexes were used in this study. Animals had free access to food and water, and were kept into regular cages under 12/12h light/dark cycle. The experimental procedures involving live animals were performed in strict accordance with institutional guidelines in compliance with national (D.L. N.26, 04/03/2014) and international law and policies (new directive 2010/63/EU). The study was approved by the Italian Ministry of Health (protocol #980/2020-PR). Additionally, the ad hoc Ethical Committee of the University of Turin approved this study. The research complies with the commonly accepted "3Rs", minimizing the number of animals used and avoiding their suffering. A total number of 43 SMA and 2 WT mice were used; no criteria for including/excluding animals during the experiment were used..

The mice were genotyped by PCR using DNA isolated from a small piece of tail. Isolation was performed with proteinase k (50 μg) in lysis buffer (10mM Tris HCl, 50mM KCl, 0.01% gelatin, 0.45% IGEPAL, 0.4% Tween-20) at 60 °C for 30 minutes

under gently shaking. The presence of the transgene was determined by PCR analysis using primers that amplify a portion of the smn gene, yielding a 420 bp product for the wild-type allele and a 150 bp product for the transgenic one. They were: smn fwd 5'- TTTTCTCCCTCTTCAGAGTGAT-3', smn wt rev 5'-CTGTTTCAAGGGAGTTGTGGC-3' and smn tg rev 5'-GGTAACGCCAGGGTTTTCC-3' as suggested by suppliers (Jackson Laboratories).

6.2.4.   ASC-EVs administration

To evaluate the therapeutic effects of ASC-EVs SMA mice were divided randomly into ASC-EVs-treated group (SMA-EVs) and PBS-treated group (SMA-PBS) (n=16 SMA-EVs, 27 SMA-PBS). ICV injections were performed at postnatal day 3 (P3) and P6: treated animals received 0.5 µg of ASC-EVs (injected volume 2 µl), while control group was injected with 2 µl of PBS.

Briefly, pups were anesthetized by hypothermia (total duration 3–5min) and their heads were immobilized on a custom neonatal stereotaxic apparatus. ASC-EVs or PBS were injected at stereotaxic coordinates of 0 mm from bregma, 0.8 mm lateral to sagittal sinus, and 1.5 mm deep with a Hamilton microsyringe, as reported in [229]. Pups were then placed on a heat pad, quickly revitalized and returned to their mother.

6.2.5.   Behavioural and motor test

The symptom progression was monitored in SMA mice by checking the body weight and by performing behavioural tests specifically designed for neonatal rodents [230]. SMA-PBS and SMA-EVs treated animals (n= 16 SMA-EVs; 23 SMA-PBS) were tested at different time points: P2, P4, P6, P8 and P10. In particular, three behavioural tests were performed on pups: I) Tail suspension test: pups were suspended by the tail for 15 seconds and a score was assigned to their hindlimb posture as follow: 4 normal hindlimb spread open; 3 not completely spread; 2 often close; 1 always close together; 0 always close together with clasping. II) Righting reflex: pups were placed on their backs on a flat surface and their failure or success in repositioning themselves on dorsal side up was evaluated within 30 seconds. III) Negative Geotaxis: for the evaluation of motor coordination and vestibular

47

sensitivity, pups from P4 were placed on an inclined surface (approximately 35° inclination) with the head facing down. The ability of the pups to turn around and climb upwards was evaluated within 60 seconds and recorded.

6.2.6. Tissue preparation

The humane endpoints were established and monitored in accordance with the Ethical Committee of the University of Turin. No mice exhibited any signs of the established endpoints in this study. For the histological analysis of brain (n = 2 WT), spinal cord (n = 5 SMA-EVs; 6 SMA-PBS), gastrocnemius and quadriceps muscles (n= 5 SMA-EVs; 7 SMA-PBS), at P10 animals were deeply anesthetized by gaseous anaesthesia and transcardically perfused with phosphate buffer 0.1 M (PB, pH 7.4), followed by paraformaldehyde (PFA) 4%. The tissues were dissected out and post-fixed in PFA 4% overnight at 4°C. They were then soaked in 30% sucrose solution overnight, embedded and frozen in cryostat medium (Killik, Bio-Optica, Milan, Italy).

First of all, in order to exclude brain damages due to ICV injections and assess the proper targeting of the cerebral ventricles, the PFA 4%-fixed WT brains (P10) were dissected and cut in 40 µm-thick sections, subsequently mounted on 4% gelatin-coated glasses. The lumbar spinal cord (L1-L5) was cut in 40 µm thick, serial, free-floating sections that were stored in an antifreeze solution (30% ethylene glycol, 30% glycerol, 10% PB; 189 mM NaH2PO4; 192.5 mM NaOH; pH 7.4) and stored at -20°C until being used. The gastrocnemius and quadriceps muscles were longitudinally cut in 20 µm sections with cryostat apparatus and directly collected on 4% gelatin-coated glasses.

For hematoxylin-eosin (H/E) staining of gastrocnemius and quadriceps muscles, another cohort of pups (n= 6 SMA-EVs; 5 SMA-PBS) were sacrificed by cervical dislocation at P10. Fresh muscles were rapidly collected, embedded in cryostat medium and cut at the cryostat in 20 µm thick transverse slices and collected directly onto 4% gelatin-coated glasses.

6.2.7. Histochemistry

For Nissl staining, brain and spinal cord sections were mounted on 4% gelatin-coated slides and air-dried overnight. Sections were then hydrated in distilled water, immersed in 0.1% Cresyl violet acetate (Sigma Aldrich) for 5 minutes and gradually placed into increasing concentrations of ethanol, cleared with xylene, and cover-slipped with Eukitt (Bio-Optica). For H/E staining, sections of gastrocnemius and quadriceps muscle were stained firstly with hematoxylin, then with eosin (Bio-Optica), dehydrated in increasing concentrations of ethanol, cleared in xylene and cover-slipped with Eukitt (Bio-Optica).

6.2.8. Immunohistochemistry

For immunofluorescence staining, the lumbar spinal cord sections were rinsed with PBS and incubated in blocking solution with 10% normal donkey serum (NDS) and 0.3% Triton X-100 in PBS for 30 minutes at RT. The sections were incubated overnight at 4°C with the following primary antibodies diluted in 0.3% Triton X-100 and appropriate 2% normal sera in PBS: anti-Cleaved Caspase-3 (1:200, Asp175, rabbit, Cell Signaling Technology, Danvers, MA, USA), anti-SMI32 (1:1000, mouse, BioLegend, San Diego, CA, USA), anti-glial fibrillary acidic protein (anti-GFAP, 1:500, rabbit, DAKO Cytomation, Agilent, Santa Clara, CA, USA), anti-ionized calcium binding adaptor molecule 1 (anti-IBA1, 1:1000, rabbit, Wako Chemicals, Neuss, Germany).

After rinsing, primary antibodies were detected with appropriate fluorochrome-conjugated secondary antibodies (all from Jackson ImmunoResearch Laboratories, West Grove, PA, USA): Alexafluor anti-rabbit 647 (1:600), Cyanin-3 AffiniPure anti-rabbit (1:200) and Cyanin-2 AffiniPure anti-mouse (1:200) diluted in PBS for 1 hour at RT. The sections were mounted on 4% gelatin-coated slices and coverslipped with the mounting medium Mowiol.

For the labelling of neuromuscular junctions (NMJs) and the following analysis of their innervation, the gastrocnemius and quadriceps muscles slices longitudinally cut were incubated for 30 min at room temperature with the Alexafluor-555-conjugated bungarotoxin (αBGTX, 1:500, Invitrogen, Milan, Italy), and overnight at 4°C with primary antibody anti-neurofilament (anti-NF, 1:200, mouse, 2H3 clone, Hybridoma

Bank, Iowa, IA, USA), diluted in 0.3% Triton X-100 in PBS and detected with Cyanin-2 AffiniPure anti-mouse (1:200; Jackson ImmunoResearch Laboratories, West Grove, PA, USA) secondary antibody. The slices were coverslipped with the mounting medium Mowiol.

Immunoreacted spinal cord and skeletal muscles were then analysed with a Leica TCS SP5 confocal laser scanning microscope (Leica Microsystems) or with Nikon Eclipse E90i epifluorescence microscope.

6.2.9.   *Quantitative Analysis*

For the MNs counting (n= 5 SMA-EVs; 6 SMA-PBS), Nissl stained-MNs in the ventral horns of the lumbar spinal cord were stereologically counted at 40X (one every fifth 40 µm-thick section was reconstructed) using a stereological technique with a computer-assisted microscope and the StereoInvestigator software (MicroBrightField Inc., Williston, VT, USA). MNs were counted when characterized by a diameter of 10 µm and located in the ventral somatic columns. The cell density was reported as MN number/mm^3.

The Cleaved Caspase-3-positive L1-L5 MNs (n= 4 SMA-EVs; 6 SMA-PBS) were quantified by counting the percentage of Casp3+/SMI-32+ double labelled cells on the total SMI32+ MNs cell population, using confocal images of the ventral horns of the lumbar spinal cord. Three spinal cord slices were evaluated for each animal.

For the analysis of astrogliosis in the ventral horn of the lumbar spinal cord, confocal images of GFAP-positive cells (n= 4 SMA-EVs; 6 SMA-PBS) and IBA-1-positive cells (n= 5 SMA-EVs; 6 SMA-PBS) were converted in black and white images, then the density of immunopositive profiles on the total area was quantified using Image J and expressed as a percentage.

Furthermore, the IBA-1-positive cells were qualitatively classified by their shape in ramified, bushy or amoeboid and the results were expressed as a percentage on the total number of IBA-1-positive cells.

To morphologically evaluate the gastrocnemius and quadriceps muscles, H/E stained muscle sections were visualized by optical microscopy (Olympus BX63; Olympus Life Science Solutions, Center Valley, PA   (n= 6 SMA-EVs; 5 SMA-PBS):   to measure the mean fibers area and Feret's max diameter, the sections were drawn and

analysed by Image J software. A total of 100 fibers per quadriceps and gastrocnemius were drawn and analysed for each animal.

Finally, for the analysis of NMJ innervation in gastrocnemius and quadriceps muscles for each animal (n= 5 SMA-EVs; 7 SMA-PBS) at least 100 NMJs/muscle were analysed with Nikon Eclipse E90i epifluorescence microscope; each NMJ was then classified in innervated, multi-innervated or denervated by looking at the number of NFs contacting the endplate and the result was expressed as a percentage on the total number of NMJs.

6.2.10. Statistical analysis

All the data were expressed as mean±standard error of the mean (SEM). Data were analysed using Two-way ANOVA (for the behavioural results) and Student t-test (for the immunofluorescence and histological analysis): p-values < 0.05 were considered significant.
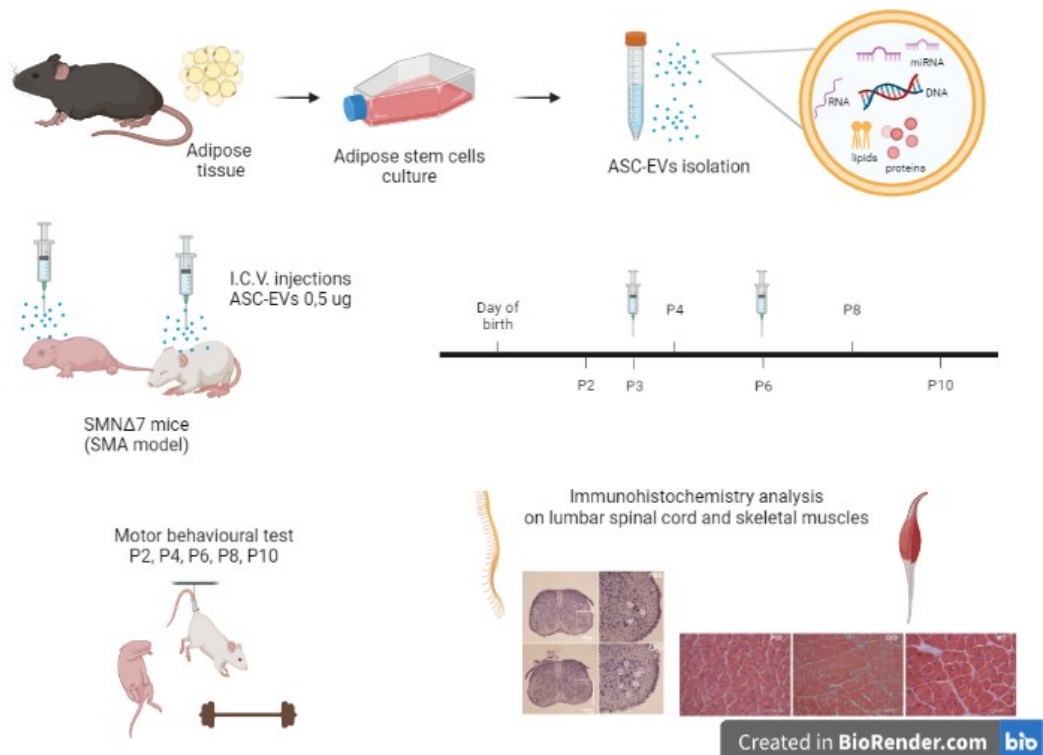
6.3. _RESULTS_

6.3.1. _Isolation and characterisation of ASC-EVs_

EVs were isolated from ASCs supernatant with an EVs isolation kit. The protein concentration was quantified and the yield of proteins for each isolation was about 200 µg/mL.

ASC-EVs were analysed and quantified by NTA: the concentration of EVs was 2.38 $\times$ 10^8 particles/mL, with a particle diameter mode of 113.6 nm (Figure 6.1A). Ultrastructure analysis of the EVs by TEM revealed round vesicles with lipid bilayers with a diameter of 50 to 150 nm. Measurements are in line with literature [160] (Figure 6.1B). By western blot we validated the presence of typical markers of EVs [231] identified through CD9 and HSP-70 antibodies, that displayed specific signals at 25 and at 75 kDa respectively. GM130 was used as negative control (Figure 6.1C). These results confirm that size, morphology, and the presence of specific protein markers are consistent with EVs.

Moreover, in a previous study regarding the proteomic analysis of ASC-EVs [232] the FL-SMN protein was not present in the extracellular vesicles content, supporting the idea that this could be a SMN-independent treatment.
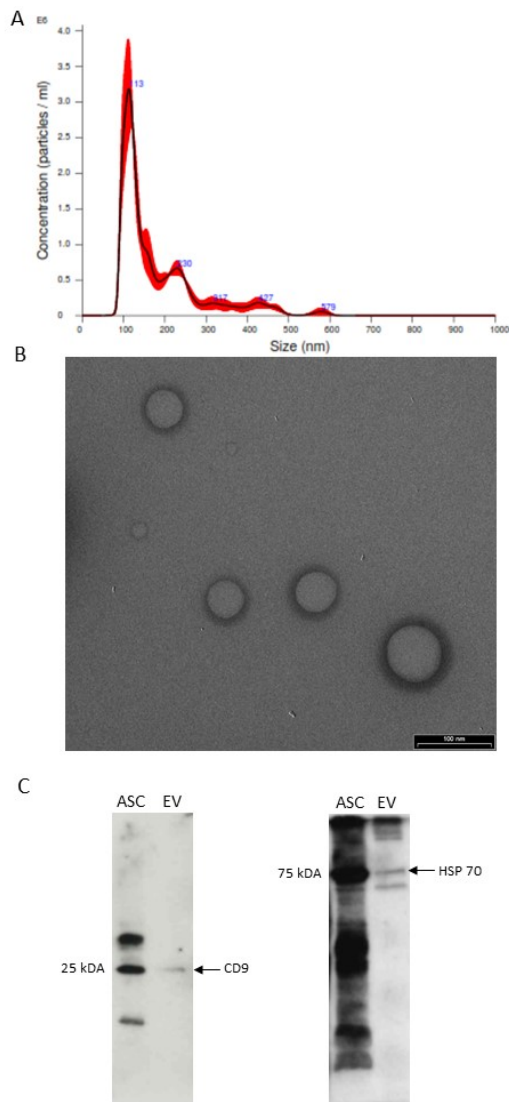
Figure 6.1. Characterization of ASC-EVs. (A) ASC-EVs size and concentration were measured and analysed by NTA. (B) Representative transmission electron microscopy images of ASC-EVs showed particles with characteristic morphology and size (scale bar 100 nm). (C) Western blot analysis of specific EVs protein markers: bands at 25, and 75 kDa were present after incubation with CD9 and HSP70 antibodies, respectively. ASCs lysates were used as positive control.

Size of ASC-EVs		
Mean (nm)	Mode (nm)	SD (nm)
181.7 ± 5.8	113.6 ± 6.7	101.2 ± 8.4
Concentration of ASC-EVs		
Concentration (particles/ml)	Concentration (particles/frame)	Concentration (centres/frame)
$2.38 \times 10^8 \pm 2.31 \times 10^7$	36.0 ± 2.4	52.0 ± 3.3

Table 6.1. NTA data output which reports mean and mode of ASC-EVs size and particle concentration with relative SD.

At P3 and P6, SMA pups received a unilateral ICV administration of ASC-EVs or PBS (2 μl). As expected, this procedure did not cause any damage to the cerebral cortex and ventricles. Moreover, the injections were well tolerated by SMA mice (Suppl. Figure 6.1).

During the entire treatment period up to the sacrifice, SMA mice body weight (Figure 6.2A) was monitored, showing no differences between SMA-PBS and SMA-EVs group. However, the body weight increase of SMA-PBS group reached the maximum value at P8, while that of SMA-EVs mice was still increasing at P10 and overall, the statistical analysis showed a significant treatment ($F_{(1, 145)}$=3.92, *p<0.05) and time ($F_{(4, 145)}$=41.99, ****p<0.0001) effect, while the interaction between treatment and time was not significant ($F_{(4, 145)}$=0.10, p>0.05).

To investigate the effect of ASC-EVs treatment, pups underwent a battery of behavioural tests from P2/P4 to P10: tail suspension, righting reflex and negative geotaxis tests.

In the tail suspension test (Figure 6.2B) the hindlimb posture was evaluated: after the injections at P3 and P6 SMA-EVs mice obtained higher scores compared to SMA-PBS mice, even if without statistical differences, in particular at P8. The statistical analysis showed a significant treatment ($F_{(1, 145)}$=12.30, ***p=0.0006) and time ($F_{(4, 145)}$=3.53, **p=0.0089) effect, while the interaction between treatment and time was not significant ($F_{(4, 145)}$=0.97, p>0.05).

The righting reflex test (Figure 6.2C) was also performed and results revealed that SMA-EVs group could complete the task in a shorter time compared to SMA-PBS group, already from P4; in particular, at P8 (after the second ASC-EVs injection, P6) the performance of the two SMA groups appeared significantly different (P8 *p<0.0428). Moreover, the statistical analysis showed a significant treatment ($F_{(1, 145)}$=12.57, ***p=0.0005) effect, while the time effect ($F_{(4, 145)}$=1.71, p>0.05) and the interaction between treatment and time ($F_{(4, 145)}$=0.78, p>0.05) were not significant.

Regarding the negative geotaxis test (Figure 6.2D), which measures the strength and motor coordination of pups, the control SMA group showed difficulties in completing the test during the whole observation period, while the treated one gradually ameliorated their motor performances, that were statistically different at

54

P10 compared to the SMA-PBS group (P10 ****p<0.0001). A significant treatment ($F_{(1, 113)}$=10.78, **p=0.0014) and time ($F_{(3, 113)}$=4.02, **p=0.0093) effect were observed, as well as the interaction between treatment and time ($F_{(3, 113)}$=5.35, **p=0.0017).

All these data suggest an overall improvement in motor performances of SMA-EVs mice compared to the SMA-PBS group, in particular after the second ASC-EVs injection.
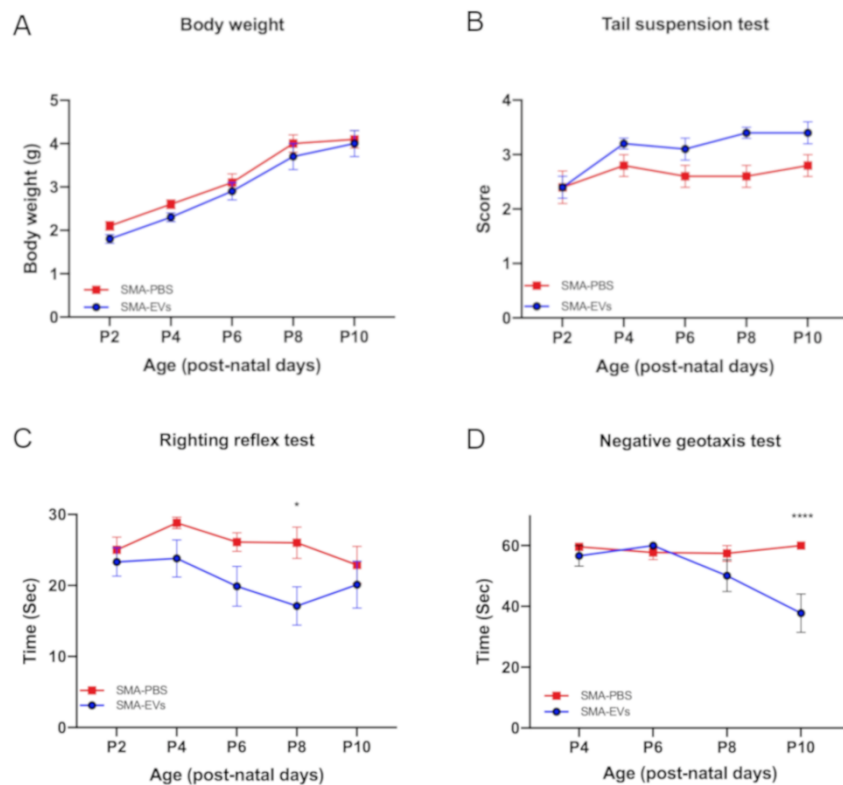
Figure 6.2. ASC-EVs treatment improves the motor performance of SMA mice. From P2/P4 to P10 the body weight measurements (A), tail suspension test (B), righting reflex test (C) and negative geotaxis test (D), were used to evaluate the motor performance of SMA mice treated with PBS (SMA-PBS, red line) or ASC-EVs (SMA-EVs, blue line). Overall the results suggest an improvement in behavioural and motor performances of SMA-EVs mice compared to the SMA-PBS group.

Data are shown as mean±SEM and were analysed by Two-way ANOVA mixed-effects model with Geisser-Greenhouse correction followed by Sidak's multiple comparison post hoc test. Statistical difference between the groups are indicated (*p<0.05; ****p<0.0001).

6.3.3. ASC-EVs administration extends the survival of lumbar MNs in SMA mice

At P10 the animals were sacrificed, lumbar spinal cords were dissected and analysed to evaluate the neuroprotective effect of ASC-EVs treatment on SMA mice. In particular, a stereological count of MNs was performed in the ventral horns of the lumbar tract (L1-L5) in both the experimental groups. The results highlighted a significantly higher MNs density in the lumbar spinal cord of SMA-EVs animals (2106.87±96.47 MNs/mm^3) compared to the SMA-PBS counterpart (1438.80±73.09 MNs/mm^3; ***p=0.0003. Figure 6.3A,B).

To further investigate the neuroprotective action of the ASC-EVs treatment in the SMA-EVs group, we then consider in the ventral horn of the lumbar spinal cord sections (L1-L5) the expression of the apoptotic marker Cleaved Caspase-3 (Casp3). The percentage of Casp3+/SMI32+ co-labelled MNs quantified by immunohistochemical analysis was significantly reduced in SMA mice treated with ASC-EVs (10.59±2.36%) compared to the SMA-PBS group (21.48±3.47%; *p=0.049. Figure 6.3C,D).

All together, these data suggest that the ASC-EVs administration is able to protect the lumbar MNs from degeneration.
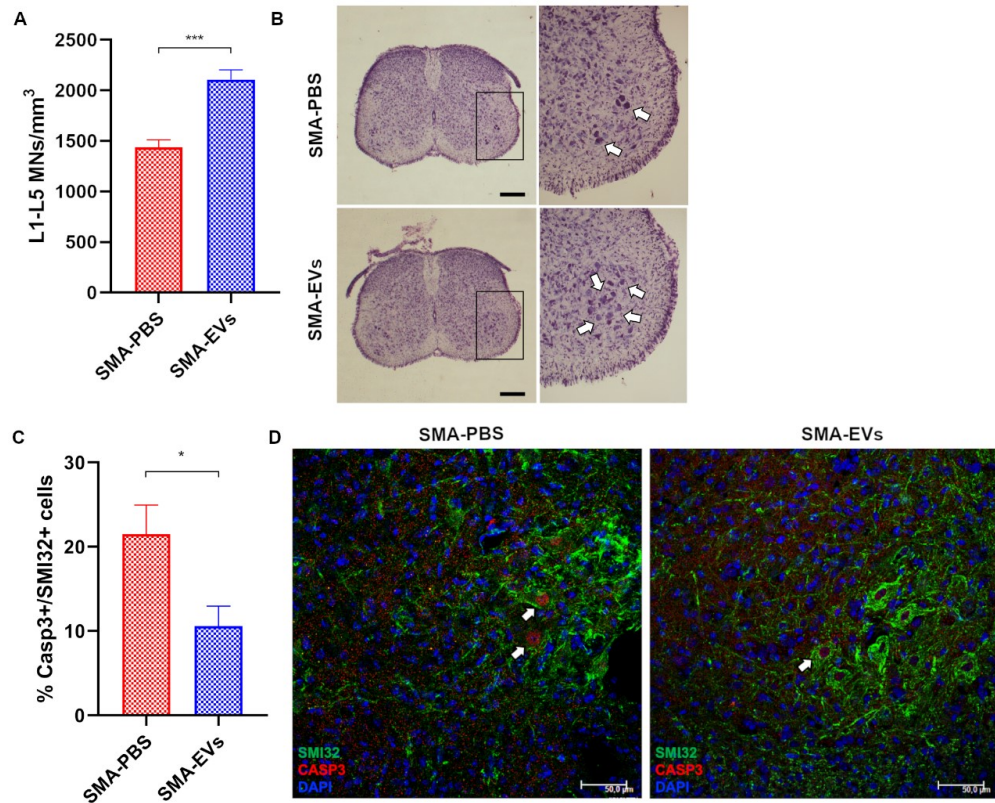
Figure 6.3. Effect of ASC-EVs administration on lumbar MNs degeneration in SMA mice. (A) The graph shows the quantification of MNs density (MNs number/volume) in the ventral horns of L1-L5 spinal cord both for SMA-PBS (red) and SMA-EVs (blue) group at P10. The treatment with ASC-EVs significantly protect MNs from neurodegeneration compared to control mice (unpaired Student t-test ***p=0.0003). (B) Representative Nissl stained sections of lumbar spinal cord of SMA-PBS and SMA-EVs mice. The arrows show stained MNs. Scale bar 500 μm. (C) The graph shows the quantification of the percentage of MNs (SMI32+ cells) expressing Casp3 in SMA-PBS (red) and SMA-EVs (blue) groups: the treatment with ASC-EVs decreased the activation of apoptotic marker Casp3 compared to control mice (unpaired Student t-test *p<0.05). (D) Representative confocal images showing Casp3+ (red) and SMI32+ (green) cells in the ventral horns of PBS- and ASC-EVs treated SMA mice. Cell nuclei are labelled by DAPI staining (blue). The arrows show Casp3+/SMI32+ cells. Scale bar 50 μm.

6.3.4. ASC-EVs treatment modulates the neuroinflammation in SMA mice

Since, besides MNs degeneration, neuroinflammation is reported in SMA as well [55], we evaluated by immunohistochemical analysis the activation rate of astrocytes

and microglia in the ventral horn of the lumbar spinal cord sections of P10 SMA animals.

In particular, our results showed that ASC-EVs treatment could significantly reduce the GFAP expression (SMA-EVs 6.16±0.315%) compared to the SMA-PBS controls (9.06±0.566%; **p=0.0048. Figure 6.4A,B).

The same analysis was carried out also to evaluate the activation of the microglia in the lumbar spinal cord of SMA mice; however, no differences in the IBA-1+ signal were observed between SMA-PBS (2.66±0.324%) and SMA-EVs mice (2.49±0.631%; p>0.05. Figure 6.4C,D). We also evaluated the morphology of microglial cells, in order to preliminary correlate their cellular phenotype with their function. Microglial cells were classified based on their shape in ramified, bushy or amoeboid (Figure 6.4E) and the results were expressed as a percentage on the total number of IBA-1-positive cells. The outcomes showed a significant difference between the two SMA groups when considering the "ramified" phenotype (typical of a steady-state microglial cells), significantly higher in the SMA-EVs group (28.41±1.64%) compared to the SMA-PBS one (19.94±3.03%; *p=0.0464. Figure 6.4F). Considering the "bushy" and "amoeboid" phenotypes, there were no statistical differences between SMA-PBS (bushy: 26.46±2.32%; amoeboid: 53.59±4.18%) and SMA-EVs pups (bushy: 22.22±1.46%; amoeboid: 48.63±1.59%), but the percentages were higher for the SMA-PBS group (Figure 6.4E,F).

These data suggest that ASC-EVs treatment is able to modulate the neuroinflammation in SMA mice, possibly contributing to delay the MN death.
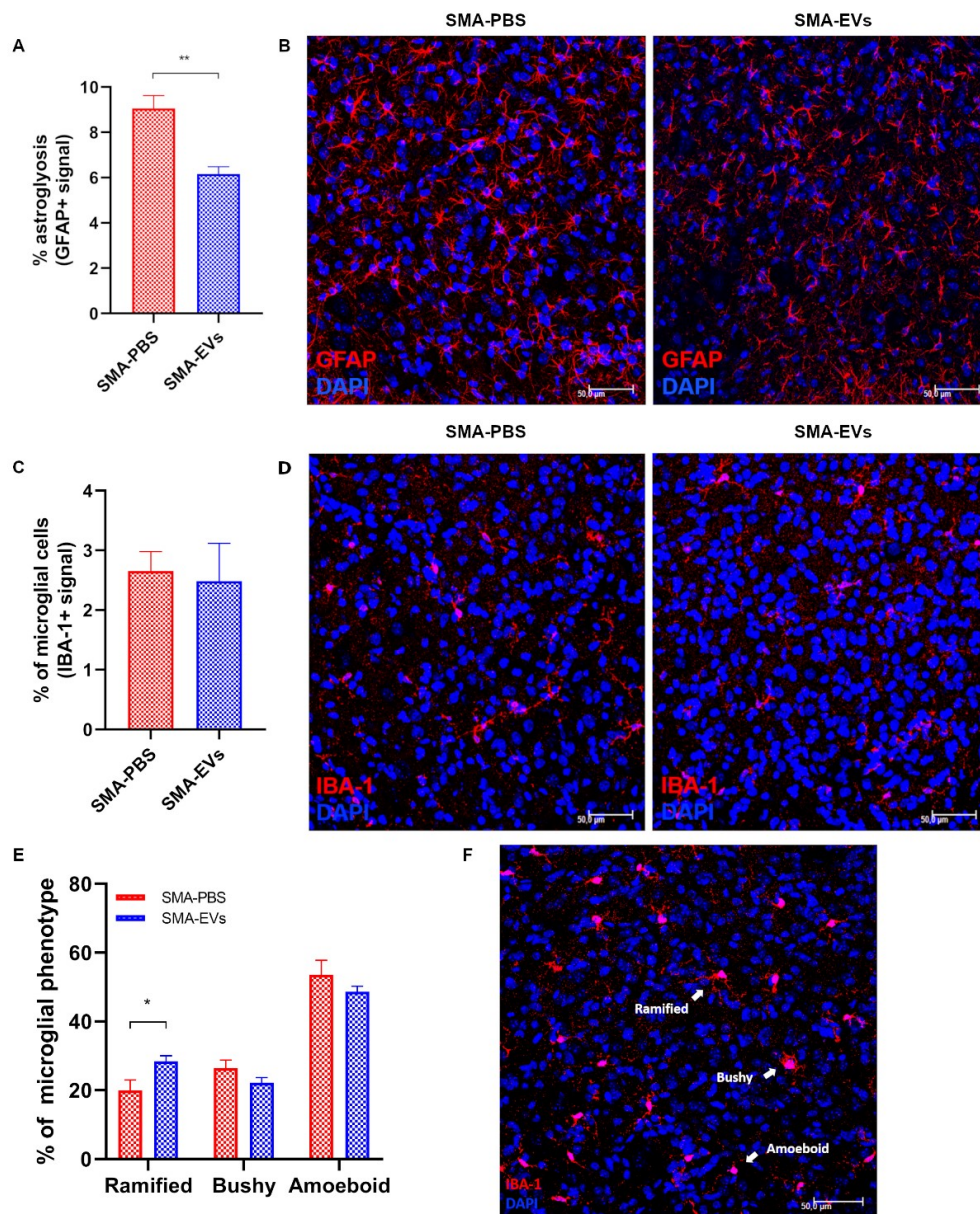
Figure 6.4. ASC-EVs treatment modulates the neuroinflammation in SMA mice. (A) The graph shows the quantification of the percentage of astrogliosis (GFAP+ signal) in the ventral horns of L1-L5 spinal cord both for SMA-PBS (red) and SMA-EVs group (blue) at P10. The ASC-EVs administration significantly decreased the percentage of GFAP-immunopositive profiles in SMA-EVs mice compared to SMA-PBS ones (unpaired Student t-test **p=0.0048). (B) Representative confocal images showing GFAP+ (red) cells in the ventral horns of PBS- and ASC-EVs treated (SMA-EVs) SMA mice. Cell nuclei are labelled

by DAPI staining (blue). Scale bar 50 μm. (C) The graph shows the quantification of the percentage of microglial cells (IBA-1+ signal) in the ventral horns of L1-L5 spinal cord both for SMA-PBS (red) and SMA-EVs group (blue) at P10. No differences in the percentage of IBA-1 immunopositive profile were observed between SMA-PBS and SMA-EVs mice (unpaired Student t-test p>0.05). (D) Representative confocal images showing IBA-1+ (red) cells in the ventral horns of PBS- (SMA-PBS) and ASC-EVs treated (SMA-EVs) SMA mice. Cell nuclei are labelled by DAPI staining (blue). Scale bar 50 μm. (E) The graph displays the microglial cell classification in ramified, bushy or amoeboid, based on their shape; the results are expressed as a percentage on the total number of IBA-1-positive cells both for SMA-PBS (red) and SMA-EVs (blue) group. A significant difference was observed regarding the ramified phenotype (typical of a steady-state microglial cells), that was higher for the SMA-EVs group compared to the SMA-PBS one (unpaired Student t-test *p=0.0464). (F) Representative confocal images showing IBA-1+ (red) microglial cells "ramified", "bushy" and "amoeboid" in the ventral horns of of spinal cord. Cell nuclei are labelled by DAPI staining (blue). Scale bar 50 μm.

6.3.5. The effects of ASC-EVs administration on skeletal muscles atrophy and NMJs maturation

Given the encouraging results observed with the motor test and in the lumbar spinal cord in SMA mice after ASC-EVs administration, we hypothesized that the central effects of our treatment could in turn positively affect also the muscular trophism and innervation at peripheral level.

Therefore, we firstly analysed the morphology of gastrocnemius and quadriceps fibers at P10 in terms of mean fibers area and Feret's max diameter. Regarding the gastrocnemius, the results did not show any differences both in the mean fibers area and in the Feret's max diameter between SMA-PBS (fibers area: 294.24±23.92 μm2; Feret's max diameter: 23.75±1.00 μm) and SMA-EVs groups (fibers area: 311.81±26.34 μm2; Feret's max diameter: 24.93±1.27 μm) (Figure 6.5A).

When considering the quadriceps muscle the morphological analysis revealed statistical differences between SMA-PBS (fibers area: 247.23±22.78 μm2; Feret's max diameter: 22.01±0.88 μm) and SMA-EVs groups (fibers area: 336.03±21.06 μm2; Feret's max diameter: 25.85±0.87 μm) both in the mean fibers area (*p=0.0188) and in the Feret's max diameter (*p=0.0127) (Figure 6.5B,C).

Secondly, we assessed the analysis on NMJs innervation and maturation by immunohistochemical reaction and we classified them as mono-innervated, multi-innervated or denervated by looking at the number of NFs contacting the endplate (Figure 6.5D). At P10 in the gastrocnemius muscle we observed an increase in the percentage of mono-innervated NMJs in SMA-EVs mice, compensated by a decrease

in the percentage of multi-innervated and denervated NMJs (SMA-EVs mono-inn.: 67.54±5.94%; multi-inn.: 15.44±8.69%; den.: 17±8.16%) compared to SMA-PBS controls (mono-inn.: 58.17±3.04%; multi-inn.: 18.1±6.32%; den.: 23.74±8.43%), even if no statistical differences were revealed (Figure 6.5E).

Similarly, in the quadriceps muscle we observed an increase in the percentage of mono-innervated NMJs in SMA-EVs mice (mono-inn.: 69.78±6%; multi-inn.: 13.94±7.90%; den.: 11.42±7.04%) compared to SMA-PBS controls (mono-inn.: 65.6±1.24%; multi-inn.: 20.99±5.99%; den.: 13.4±5.63%), with no statistical difference between the two groups (Figure 6.5F).

Overall, these results suggest that ICV ASC-EVs treatment can also partially counteract the muscular atrophy, in particular of early SMA affected muscles as quadriceps.
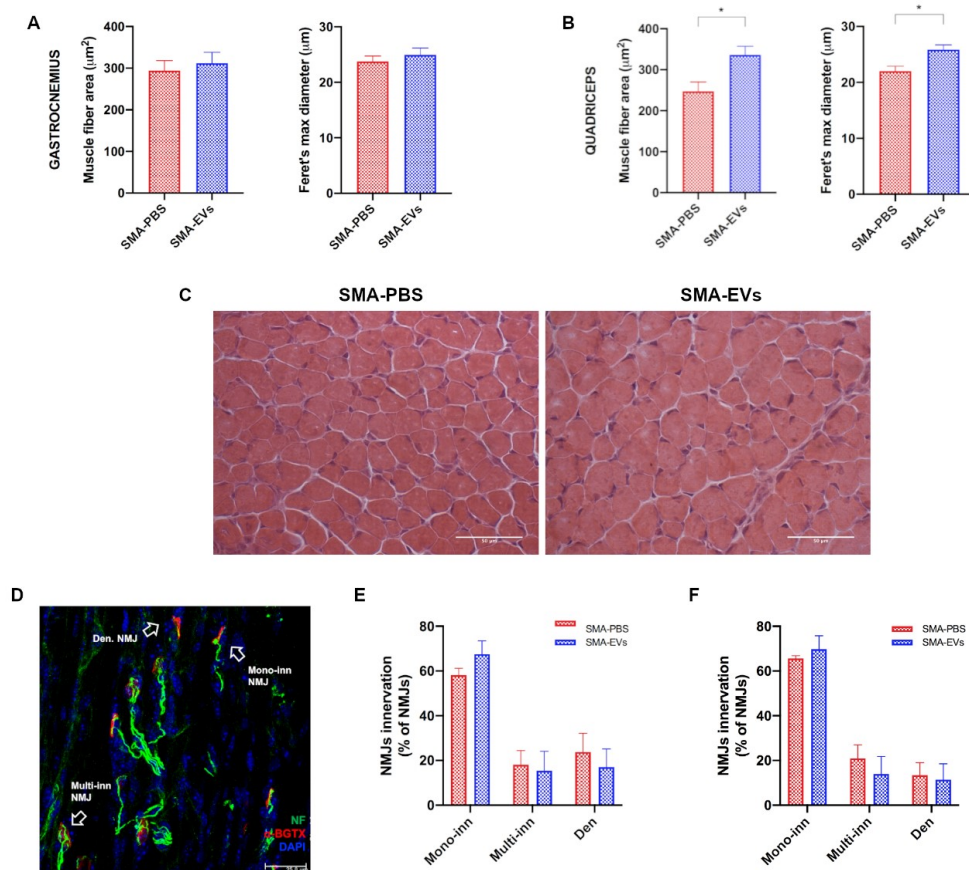
Figure 6.5. Effect of ASC-EVs treatment on skeletal muscles of SMA mice. The graphs show the quantitative analysis of the mean fiber area and Feret's max diameter of

gastrocnemius muscle (A) and quadriceps muscle (B) in SMA mice treated with PBS (SMA-PBS, red) or with ASC-EVs (SMA-EVs, blue). ASC-EVs treatment can partially rescue the atrophy of skeletal muscle fibers in SMA mice. (C) Hematoxylin/eosin (H/E) stained representative images showing SMA-PBS, SMA-EVs quadriceps fibers. Scale bar 50 μm. (D) Representative confocal image showing NMJs (αBGTX, red; NF-H, green, DAPI blue) in quadriceps muscle. The arrows show three different NMJs phenotypes: mono-innervated (a single NF is contacting the endplate), multi-innervated (several NFs are contacting the endplate) and denervated (no co-localization between NF-H and αBGTX). Scale bar 25 μm. The graphs show the quantification of the percentage of mono-innervated, multi-innervated and denervated NMJs in gastrocnemius muscle (E) and quadriceps muscle (F) in SMA mice treated with PBS (SMA-PBS, red) or with ASC-EVs (SMA-EVs, blue). ASC-EVs treatment can only partially limit the muscular atrophy and fibers denervation of SMA mice. Statistical difference between the groups are indicated (unpaired Student t-test *p<0.05).
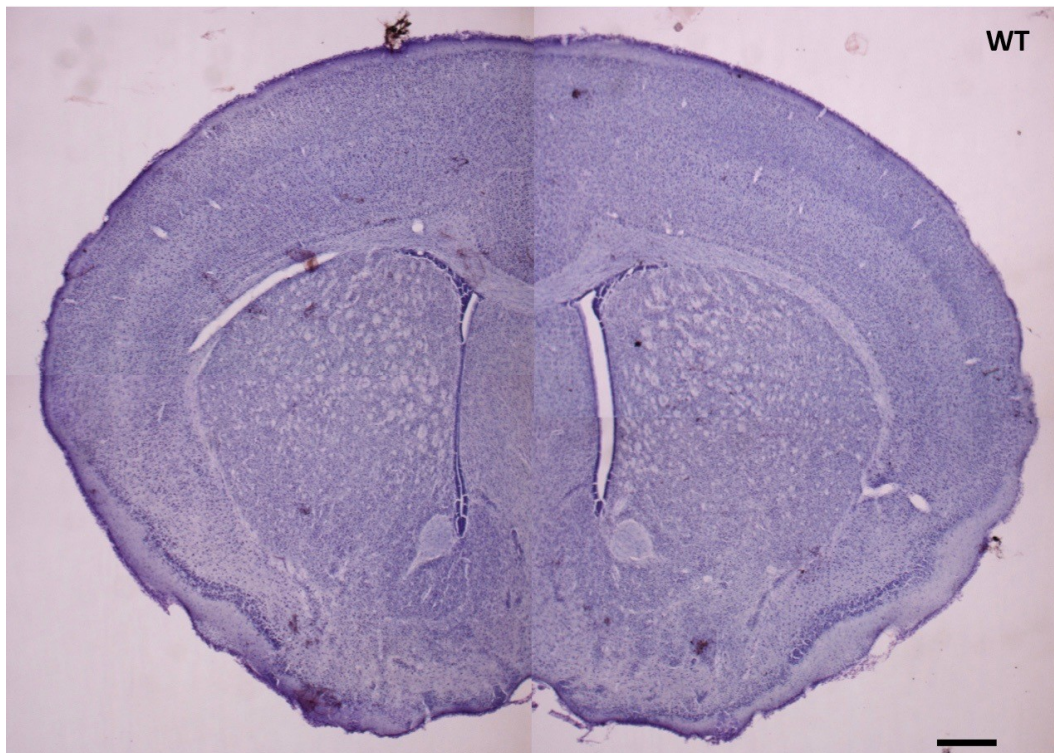
Suppl. Figure 6.1. Evaluation of the invasiveness of the surgery in a WT animal. The image shows a section of P10 WT brain after ICV administration of 2 μl of ASC-EVs at P3 and P6: the brain tissue did not show any lesions in the areas interested by the injections and ventricles appear intact . Scale bar 500 μm.

6.4. DISCUSSION

The pathogenesis of SMA is linked to the deficiency of the full-length SMN protein due to deletion or mutation on the *SMN1* gene. Several SMN-dependent therapeutic strategies have been exploited to restore the level of SMN by correcting the *SMN2* gene splicing as both Nusinersen (Spinraza, Biogen) and Risdiplam (Evrysdi, Roche) [233, 234] or by delivering a functional copy of *SMN1* gene into cells for its expression, as Onasemnogene abeparvovec (Zolgensma, Novartis) [235]. Besides the remarkable results obtained with these approved drugs, some issues and limitations remain, such as still unknown long-term effects, the possible treatment-related toxicity, and the high cost of these therapies. Furthermore, another relevant limitation concerning SMN-dependent therapies is that these strategies overlook other molecular and cellular pathways involved in SMA pathogenesis. A way to overcome this problem could be to implement SMN-dependent therapies with SMN-independent ones to exploit their synergistic effect [236].

In this regard, stem cells therapy has the advantage of counteracting pathogenic pathways modulating several molecular and cellular mechanisms, given their ability to reach damaged sites where they differentiate and stimulate tissue repair and regeneration. However, stem cells therapeutic effects were later demonstrated to be due to their indirect and paracrine effect obtained through the release of EVs, rather than to their engraftment in damaged tissues. Indeed, EVs are able to recapitulate the major advantages of their cells source transferring their cargo (protein, lipids, mRNAs and miRNAs) to nearby cells and avoiding all the risks associated to cells therapy as well [221, 237].

With all these characteristics, EVs are a promising tools for several neurodegenerative diseases [238]: as reported by Wang and colleagues MSC-derived EVs improved the cognitive impairments and reduced the hippocampal β-amyloid aggregation and neuronal loss in a murine model of Alzheimer disease [226]. Intravenous MSC-EVs administration improved motor deficits, reduced brain atrophy and modulated brain neuroinflammation in a progressive model of multiple sclerosis [227] and ameliorate chronic experimental autoimmune encephalomyelitis pathogenesis [212]. In previous studies we demonstrated that ASC-EVs exerted a neuroprotective effect in an *in vitro* model of ALS [196] as well as in the

SOD1(G93A) murine model: indeed, we showed that repeated administration of ASC-EVs improved motor performance, protected lumbar MNs, NMJs and skeletal muscles and decreased the glial cell activation in treated animals [208].

In this study, we investigated whether ASC-EVs could ameliorate the progression of another motor neuron disease such as SMA, different from ALS for its etiopathogenesis but with several pathological mechanisms in common. Therefore, we treated SMA pups with ICV injections at two different time points (at P3 and P6), and sacrificed the animals at P10 to evaluate the effect of the treatment.

From P2 to P10, mice underwent a battery of motor tests to follow the disease progression: we observed that the treatment with ASC-EVs improved the motor performance of treated animals; in particular, after the second injection, we could appreciate major effects in the righting reflex and negative geotaxis tests.

At the lumbar level of spinal cord, ASC-EVs treatment efficiently counteracted the MN degeneration compared to the vehicle-treated group, possibly explaining the observed improved motor performances of treated mice. From our previous proteomic study we know the ASC-EVs content, in which we did not detect the presence of the FL-SMN protein, thus supporting the idea that ASC-EVs act as an SMN-independent treatment in SMA mice. On the other side, ASC-EVs content comprises several proteins able to influence different cellular pathways, as for example the apoptotic process: in particular, the analysis pointed out the presence of proteins involved in the PI3K-Akt signalling pathway like the insulin-like growth factor (Igf1) [232]. Indeed through this signalling pathway, Igf1 protein, after binding with its receptor Igf1R, activates Akt, which prevents the apoptosis by inhibiting the pro-apoptotic protein Bad and stimulates cells proliferation [53, 239]. Furthermore, it has been already demonstrated that PI3K/Akt pathway is affected in SMA animals [240] and Akt phosphorylation was found to be reduced in SMA mice MNs primary cultures [241]. Therefore, we evaluated the expression of the apoptotic marker Cleaved Caspase-3, that is upregulated in *in vitro* [241] and *in vivo* [229] SMA models. What we observed was a significant reduction of Cleaved Caspase-3-positive lumbar MNs in SMA-EVs animals compared to control, confirming the neuroprotection efficacy of ASC-EVs treatment.

As reported in literature, neuroinflammation is observed in SMA and it can negatively influence the MNs survival through the release of pro-inflammatory

molecules [55]. Since SMN-deficient astrocytes showed alteration and impairments [63] as well as increased expression of GFAP [62], we analysed the activation of astrocytes in lumbar spinal cord and the outcomes showed a significant reduction of the percentage of astrogliosis in the animals treated with ASC-EVs. Also microglia seems involved in the pathogenesis of SMA [218]; Tarabal and colleagues confirmed the presence of activated microglia in the lumbar spinal cord in a rodent SMA model [66]. In our study we could not observed any differences in the total number of activated microglia between control and treated group. However, we performed a qualitative classification based on the shape of IBA-1 positive cells into ramified, bushy or amoeboid. We observed a significant increase of the ramified phenotype (typical of steady-state microglial cells [242, 243]) for the treated group compared to the control one. We also observed a decrease of the bushy and amoeboid phenotype (respectively representing an intermediate activation state with morphological transformations/de-ramification in response to neuroinflammated environment and a fully activated and phagocytic microglia), although not significant.

In addition, at the peripheral level we evaluated skeletal muscles that are known to show atrophy and denervation because of neurodegeneration [74] and the crosstalk between MNs and muscles. From a morphological point of view (muscle fiber area and Feret maximum diameter) only quadriceps muscle showed a significant difference between treated and control group, meaning a less severe level of muscle atrophy. This is in line with other studies that demonstrated that quadriceps is early affected during the disease progression [244] as a consequence of selective vulnerability of the MNs innervating proximal muscles [245]. Therefore, it could be possible that the ASC-EV neuroprotective effect on MNs through the delivery of molecules and proteins involved, among other mechanisms, in cell proliferation and angiogenesis (like Igf-1 and Rnase4 both identified in our previous proteomic analysis [232]) could consequently positively influence also the muscular trophism. In SMA mouse models (and in human patients as well) NMJs developmental impairment is also reported including several hallmarks such as immaturity, denervation and NF aggregation [68, 70]. In both the analysed muscles, ASC-EVs treatment could only partially impact on the maturation and innervation of NMJs with a mild increase of mature mono-innervated NMJs and a consequently reduction of immature multi-innervated and denervated NMJs.

All together, here we demonstrated that ASC-EVs induced beneficial effects in SMNΔ7 mice model of a severe SMA, recapitulating the neuroprotective effects of their parental mesenchymal stem cells. Indeed, we confirmed their ability to counteract the disease progression and in particular the degeneration of MNs and the neuroinflammation in the lumbar spinal cord. ASC-EVs seem to be promising candidates for SMA therapy, possibly in combination with SMN-dependent drugs to boost their effects, even if the mechanisms of action involved remain to be better clarified and further studies could explain the EVs homing and uptake ability of, after their administration. Indeed, it is crucial to understand EVs biodistribution in the target organs to be able to predict their therapeutic response. Perets and co-workers recently developed a system to track the migration and homing of EVs derived from bone marrow MSCs *in vivo* in different brain diseases (including stroke, autism, Parkinson's and Alzheimer's diseases). They found that the accumulation of MSC-EVs correlates with inflammatory signals in pathological brains [246, 247] and this could be strictly related to the markers expressed on their surface, such as integrins [248].

Finally, the ICV injections used in this study was chosen to directly deliver ASC-EVs to the central nervous system (CNS); indeed, the passage of the blood-brain barrier and the delivery of therapeutic agents efficiently to the CNS represents one of the main issues in the treatment of neurodegenerative diseases. However, the chosen administration route remains controversial due to its invasiveness. To overcome this problem, the intranasal administration route represents a very attractive strategy as it is a non-invasive way, it avoids the hepatic metabolism and the systemic absorption and a multidose therapeutic regimen, with the assistance of simple devices (drops, aerosol, spray), becomes more accessible even for patients with neurodegenerative disorders [249, 250]. Several studies reported beneficial effects of EVs injected via the i.n. route in different models, as in a mouse model of Alzheimer's disease [204], in the treatment of brain inflammatory diseases [251] and in our already published work using an *in vivo* ALS model [208]. Further efforts in this sense could be done also for SMA condition, in order to deliver ASC-EVs to the CNS in a tolerable and easy way, as well.

7. EXPERIMENT 2

EXTRACELLULAR VESICLES FROM ADIPOSE-DERIVED STEM CELLS: THERAPEUTIC EFFECT ON A MURINE MODEL OF AMYOTROPHIC LATERAL SCLEROSIS

PART 1

This material was part of the following published article: Bonafede R, Turano E, Scambi I, Busato A, Bontempi P, Virla F, Schiaffino L, Marzola P, Bonetti B, and Mariotti R. ASC-Exosomes Ameliorate the Disease Progression in SOD1(G93A) Murine Model Underlining Their Potential Therapeutic Use in Human ALS. Int J Mol Sci. 2020;21(10):3651.

NOTE: In this article authors referred to extracellular vesicles as "exosomes", since it was still not updated to the nomenclature proposed by ISEV. Therefore, it is possible to find "exosomes/EXO" in some of the graphs reported in this chapter; however, it has to be intended as "extracellular vesicles/EVs" instead.

7.1. *INTRODUCTION*

Amyotrophic lateral sclerosis (ALS) is a fatal neurodegenerative disease characterized by the progressive degeneration of motor neurons (MN) in the primary motor cortex, brainstem, and spinal cord [252]. The disease is sporadic in 90%–95% of cases, while it is familial in the remaining cases (with an autosomal dominant, autosomal recessive, or X-linked inheritance), and 20% of the familial ALS are due to mutations in the gene encoding for $Cu2+/Zn2+$ superoxide dismutase (SOD1) [253]. The mechanisms underlying the neurodegeneration of the disease are complex and still need to be clarified [115].

Transgenic mice overexpressing the human SOD1 gene with a reported G93A mutation (SOD1(G93A)) is the most widely used murine model to study ALS. This model exhibits the clinical signs and the pathological features of human patients, and provides an optimal *in vivo* model for investigating the pathogenesis of disease and for testing new therapeutic approaches [254].

Due to the complexity of the pathogenetic mechanisms involved in this neurodegenerative disorder, to date, there is no effective treatment available [255]. A promising therapeutic approach in neurodegenerative diseases is represented by stem cells that are able to self-renew, differentiate, and home to damage sites, which contribute to tissue repair and regeneration. Mesenchymal stem cells (MSC) are considered to be the best candidates and, among these, adipose-derived stem cells (ASCs) are accessible in large amounts and allow an easily autologous cell transplantation [256].

Several studies, including ours, have already demonstrated the beneficial effects of stem cells after their transplantation in murine models of ALS. The cells delayed the symptom progression of the disease, improved the function of the neuromuscular junction, and decreased the inflammatory response of the animals, indicating that they could promote neuroprotection [153, 257-259]. However, despite the encouraging results concerning stem cell treatment, migration, engraftment, and differentiation of stem cells at the sites of injury were reported rarely. For these reasons, the hypothesis that stem cells exert their therapeutic activity through secreted molecules and extracellular vesicles (EVs) is plausible [115, 260]. EVs are 50–150 nm in diameter and play important roles in intercellular communication, recapitulating the effect of stem cell transplantation by transferring biologically active molecules to recipient cells, altering their gene expression and behavior [154]. Several studies have suggested that EVs isolated from stem cells are involved in neuronal protection, nerve regeneration, neurological recovery, and synaptic plasticity. These vesicles can be exploited as a therapy instead of their derived parental cells, avoiding the limitations and risks associated with cell transplantation (reviewed in [261]).

In the present study, we tested the neuroprotective effect of EVs isolated from ASCs (ASC- EVs) in the SOD1(G93A) murine model of ALS. Moreover, we compared the effect of two different routes of EVs administration, i.e., intravenous (i.v.) and intranasal (i.n.). First, we administered ASC-EVs i.v., as previously done with ASCs [153]. Furthermore, we assessed the i.n. delivery, since it is easily transferable to ALS patients avoiding their hospitalization and represents a noninvasive way to deliver EVs directly to the CNS.

In this study, we demonstrated, for the first time, that repeated administration of EVs (i.v. or i.n.) improved the motor performance; protected the lumbar MN,

neuromuscular junction (NMJ), and muscle; and decreased the glial cells activation in treated SOD1(G93A) mice. These data contribute by providing additional knowledge for the promising use of ASC-EVs as a novel cell-free therapy in ALS.

7.2. *MATERIALS AND METHODS*

7.2.1. *ASCs Culture and ASC-EVs isolation and characterization*

Murine ASCs were obtained from inguinal adipose tissues of C57BL/6 mice as reported in paragraph 6.2.1. EVs were isolated from the culture medium of ASCs and characterized as reported in paragraph 6.2.2.

7.2.2. *Animals*

Experiments were performed using transgenic mice overexpressing human SOD1 carrying a Gly93-Ala mutation (SOD1(G93A)) (strain designation B6SJL–TgN[SOD1–G93A]1Gur, stock number 002726) and wild-type (WT) mice (B6SJL) obtained from Jackson Laboratories (Bar Harbor, ME, USA). Animals were maintained under controlled environmental conditions (temperature, humidity, 12 h/12 h light/dark cycle, water, and food ad libitum) and veterinarian assistance. The research complies with the commonly accepted "3Rs". The experiments were performed with the approval of the Animal Care and Use Committee of the University of Verona (CIRSAL), and the Italian Ministry of Health, in strict adherence to the European Communities Council (2010/63/EEC) directives (project identification code 710/2018-PR, approved 24/09/2018), minimizing the number of animals used and avoiding their suffering. Transgenic mice were identified by a polymerase chain reaction specific for human SOD1 gene (primers for SOD1 gene were forward (113) 5'-CATCAGCCCTAATCCATCTGA-3' and reverse (114) 5'-CGCGACTAACAATCAAAGTGA-3'; while for the housekeeping gene interleukin-2 receptor (IL-2R) the primers were forward (42) 5'-CTAGGCCACAGAATTGAAAGATCT-3'; reverse (43) 5'-GTAGGTGGAAATTCTAGCATCATCC-3').

7.2.3. *Motor tests*

The progression of the disease was monitored starting at 50 days by careful motor performance examination. In order to test the efficacy of the treatment, SOD1(G93A) mice were weekly evaluated blinded for body weight, neurological score test, paw grip endurance (PaGE) test, and rotarod test. The neurological score

test was evaluated as follows: 4, normal (no sign of motor dysfunction); 3, hind limb tremors were present when the mice were suspended by tail; 2, gait abnormalities; 1, dragging at least one hind limb; and 0, inability to right itself in 30 sec when the animal was placed in the supine position. The PaGE test was used to assess the grip strength of the animals. The test was performed by placing the animal on a metal grid and quickly turning it over. The score was measured by the length of time that the mouse was able to grip onto the grid. Each mouse was given up to two attempts to hold onto the inverted grid with an arbitrary cut-off time of 120 s. The rotarod test was used to assess the motor coordination of the animals. The mice were placed in a rotor tube (Acceler Rota-Rod 7650, Ugo Basile, Varese, Italy) at a constant speed of 16 rpm. The cut-off time was settled at 180 sec and three attempts were given to mice that failed the test, with a resting phase of 5 min. The longest latency time was registered.

The animals failed the PaGE test or the rotarod test when they were not able to reach the cut-off time. The onset was established when the mouse failed the PaGE or rotarod test. When the neurological score was equal to zero, the animals were sacrificed, and the survival time was recorded.

7.2.4. ASC-EVs administration

To test the therapeutic efficacy of ASC-EVs, a total of 56 SOD1(G93A) male mice were used in the experimental paradigm. The ASC-EVs were administered in SOD1(G93A) mice intravenously (10 treated mice and 10 control mice) or intranasally (10 treated mice and 10 control mice). The ASC-EVs administrations were performed from the onset of the clinical sign until the end stage, every 4 days. For each injection, the treated mice were injected with 1 μg of ASC-EVs, while the control mice received sterile PBS. The total amount of injected solution was 100 μL for an intravenous injection and 10 μL for i.n. administration.

A third group of animals was used. These SOD1(G93A) mice (8 treated mice and 8 control mice) received ASC-EVs intranasally every 4 days but, in this case, the administrations were performed from the onset of the clinical sign until 15 weeks of life. This time point represents an intermediate point between the onset and the end

stage of the disease, when the motor performance was statistically significant different between the control versus the treated groups.

7.2.5.   Lumbar spinal cord MNs stereological count

At the end stage (19 weeks) or at 15 weeks of life, the SOD1(G93A) mice (n = 5 per group) were deeply anesthetized and transcardially perfused with PBS 0.1 M followed by paraformaldehyde 4%. The spinal cord was dissected out and 2 h of post-fixation was performed. The lumbar tract was soaked in 30% sucrose, included in OCT and serially cut at 15 μm with cryostat apparatus. The sections were mounted on Surgipath® Apex™ Superior Adhesive Slides (3800080E, Leica Biosystems Italia, Milan, Italy).

For Nissl staining, the slides were air-dried, and then hydrated with H2O for 30 sec. The sections were stained with 0.2% cresyl violet solution for 8 min and gradually placed into increasing concentrations of ethanol, cleared with xylene, mounted with Entelan and covered with a cover glass. The MN of the ventral horn in the lumbar spinal cord tract (lateral and medial MN of L1-L5 segments) were counted blinded every 100 μm (every 6/7 slide) by the operator using a computer-assisted microscope (Olympus BX6 with Retiga 2000R camera, Center Valley, PA) with the Stereoinvestigator software (MicroBrightField, Williston, VT, USA) at 40× magnification. Cells with nucleoli on the plane of focus, size and shape typical of MN were counted. The values from the sections were computed for the summation, the mean number was then computed from the average number derived from each animal.

7.2.6.   Immunohistochemistry of lumbar spinal cord

To investigate the activation of astrocytes and microglia cells in the lumbar tract of the spinal cord, immunohistochemistry for light microscopy was performed. The sections were incubated for 10 min in 3% H2O2 to quench endogenous peroxidase and preincubated for 1 h in 5% of NGS in PBS and 1% BSA. The slides were incubated overnight in anti-mouse GFAP or Iba1 antibodies to recognize astrocytes and microglia, respectively, (GFAP 1:500, Z0334 Dako; Iba1 1:500 019–19741 Wako) in 1% NGS in PBS. The sections were washed and incubated for 1 h in

72

biotinylated goat anti-rabbit IgG (1:100, Vector Laboratories). The avidin-biotin peroxidase kit (ABC kit; Vector) and Novared kit (Vector) as signal revelation system was used. After mounting on slides, the sections were dehydrated through increasing grades of ethanol, cleared in xylene, and coverslipped with Entellan (Merck, Darmstadt, Germany). For the analysis, cells were counted every 100 μm for a total of 30 sections for each animal. The astrocytes and microglial cells (GFAP or CD11b labelled cells) of the lumbar tract (L1-L5) were visualized and counted using a computer-assisted microscope (Olympus BX6 with Retiga 2000R camera) with the Stereoinvestigator software (MicroBrightField, Williston, VT, USA).

7.2.7. *Immunohistochemistry of NMJs and Hematoxylin-eosin staining*

WT (n = 5) and SOD1(G93A) mice PBS- or EVs-treated (n = 5 per group) were deeply anesthetized and transcardially perfused with PBS 0.1 M followed by paraformaldehyde 4%. The hindlimb gastrocnemius muscle was dissected out, post-fixed for 2 h, soaked in 30% sucrose, included in OCT, and longitudinally cut at 20 μm with cryostat apparatus. The sections were mounted on Surgipath® Apex™ Superior Adhesive Slides (3800080E, Leica Biosystems Italia, Milan, Italy). The sections were washed with PBS Triton for 20 min and stained for postsynaptic acetylcholine receptors using CF543 conjugates α-bungarotoxin (αBTx, 1:500, Biotium, DBA Italia Srl, Milan, Italy) for 25 min at room temperature. The sections were washed and incubated for 1 h in 10% NDS and 0.3% Triton X-100 in PBS. Presynaptic motor terminals were labelled using anti-neurofilament H (NF-H; 1:100, Chemicon, Merck, Milan, Italia) overnight at 4 °C. After washing, the sections were incubated with species-specific Alexa Fluor 488 secondary antibody in 2% NDS in PBS (1:1000; Invitrogen, Thermo Fisher Scientific, Milan, Italy) for 1 h at room temperature. After washing, the sections were incubated with DAPI (1:1000; Santa Cruz Biotechnology, DBA Italia Srl, Milan, Italy) for 3 min at room temperature. Sections were washed and mounted with Dako Fluorescence Mounted Medium (Agilent, CA; USA) and dried prior to analysis.

For hematoxylin-eosin (HE) staining, the hindlimb gastrocnemius muscle was transversely cut at 20 μm with cryostat apparatus. The sections were stained with hematoxylin for 40 s, washed with tap water, immersed in eosin for 30 s, and washed

with tap water. The sections were dehydrated in ascending alcohol solutions, cleared with xylene, and coverslipped with Entellan (Merck, Darmstadt, Germany). The sections were visualized by optical microscopy (Olympus BX63; Olympus Life Science Solutions, Center Valley, PA). A total of 100 fibers were examined for each animal. The image J software was used to measure the area of gastrocnemius muscle fiber in each group.

7.2.8. *Statistical analysis*

Concerning the motor performance, two-way univariate analysis of variance (ANOVA) and Bonferroni post-hoc tests were performed to evaluate differences between the two animal groups. Data are expressed as mean ± standard error of the mean (SEM). Survival data of the animals were analyzed by Gehan–Breslow–Wilcoxon test. The stereological MN count, immunohistochemistry analysis of glial cells, and data of NMJ immunohistochemistry were analyzed using a two-tailed Student's test to evaluate differences between groups. Data are reported as mean ± SEM. For all statistical analysis and graphs, GraphPad Prism 5 Software was used, and significance was accepted at $p < 0.05$.
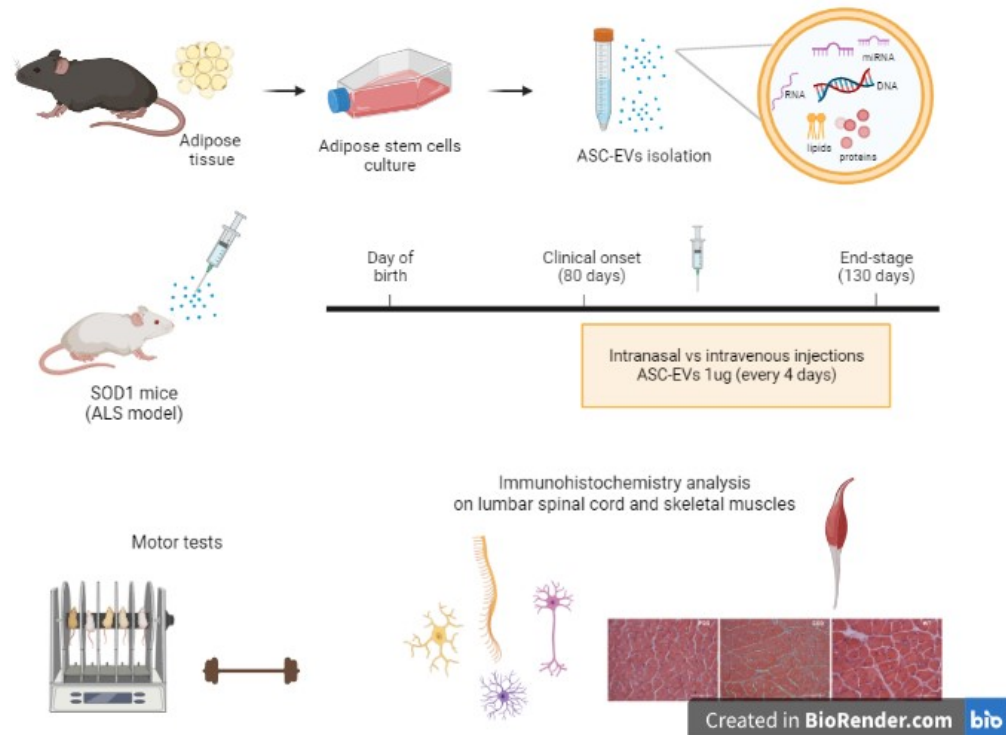
7.3. *RESULTS*

7.3.1. *Isolation and characterization of ASC-EVs*

Refer to paragraph 6.3.1.

7.3.2. *ASC-EVs administration improves motor performance of SOD1(G93A) mice*

In order to test the possible beneficial effect of ASC-EVs in SOD1(G93A) mice, specific motor tests were performed to evaluate the disease progression in EVs- and PBS-treated mice. Furthermore, we tested two different routes of EVs administration, i.v. and i.n. We administered ASC-EVs intravenously in order to compare their effect with that obtained with ASCs [153] and demonstrated that ASCs act through the release of extracellular vesicles. The i.v. administration of ASC-EVs was started from the clinical onset of pathology (defined in the Material and Method section) and determined an improvement of the grip strength of the mice, monitored with the paw grip endurance (PaGE) test (Figure 7.1A). The graph shows that the mice started to fail the test at the beginning of 10 weeks of life, which was the time when they started to receive ASC-EVs injections. The performance of the mice progressively declined during the following weeks, when the mice treated with EVs showed a better performance as compared with the PBS group, with a statistically significant difference at 11, 14, and 15 weeks of life ($p = 0.0494$, $p = 0.0308$, and $p = 0.0102$, respectively) (Figure 7.1A). The improvement of motor performance after administration of ASC-EVs was comparable with ASC treatment [153].

75
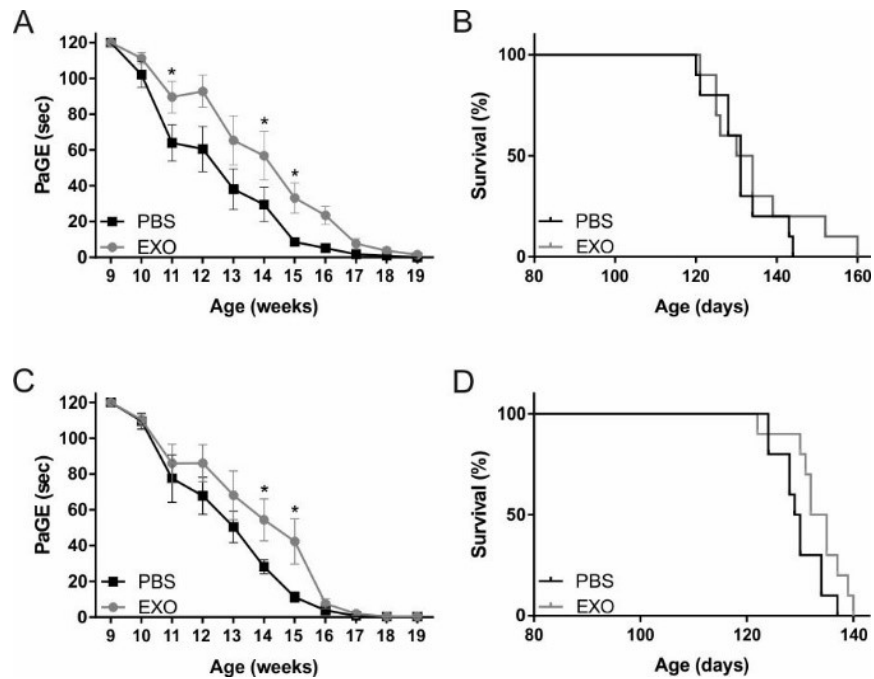
Figure 7.1. Motor performances and survival of human SOD1 gene with a G93A mutation (SOD1(G93A)) mice treated intravenously (A, B) and intranasally (C, D). (A, C) The graphs show the motor performances of SOD1(G93A) mice treated with PBS (black line) or with ASC-EVs (EXO, grey line). The paw grip endurance (PaGE) test shows a global improvement of motor performance of the EXO-treated mice as compared with the PBS group, with significant differences at 11, 14, and 15 weeks (* p = 0.0494, * p = 0.0308 and * p = 0.0102, respectively) with i.v. treatment (A) and significant differences at 14 and 15 weeks (* p = 0.0219 and * p = 0.0431, respectively) with i.n. treatment (C). Data are reported as mean ± SEM. (B, D) The graphs show the survival rate of SOD1(G93A) mice treated with PBS (black line) or with ASC-EVs (EXO, grey line). Graphs show the percentages of occurrence of the events.

In order to assess the effect of an alternative route of administration of ASC-EVs, the mice were treated intranasally from the beginning of 10 weeks of life (clinical onset of disease) until the end stage (19 weeks of life). An improvement of the grip strength of the EVs-treated mice was obtained as compared with the PBS group, with a statistically significant difference at 14 and 15 weeks of life (p = 0.0219 and p = 0.0431, respectively) (Figure 7.1C).

The PaGE test showed that the beneficial effect of ASC-EVs persists for six weeks and the motor performance progression was similar, irrespective of the route of delivery. In both cases, the beneficial effect observed in ASC-EVs treated mice disappeared around week 17 of life, whereas no differences were reported between EVs- and PBS-treated mice (Figure 7.1A,C).

Concerning the rotarod test, no significant difference was observed among the mice that received ASC-EVs or PBS with different routes of administration (i.v and i.n.). It is possible that we did not observe any differences since the motor coordination results evaluated by the rotarod test usually altered in the late phase of the disease, at the time when the ASC-EVs reduced their efficacy in terms of muscle strength (as shown by the PaGE test).

The graphs regarding the survival of the mice show that both treatments exerted no significant effect, although some EVs-treated mice had a prolonged lifespan as compared with the PBS-treated mice (Figure 7.1B,D).

7.3.3.   *ASC-EVs administration protects lumbar spinal cord MNs from neurodegeneration*

To evaluate the neuroprotective effect of ASC-EVs in the SOD1(G93A) mice, the stereological count of lumbar MN was performed on sections from L1–L5 metamers of the spinal cord. To evaluate the MN loss during the disease progression, a third group of untreated SOD1(G93A) mice was sacrificed at the preclinical stage of the disease (week seven). A significant loss of MN was observed in PBS-treated mice at 19 weeks of life, with both routes of treatment (with $p = 0.0026$ in the i.v. treatment and $p = 0.001$ in the i.n. treatment) showing a progressive loss of MN of about 50% due to the disease progression as compared with untreated mice sacrificed at seven weeks of life (Figure 7.2A and Figure 7.3A). The i.v. ASC-EVs administration determines a significant increase in surviving MN as compared with the PBS mice at the end-stage of the disease (19 weeks, $p = 0.0078$) (Figure 7.2A). This data indicates that ASC-EVs are able to protect MN from death, as shown in a representative image of PBS- and EVs-treated mice (Figure 7.2B).

The same neuroprotective effect was observed after i.n. administration of ASC-EVs at 19 weeks of life ($p = 0.034$, Figure 7.3A).

For the i.n. administration, an additional group of mice was used. This group received ASC-EVs from the onset of the clinical sign until week 15 of life, which was the time when the mice were sacrificed. Week 15 represents the time point when the difference in the motor performance of the mice was statistically significant for the PBS-treated versus EVs-treated groups (see Figure 7.1C).

77

At week 15, we did not observe a significant difference in the number of lumbar MN in the EVs-treated as compared with the PBS-treated mice. Moreover, the MN number of untreated mice, at the preclinical stage of the disease (week seven) as compared with PBS-treated mice, was not significantly decreased (Figure 7.3A). However, the PBS-treated mice sacrificed at week 15 of life showed 22.9% MN loss as compared with the untreated mice at the preclinical stage of the disease (week seven), whereas the EVs-treated mice showed a lower percentage of MN loss (10.4%) than the PBS-treated mice, which underlines the effect of EVs also at this stage of disease (Figure 7.3B). Finally, the progressive MN death during the disease course in the PBS-treated mice reached 56.2% after 19 weeks of life, whereas, in the EVs-treated mice, the percentage of MN death was 26.7% (p=0.034, Figure 7.3B,C). Altogether, these results indicate that ASC-EVs treatment is able to protect the lumbar spinal cord MN from degeneration.
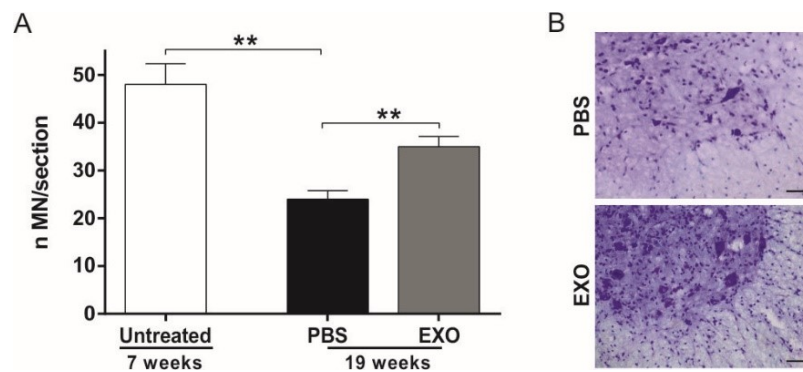
Figure 7.2. Effect of i.v. ASC-EVs treatment on motor neurons (MN) survival in SOD1(G93A) mice. (A) The graph shows the significant progressive loss of MN during the disease progression (as compared with untreated mice at week 7 and PBS-treated mice at the end stage of the disease, ** p = 0.0026). The i.v. treatment with ASC-EVs (EXO) significantly increases the MN survival in the lumbar section (L1–L5) of the spinal cord as compared with the PBS-treated group (** p = 0.0078). Data are shown as mean ± SEM; (B) Representative Nissl staining of the lumbar spinal cord MN of PBS- and ASC-EVs (EXO) treated mice. Note that a higher MN number in the mice that receive EVs treatment as compared with the PBS group. Magnification 20×, scale bar 50 μm.
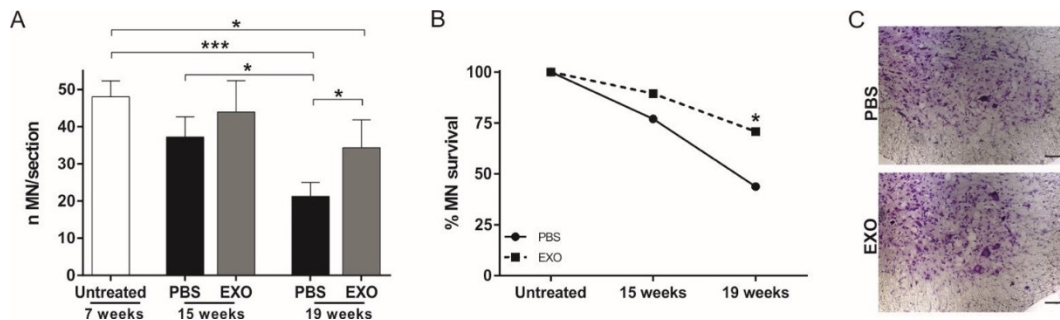
Figure 7.3. Effect of i.n. ASC-EVs treatment on MN survival in SOD1(G93A) mice. (A) The graph shows the significant progressive loss of MN during the disease progression. At the end stage of the disease (19 weeks of life), the i.n. treatment with ASC-EVs (EXO) significantly increases the MN survival in the lumbar section (L1–L5) of the spinal cord as compared with the PBS-treated group (* p = 0.034). Data are reported as mean ± SEM (untreated versus PBS 19 weeks *** p = 0.001; untreated versus EXO 19 weeks * p = 0.049; PBS 15 weeks versus PBS 19 weeks * p = 0.049); (B) The graph shows the percentage of MN during the disease progression. Note, the ability of ASC-EVs to protect MN from death. Data are reported as the percentage of surviving MN (* p = 0.034); (C) Representative Nissl staining of the lumbar spinal cord MN of the PBS and ASC-EVs (EXO) treated mice. Note, a higher MN number in mice that receive EVs treatment as compared with the PBS group. Magnification 20×, scale bar 50 μm.

7.3.4. *ASC-EVs administration preserves neuromuscular junctions functionality and skeletal muscle fiber morphology*

As reported above, the mice treated with ASC-EVs showed a significant improvement in motor performance as compared with the PBS-treated mice at 14 and 15 weeks of life. Since this data were not supported by a higher significant MN survival of EVs-treated animals at these intermediate time points, we analyzed the NMJ and the skeletal muscle fibers in EVs- and PBS-treated mice at 15 weeks of life. The NMJ with complete or partial colocalization of presynaptic NF-H and the postsynaptic α-bungarotoxin (αBTx) were defined as innervated, while the total loss of colocalization indicated the degeneration of the NMJ (Figure 7.4A). At 15 weeks of life, a significant difference (p < 0.0001) of innervated NMJ was reported in wild-type (WT) mice as compared with the SOD1(G93A) PBS- or EVs-treated mice, indicating the hindlimb NMJ degeneration of the SOD1(G93A) mouse model. Interestingly, the SOD1(G93A) mice treated with ASC-EVs showed a higher innervated NMJ number as compared with PBS-treated mice (p = 0.0006) (Figure 7.4B). This result indicates that ASC-EVs treatment preserves the NMJ, slowing down the degeneration of MN and, consequently, the detachment of the axons from the muscle.

79

In addition to the NMJ, we analyzed the morphological changes of the gastrocnemius muscle (Figure 7.4C). Compared to the WT mice, hematoxylin-eosin (HE) staining of PBS-treated mice showed enhanced endomysial space, degenerated fibers with reduced diameter, and a significantly decreased muscular fiber area (Figure 7.4C,D, p = 0.0034). Interestingly, the ASC-EVs treatment attenuated the degeneration of fibers with an average muscular fiber area significantly increased as compared with the PBS group (p = 0.0410), and without significant differences with the WT mice (Figure 7.4C,D).
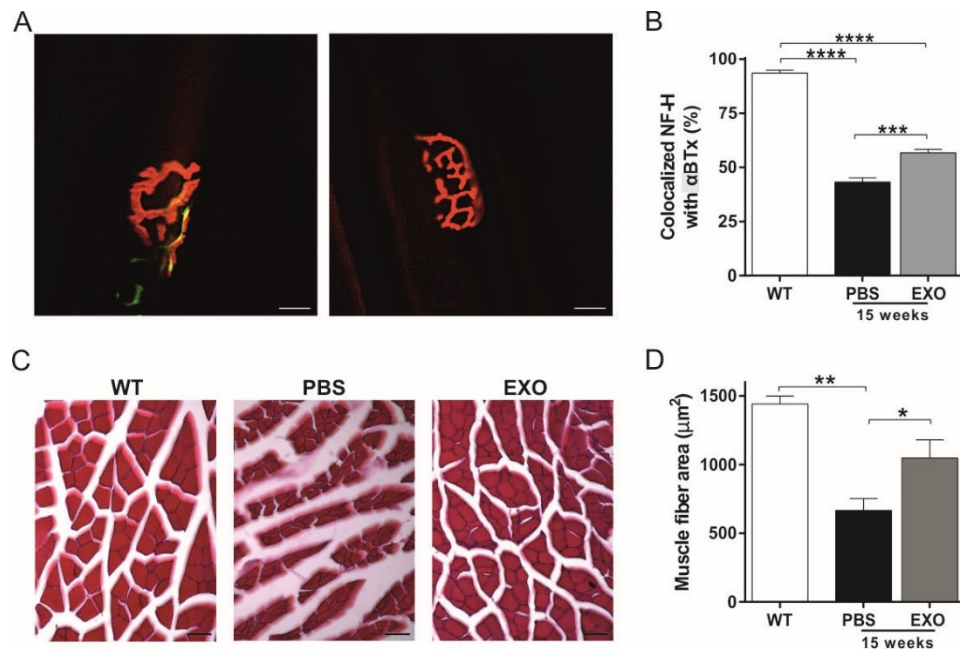
Figure 7.4. Effect of i.n. administration of ASC-EVs on skeletal muscle of SOD1(G93A) mice. (A) Representative images of the correct architecture of the neuromuscular junction (NMJ), in which a colocalization of presynaptic NF-H (green) and αBTx (red) is showed (left). On the right is reported the degeneration of the NMJ, in which non colocalization between NF-H (green) and αBTx (red) is reported, due to presynaptic loss of neurofilament that leave to denervation. Magnification 40×, scale bar 25 μm; (B) The graph shows a significant decrease in colocalization of NF-H and αBTx in SOD1(G93A) mice at 15 weeks of life as compared with the wild-type (WT) mice (**** p < 0.0001 comparing WT mice with both PBS- or EVs-treated SOD1(G93A) mice). Note that ASC-EVs treated mice (EXO) showed a significant increase in NMJ with presynaptic terminals colocalized with αBTx as compared with the PBS group (*** p = 0.0006). Data are shown as mean ± SEM; (C) Representative images of hematoxylin-eosin (HE) staining in the WT mice and the SOD1(G93A) mice treated with PBS or ASC-EVs (EXO) at 15 weeks of life. Note, the reduced degeneration of the skeletal muscle in ASC-EVs treated mice. Magnification 20×, scale bar 50 μm; (D) The graph shows the quantitative analysis of the average fiber area in the groups of mice. A significant decrease in fiber area in the PBS-treated SOD1(G93A) mice at 15 weeks of life was detected as compared with the WT mice (** p = 0.0034). Note that ASC-EVs treated mice (EXO) showed a significant increase in fiber area as compared with the PBS group (* p = 0.0410). Data are shown as mean ± SEM.

7.3.5. Effect of ASC-EVs administration on glial cells

Analysis of glial cells was performed on the lumbar section of the spinal cord of EVs- and PBS-treated mice. We found a progressive increase in astrocyte activation during the disease course (comparing mice at the preclinical stage of the disease to the PBS-treated mice and at 15 and 19 weeks), which reached a significant difference at 19 weeks for both i.v. and i.n. treatments ($p = 0.05$ and $p = 0.006$, respectively, Figure 7.5A,B).

In mice treated intravenously, a tendency to downregulate the GFAP-reactive astrocyte in EVs-treated SOD1(G93A) mice was evident, although the difference with PBS-treated mice was not significant (Figure 7.5A). Interestingly, i.n. EVs-treated mice showed a trend of astrocytosis reduction as compared with the PBS group at week 15. This reduction became significantly different at week 19 ($p = 0.03$, Figure 7.5B,C), demonstrating the effect of i.n. EVs treatment on reducing astrocyte activation at the late stage of ALS disease (Figure 7.5C).

Concerning the number of microglial cells, no difference was observed in the lumbar spinal cord of EVs- and PBS-treated mice, at any time points.
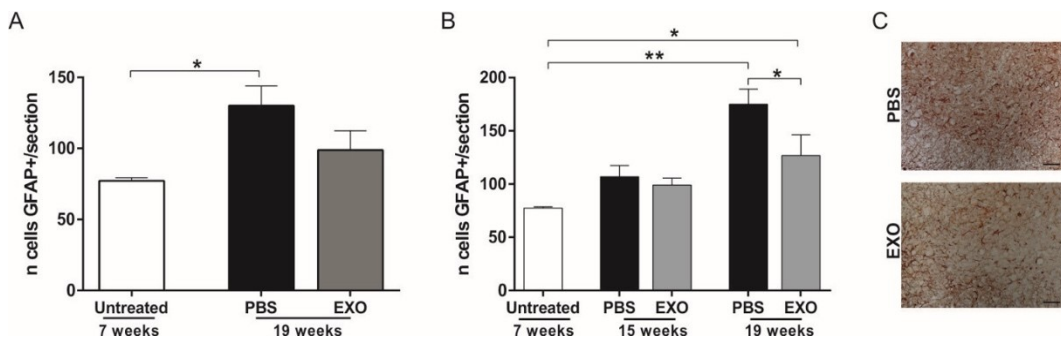
Figure 7.5. Effect of i.v. and i.n. ASC-EVs treatment on astrocytosis in SOD1(G93A) mice. (A) The graph shows the number of GFAP+ cells in the lumbar section (L1–L5) of the spinal cord, comparing untreated with i.v. treated SOD1(G93A) mice. Note, the progressive increase of astrocytosis during the disease progression, and a trend in ASC-EVs (EXO) treatment to decrease astrocyte activation (* $p = 0.05$); (B) The graph shows the number of GFAP+ cells in the lumbar section (L1–L5) of the spinal cord, comparing untreated with i.n. treated SOD1(G93A) mice sacrificed at 15 and 19 weeks of life. At the end stage of the disease, note, a significant difference in decreasing astrocyte activation in ASC-EVs treated mice (EXO) as compared with the PBS group (* $p = 0.03$ ** $p = 0.006$); (C) Representative staining of the lumbar spinal cord of the PBS and ASC-EVs (EXO) treated mice. Note, a lower number of GFAP+ cells in the ASC-EVs treated mice as compared with the PBS-treated mice. Magnification 20×, scale bar 50 μm.

7.4. *DISCUSSION*

The development of new therapies for ALS is crucial to improve the quality of life of patients and extend their survival. Many studies have been conducted in order to develop pharmacological/cell therapies [262-264], but the challenge is still open. It is known that ALS is a multifactorial disease, since different pathogenetic mechanisms are involved in MNs degeneration [115]. All pharmacological treatments tested for ALS have usually been focused on single or few altered cellular pathways, and all clinical trials have failed to show any significant results [255]. The stem cell therapy has the advantage that it can act via multiple mechanisms, simultaneously counteracting different pathogenetic pathways and providing a more effective treatment for ALS patients [115]. The therapeutic efficacy of stem cells of different origins has been evaluated in experimental models of ALS, with encouraging results [153, 257-259].

It has emerged that the beneficial function of MSC could be mediated by the release of extracellular vesicles, as EVs, rather than their engraftment and differentiation [237]. A therapy based on the use of EVs would prevent all the risk associated with cells transplantation and would require administering only the fraction responsible for the beneficial effect of stem cells [265]. The EVs transfer functional molecules (in particular proteins, mRNA, and miRNA) to other cells, modulating their activity, and maintaining the integrity of their cargos from proteases and nucleases degradation. Moreover, among the extracellular vesicles, EVs are the only ones that can cross the blood-brain barrier thanks to their small dimension, a feature that renders these vesicles more interesting as a therapeutic approach in several neurodegenerative diseases [261]. With evidence that extracellular vesicles recapitulate the effect of stem cells, several works have tested their therapeutic efficacy in neurodegenerative disease models. The EVs reduce the pathological accumulation of the β-amyloid peptide in an *in vitro* model of Alzheimer's disease stimulating their proteolysis [184], protecting dopaminergic neurons from apoptosis after oxidative stress [194], and showing a neuroprotective effect in an *in vitro* model of ALS [196]. In this regard, the proteomic analysis of EVs, correlating the protein content to the anti-apoptotic effect, was useful to understand the mechanisms by which ASC-EVs exert their beneficial effect [232]. In the *in vivo* model of the disease, EVs are able to promote neural plasticity

and functional recovery after stroke in rats via the transfer of miRNA-133b [266], induce neurite outgrowth and improve neuroregeneration after traumatic brain injury in C57BL6 mice [267], and ameliorate chronic experimental autoimmune encephalomyelitis [212]. Moreover, EVs isolated from a different source of MSC alleviate inflammation and prevent cognitive and memory impairments after status epilepticus [268], alleviate neuroinflammation and reduce β-amyloid accumulation in a mouse model of Alzheimer's disease [185], and suppress inflammatory response enhancing the regeneration of mice spinal cord after injury [269].

In the present study, we investigated whether ASC-EVs exert a protective effect *in vivo* in transgenic SOD1(G93A) mice of ALS. We decided to administer ASC-EVs every four days, since this experimental paradigm presents an optimal compromise between frequency and route of administration, above all for chronic intravenous administration in which more frequent injections could be harmful to the mice and not allow the regeneration of epithelial vein tissue. We demonstrated that repeated i.v. or i.n. administrations of ASC-EVs improved the motor performance from week 11 to week 15 of life as compared with the controls (PBS-treated mice). From week 17 of life, the beneficial effect observed in ASC-EVs treated mice disappeared and no differences in motor performance were observed as compared with the PBS group. This data indicates that, at the late phase of the disease, when the interaction between MN and NMJ is highly compromised [270], the dose of ASC-EVs used was inefficient, underling that this treatment could be dose-dependent, as already demonstrated in other experimental studies [271-273].

As reported in the literature, in SOD1(G93A) mice, there is a progressive lumbar MN degeneration during the progression of the pathology [274]. This result is also confirmed by our study, which showe 22.9% MN loss at week 15 and 56.2% MN loss at week 19. Interestingly, we demonstrated that ASC-EVs treatment was able to protect lumbar MN degeneration during the disease progression, showing a progressively increased percentage of MN survival between 15 and 19 weeks of life, being significant at the last time point. In addition to survival, our data suggest that ASC-EVs improves the function of MN, as indicated by a significantly higher number of preserved NMJ and skeletal muscle fibers at 15 weeks of life.

Neuroinflammation, determined by astrogliosis, microgliosis, and infiltration of immune cells, is a common characteristic of ALS and other neurodegenerative

83

diseases. In particular, through the release of soluble factors, astrocytes exert a potent toxic property on MN, contributing to their neurodegeneration [275, 276]. It has been reported that EVs derived from stem cells suppress the activation of neurotoxic astrocytes after traumatic spinal cord injury, ischemia, and epilepsy [269, 277, 278]. In our study, we demonstrate that ASC-EVs are able to decrease astrocytes activation but not the total number of activated microglial cells.

The route of delivery of ASC-EVs could also have profound relevance. In this study, we tested the intranasal administration, which represented a noninvasive procedure that allowed repetitive dispensation and an efficient delivery of the vesicles to the brain. These characteristics make the i.n. administration an efficient approach to deliver EVs to the regions involved in this neurological disease, since earlier studies have shown that the systemic administration of EVs determined an accumulation in the spleen and the liver [279, 280]. Moreover, these features would allow an easy and more effective transferability of ASC-EVs treatment for patients with neurological diseases.

7.5. *INTRODUCTION*

When considering EVs treatment, the identification of the route and frequency of administration, the dose and the time of administration to obtain therapeutic effects in preclinical models, appears to be one of the critical problems which is then also translated into humans [281].

Based on the promising results of this first part of the study that demonstrated a neuroprotective role of ASC-EVs administered both via i.v. and i.n. injections in SOD1(G93A) mice, we focus on the second route of administration being less invasive and equally efficient. However, despite the good results of treated animals regarding the disease progression and the histological analysis, no differences were observed concerning the survival of ASC-EVs treated SOD1(G93A) mice.

For these reasons, the aim of this second part of the study was to optimize the intranasal experimental paradigm of ASC-EVs treatment in the SOD1(G93A) model comparing the previous results with a higher dose treatment (3 μg) administered every four days till end-stage. In light of this first experiment and of the previous results, we identified a time window in which ASC-EVs seem to have a more powerful therapeutic effect (3rd-4th week after onset) and a second experimental plan was set up with a lower ASC-EVs dose (1 μg) tested with daily i.n. injections, this time.

The obtained results highlighted that a higher dose was not toxic for animals and could slow down the disease progression and preserve MNs degeneration as the corresponding low-dose. However, also in this case the treatment didn't affect the survival of animals. Regarding the ASC-EVs daily injections with 1 μg, it appeared to be more effective in the week immediately after the clinical onset at the beginning of the treatment. This evaluation could be useful in determining the correct ASC-EVs dose and therapeutic regimen.

7.6. MATERIALS AND METHODS

7.6.1. ASCs Culture and ASC-EVs isolation and characterization

Murine ASCs were obtained from inguinal adipose tissues of C57BL/6 mice as reported in paragraph 6.2.1. EVs were isolated from the culture medium of ASCs and characterized as reported in paragraph 6.2.2.

7.6.2. Animals

Experiments were performed using transgenic mice overexpressing human SOD1 carrying a Gly93-Ala mutation (SOD1(G93A)) (strain designation B6SJL–TgN[SOD1–G93A]1Gur, stock number 002726) and wild-type (WT) mice (B6SJL) obtained from Jackson Laboratories (Bar Harbor, ME, USA) as reported in paragraph 7.2.2.

7.6.3. Motor test

The progression of the disease was monitored as reported in paragragh 7.2.3.

7.6.4. ASC-EVs administration

To test the therapeutic efficacy of ASC-EVs, a total of 22 SOD1(G93A) male mice were used in the experimental paradigm. In the first experimental plan, ASC-EVs were administered in SOD1(G93A) mice intranasally (7 treated mice and 5 control mice) from the onset of the clinical sign until the end stage, every 4 days. For each injection, the treated mice were injected with 3 μg of ASC-EVs, while the control mice received sterile PBS. The total amount of injected solution was 10 μL for intranasal administration.

In the second experimental plan, SOD1(G93A) mice (6 treated mice and 4 control mice) received 1 μg of ASC-EVs intranasally every day from the onset of the clinical sign until 15 weeks of life. This time point represents an intermediate point between the onset and the end stage of the disease, when the motor performance was statistically significant different between the control versus the treated groups.

7.6.5. *Lumbar spinal cord MNs stereological count*

At the end stage (19 weeks) or at 15 weeks of life, the SOD1(G93A) mice were deeply anesthetized and transcardially perfused with PBS 0.1 M followed by paraformaldehyde 4%. The spinal cord was dissected out as reported in paragraph 7.2.5. For Nissl staining, refer to paragraph 7.2.5.

7.6.6. *Statistical analysis*

For all statistical analysis refer to paragraph 7.2.8.
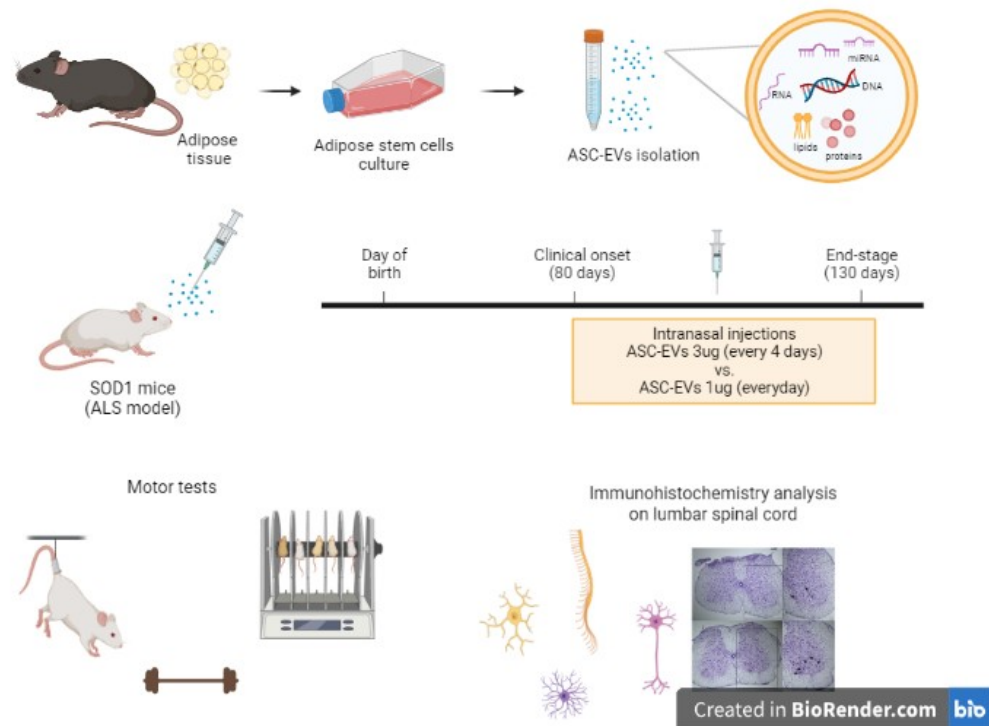
7.7. RESULTS

7.7.1. Isolation and characterization of ASC-EVs

Refer to paragraph 6.3.1.

7.7.2. ASC-EVs administration improves motor performance of SOD1(G93A) mice

To evaluate the disease progression in ASC-EVs- and PBS-treated mice, specific motor tests were performed. The treatment determined an improvement of the grip strength of mice, monitored with the paw grip endurance (PaGE) test for the treated group animals (ASC-EVs 3 µg) when compared to the control group with a significant difference at the 3rd week (***p=0.0009) and at the 4th week from the clinical onset (*p=0.0203) (Figure 7.6A). However, the treatment didn't affect the survival of the mice (Figure 7.6B).

In light of these results, we identified the time window in which ASC-EVs exerted the greater therapeutic effect (3rd-4th week after clinical onset) and we tested the second ASC-EVs treatment (1 µg, daily injections): in this case we observed a significant amelioration of the motor performances after the 1st week of treatment with ASC-EVs (*p=0.0316) (Figure 7.6C).

Concerning the rotarod test, no significant differences were observed between the mice that received ASC-EVs or PBS with both therapeutic regimen (3 µg and 1 µg) (Data not shown).
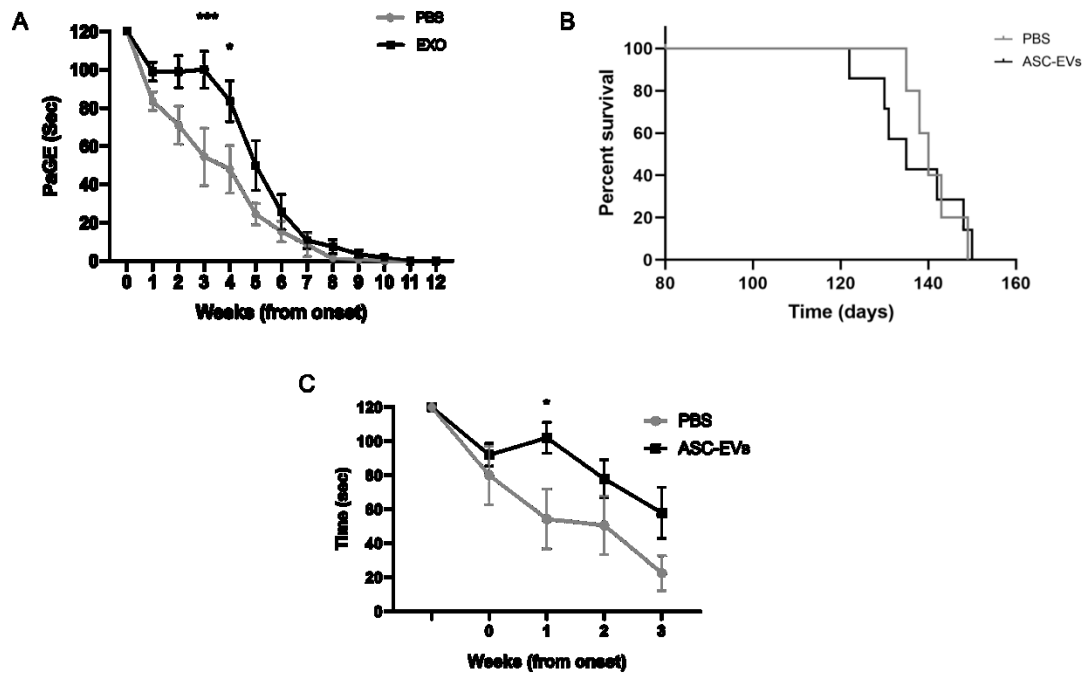
Figure 7.6. Motor performances and survival of SOD1(G93A) mice treated with ASC-EVs 3 μg every four days (A, B). (A) The paw grip endurance (PaGE) test shows a global improvement of motor performance of the ASC-EVs-treated mice as compared with the PBS group, with significant differences at 3 and 4 weeks after clinical onset (***p=0.0009, *p=0.0203 respectively). (B) The graph shows the survival rate of SOD1(G93A) mice treated with PBS or with ASC-EVs: no significant differences between group were observed. (C) Motor performances of SOD1(G93A) mice treated with ASC-EVs 1 μg every day. Significant difference was observed 1 week after clinical onset (*p=0.0316). Data are reported as mean ± SEM.

7.7.3. *ASC-EVs administration protects lumbar spinal cord MNs from neurodegeneration*

In order to evaluate the neuroprotective effect of ASC-EVs (3 μg, every four days) in the central nervous system we assessed a stereological MNs count in the ventral horns of L1-L5 spinal cord sections at the end stage of the disease. The results of the analysis showed a significant reduced loss of lumbar MNs in the ASC-EVs treated SOD1(G93A) mice compared to the control littermates (**p=0.0023) (Figure 7.7A,B).

The same analysis was performed on the second experimental plan (ASC-EVs 1 μg, daily injections): the evaluation of the neuroprotection of ASC-EVs treatment at the time of sacrifice (3rd week after clinical onset) didn't showed any statistical differences compared to the control group (Figure 7.7C). This could be due to the fact that the sacrifice is performed at an early phase of the disease and the

neurodegeneration of lumbar MNs could be still not clearly evident in not treated animals as well.
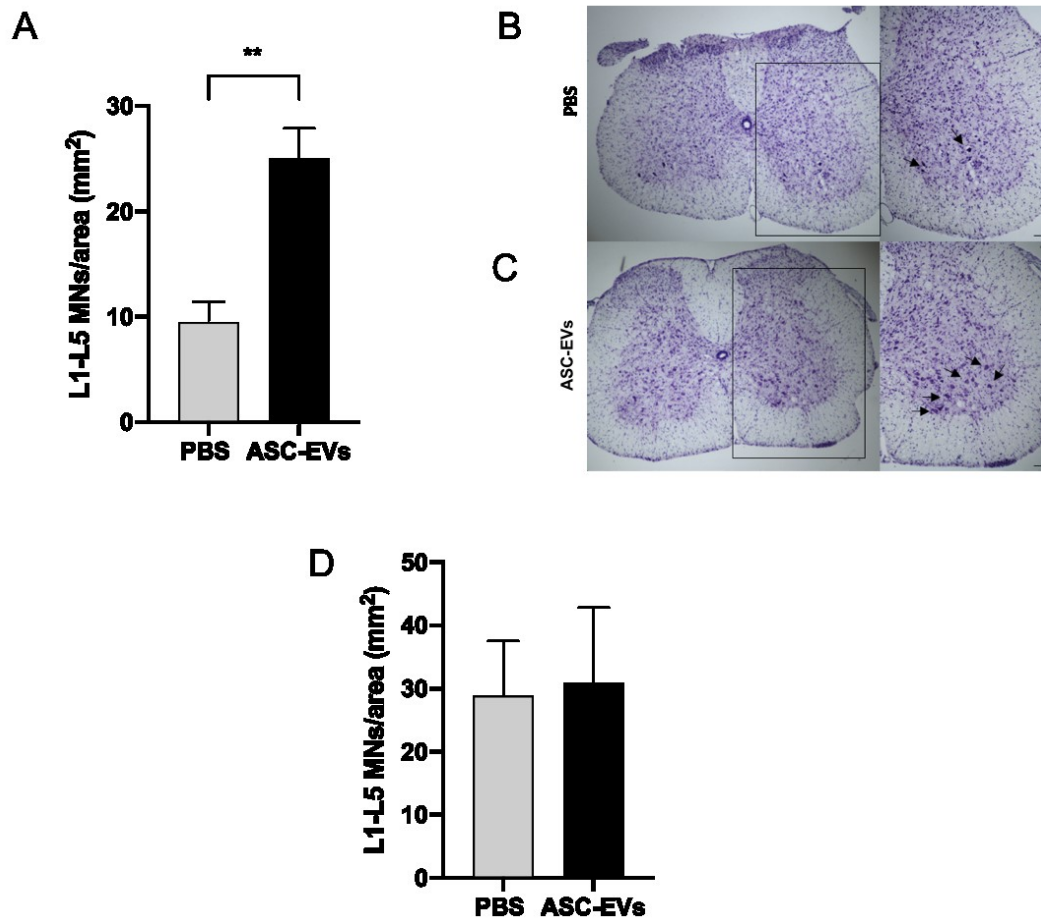
Figure 7.7. Effect of ASC-EVs treatment on lumbar MNs survival in SOD1(G93A) mice. (A) The graph shows a significantly higher motor neuron survival for the ASC-EVs group (3 µg, every four days) compared to the PBS group (**p=0.0023). Representative Nissl staining of lumbar spinal cord MN of PBS (B) and ASC-EVs (C) treated mice. (D) The second treatment with ASC-EVs (1 µg, daily injections) didn't exert any statistical difference compared to control. Data are shown as mean±SEM; Magnification 20×, scale bar 50 µm.

7.8. *DISCUSSION*

For novel therapeutics and EVs-based treatment the route of administration is important since it directly precedes how they interact with the body. Important evaluation has to be done also considering the optimal dose, time window and timing of administration for EV-based therapeutics [281].

Zhang and colleagues demonstrated that MSC-derived EVs significantly improve functional recovery in rats after TBI [282]. However, determining the dose- and time-dependent efficacy of EVs for the treatment of this condition was crucial. Indeed, authors demonstrated that the EVs treatment data starting at 1 day post-TBI provided a significantly greater improvement in functional and histological outcomes than EVs treatments at 4 or 7 days after injury. Moreover, their data indicates that a higher dose of EVs does not provide additional beneficial effects compared with a lower one. These results strengthen the idea that EVs can have a wide range of effective doses and therapeutic windows depending on the definition of the pathological conditions.

In this part of the study, we tried to optimize the intranasal delivery route of ASC-EVs in SOD(G93A) mice model based on our previous results. For this purpose, we compared 3 μg injections every 4 days with 1 μg injections daily. We observed that, in particular regarding the motor performances, the higher dose seems to better counteract the disease progression in a more advanced phase of the disease compared to the lower and daily dose that significantly improved the motor test in a shorter time window closer to the clinical onset. However, the higher dose was insufficient to affect the survival of treated animals.

This could be useful to establish a work interval for the each ASC-EVs doses and a possibility could be to use not only a single dose but possibly including a mixed multi-dose regimen, for example taking in consideration a lower concentration with a higher frequency in the first phase of disease progression and a higher and chronic dose subsequently. This, in view of a treatment for a neurodegenerative disease, it appears to be potentially a good strategy. Subsequent studies will allow the use of mixed regimens of times and doses to try to obtain evident improvements and, hopefully, an increase in survival of SOD1(G93A) mice.

8. EXPERIMENT 3

EXTRACELLULAR VESICLES FROM ADIPOSE-DERIVED STEM CELLS DIFFUSED THROUGH AN EPITHELIUM: NEUROPROTECTIVE EFFECT ON *IN VITRO* MODELS OF NEURODEGENERATION

8.1. *INTRODUCTION*

Neurodegenerative and inflammatory diseases of the central nervous system (CNS) have a strong social and economic impact all over the world. Currently, there is no cure for the vast majority of these diseases. The available treatments aim to slow down the progression of neurodegenerative diseases, relieve pain and improve symptoms. Therefore, the treatment of these diseases represents one of the main medical and social challenges in our society.

However, the BBB is one of the obstacles to overcome in the development of therapies for CNS diseases, making difficult the clinical use of many therapeutic agents. Currently, the principal therapeutic routes are by intracranial or intravenous injections, which can be quite invasive; thus, it became necessary to evaluate less invasive approaches for translational clinical applications. The intranasal (i.n.) route is an attractive strategy that has gained much interest as a non-invasive administration route to deliver therapeutic agents to the brain via neural pathways [283, 284]. In the context of cellular therapies, beneficial effects of injecting MSCs and their vesicular counterpart via the i.n. route have been reported [285, 286]: Losurdo and co-workers used i.n. administration of EVs derived from cytokine-preconditioned MSCs to induce neuroprotection and immunomodulation in 3xTg AD mice, thereby damping the activation of microglial cells, increasing the density of dendritic spines, and modulating the inflammatory status of treated mice [204].

Although small particles such as EVs are able to bypass the BBB obstacle, the mechanisms of penetration of biological barriers (such as epithelia and endothelia) at the CNS level and more in general in the human body are still poorly understood. For this reason, the evaluation of the mechanisms of transportation are required, also for the development of new intranasal drugs: a possibility is using *in vitro* models suitable for further investigate these aspects and the biodistribution of EVs.

In this study we exploit the RPMI 2650 cell line, derived from human nasal carcinoma, that well summarizes the characteristics of a human epithelium and that is capable of mimicking one of the physiological conditions and obstacles that the compounds must overcome to reach the target sites [287].

In previous studies of our group, the neuroprotective efficacy of ASC-EVs was demonstrated in *in vitro* [196] ALS models and *in vivo* SOD1(G93A) mice, when administered intravenously and intranasally [208]. Here, we investigated the ability of ASC-EVs to induce the neuroprotective effect following oxidative stress on two different cell lines (SH-SY5Y, human neuroblastoma cell line and NSC-34, motor neuron cell line), as observed in the past in other models, also following their passage through an epithelial barrier. The results showed that the viability percentage of cells treated with ASC-EVs following the oxidative stress was higher than the control counterpart, in particular for the SH-SY5Y cell line, confirming that ASC-EVs maintain their functionality even after passage through RPMI 2650 cells.

Finally, we used a protocol of fluorescent EVs staining [288] to allow their detection, discrimination from other EVs normally released by all cells types and confirming their role in migration and internalization by injured cells.

8.2. *MATERIALS AND METHODS*

8.2.1. *ASCs Culture and ASC-EVs isolation and characterization*

Murine ASCs were obtained from inguinal adipose tissues of C57BL/6 mice as reported in paragraph 6.2.1. EVs were isolated from the culture medium of ASCs and characterized as reported in paragraph 6.2.2.

8.2.2. *Cell culture*

The SH-SY5Y human neuroblastoma cell lines were cultured in Dulbecco's Modified Eagle Medium/Nutrient Mixture F-12 (DMEM-F12) supplemented with 10% heat-inactivated fetal bovine serum (FBS), 25mM of HEPES solution (4-(2-hydroxyethyl)-1-piperazineethanesulfonic acid) and 1% antibiotics (100IU/ml penicillin and 100µg/ml streptomycin) at 37 °C in a 5% CO_2 atmosphere.

The NSC-34 motor neuron-like cell line was purchased from CELLutions Biosystems Inc (Ontario, Canada). NSC-34 cells were grown in DMEM 1X GlutaMAX-I supplemented with 10% heat-inactivated FBS and 1% antibiotics (100IU/ml penicillin and 100µg/ml streptomycin) at 37 °C in a 5% CO_2 atmosphere.

The RPMI 2650 human nasal carcinoma cell lines (DSMZ, Braunschweig, Germany, Cat. No. ACC 287) were cultured in Eagle's Minimum Essential Medium (MEM) supplemented with 10% heat-inactivated FBS, 1% L-glutamine and 1% No Essential Aminoacids (NEAA) and 1% antibiotics (100IU/ml penicillin and 100µg/ml streptomycin) at 37 °C in a 5% CO_2 atmosphere.

The RPMI 2650 cells were cultured ($6x10^4$ cells) in a transwell system on a 0.4µm pore size PET membrane (Corning), in LLI mode (liquid-liquid interface) for the first 7 days of culture, subsequently in ALI mode (air-liquid interface) till the experimental day (19th day of culture). All reagents for cell cultures were purchased from GIBCO Life technologies (Milan, Italy).

8.2.3. RPMI 2650 epithelial model validation and characterization

The integrity of the RPMI 2650 epithelial layer was monitored with trans-epithelial electrical resistance (TEER) measurements using epithelial voltohmmeter (EVOM2, WPI, USA) with electrodes (STX2) at different time points (15th, 18th, 19th, 21th, 25th day of culture). For each experimental condition, three measurements were performed in different random fields of the well, then an average was calculated. The values were then corrected by subtracting the mean resistance of blank porous membranes and multiplicated to the effective membrane growth area (0.3 cm^2) as reported in [287].

Alcian blue staining for mucus detection was performed on RPMI 2650 cell layer (previously fixed with paraformaldehyde 4% in PBS at RT for 15 minutes) using 100 µL alcian blue stain (1% (w/v) in 3% (v/v) acetic acid/water at pH 2.5) for 15 min. The images were acquired through inverted microscope Leica DM IL LED and analysed using ImageJ software. The intensity of blue stains was calculated as RGB_B ratio$=RGB_B/(RGB_R+RGB_G+RGB_B)$ to quantify stained mucin. Measurements were performed into 5 random fields from each condition.

For tight junctions immunofluorescence staining, the RPMI 2650 cell layer was rinsed with PBS and incubated in blocking solution with 10% normal donkey serum (NDS) and 0.3% Triton X-100 in PBS for 30 minutes at RT. The cell layer was incubated overnight at 4°C with anti-occludin antibody (1:1000, rabbit, Wako Chemicals, Neuss, Germany). After rinsing, primary antibodies were detected with appropriate fluorochrome-conjugated secondary antibodies prior to analysis.

8.2.4. ASC-EVs and H$_2$O$_2$ cell treatment on neuronal cells

To investigate the neuroprotective effect of ASC-EVs, SH-SY5Y (2×10^4 cells) or NSC-34 (2.5×10^4 cells) cells were used. For each condition, 3 replicates were performed. During the experiment the cells were maintained in FBS 1% to avoid contamination with vesicles from serum.

Oxidative stress was performed by adding H$_2$O$_2$ (100µM) on SH-SY5Y or NSC-34 cells for 6 hours of treatment. Control counterpart was treated with PBS. In concomitance, ASC-EVs (10µg/ml) were added above the RPMI 2650 cells to cross the epithelium.

The effect of ASC-EVs through the RPMI 2650 layers on neuronal-like cells was detected measuring the viability of the cells plated on the bottom of the transwell system: after 6 hours treatment SH-SY5Y or NSC-34 were fixed using paraformaldehyde 4% in PBS and labelled with DAPI (4',6-diamidino-2-phenylindole) for 20 minutes. Cell counting was performed with Olympus BX51 microscope equipped with an ultraviolet excitation U-MWU2 filter wideband at 330-385nm and confirmed by EVOS-FL auto microscope. Ten random fields were counted for each well, then an average was calculated to obtain the percentage number of survive cells. All the images were analyzed by ImageJ software.

8.2.5.   ASC-EVs fluorescent labelling

ASC-EVs labelling with 1mM Vybrant™ DiO Cell-labelling solution (Invitrogen) was performed according to the manufacture's protocol and as reported in [288]. Briefly, the dye labelling solution was added in ASCs culture medium and incubated at 37°C for 30 minutes. Subsequently the dye labelling was discarded by washing and ASC-EVs were isolated and characterized as described in 6.2.2.

Fluorescent labelled ASC-EVs and the appropriate control counterparts were incubated with NSC-34 cells with or without H_2O_2 (100μM) oxidative stress for 6 hours treatment to evaluate the EVs uptake by injured motor neuron-like cells. Cells images was acquired by confocal microscopy.

8.2.6.   Statistical analysis

All the data were expressed as mean±standard error of the mean (SEM). Data were analysed using One-way ANOVA. p-values < 0.05 were considered significant.

Day 0
Cells seeding
Liquid-liquid mode

Day 15
TEER
measurements

Day 7
Air-liquid (ALi)
mode

Day 19
Epithelial layer ready for
experiments

RPMI 2650 cells

RPMI 2650 cells layer
characterization

TEER measurements

IF for tight junctions

IHC for mucus presence

ASC-EVs isolation and characterization

ASC-EVs

RPMI 2650 cells

ROS

SH-SY5Y or NSC-34 cells

Day 0

Day 18

Day 19

Day 19 + 6h

H_2O_2+ EVs treatment

RPMI seeding

Neuronal cells seeding

Cell fixing and counting

Created in BioRender.com

8.3. RESULTS

8.3.1. Isolation and characterization of ASC-EVs

Refer to paragraph 6.3.1.

8.3.2. RPMI 2650 epithelial model validation and characterization

RPMI 2650 were used as an *in vitro* model of human epithelium (Figure 8.1A). The correct formation of epithelium was monitored until 25 days of culture by TEER measurements: the obtained values showed an increase of resistance starting from day 15 with a peak around the nineteenth day ($117 \pm 4\ \Omega\ cm^2$; Figure 8.1B). The obtained values reflect those typically reported in literature. The formation of the epithelium was also confirmed by observing the presence of visible mucus with Alcian Blue staining (Figure 8.1C) and the presence of tight junctions was observed in immunofluorescence with anti-occludin antibody (Figure 8.1D). The following experiments on RPMI 2650 cells have been performed around the 19th day of culture, when the epithelium reached the optimal conditions in all the characterization analysis taken in consideration.
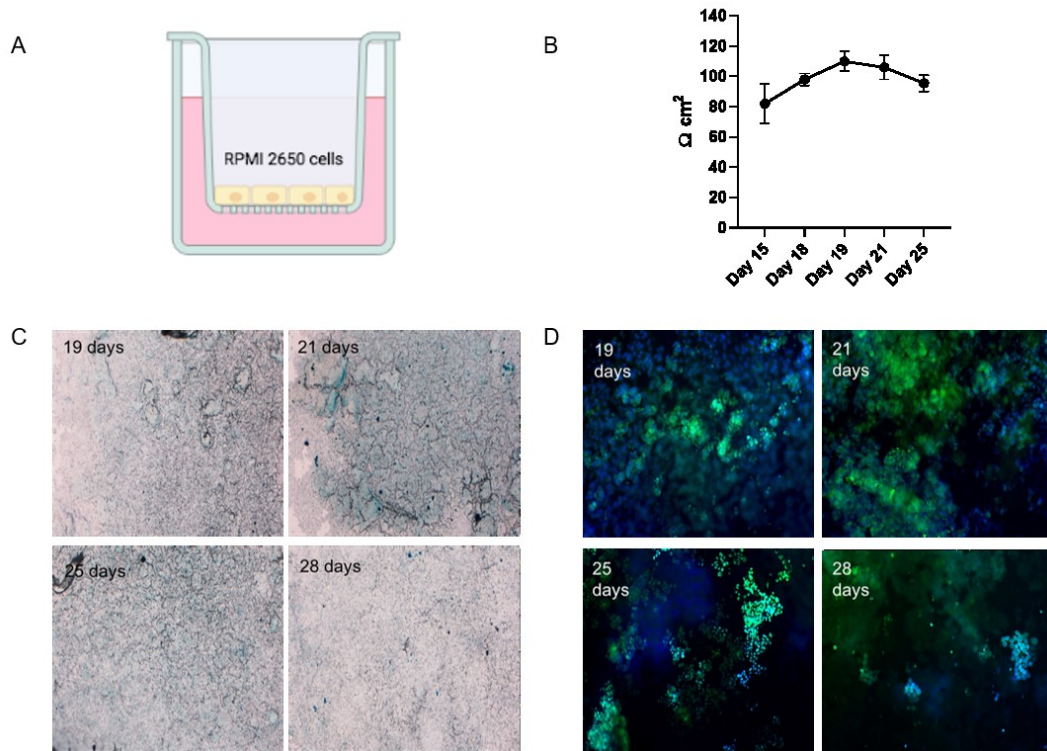
Figure 8.1. RPMI 2650 epithelial cells were used as a model of epithelium *in vitro*. Schematic representation of the transwell system used to culture RPMI 2650 cells (A). This cell line was cultured to reach a sub-confluence until Transepithelial electrical resistance (TEER) values resulted compatible with the formation of the epithelium. The result was achieved around 19 days of cells culture (B). The formation of the epithelium was also confirmed by observing the presence of visible mucus with Alcian Blue stain (C) The presence of tight junctions were observed in immunofluorescence with anti-occludin antibody (D) Scale bar: 500 nm). Data are shown as mean ± SEM.

8.3.3. *Neuroprotective effect of ASC-EVs on injured neuronal cells*

To elicit the oxidative cell damage in SH-SY5Y and NSC-34 cells H_2O_2-induced cytotoxicity was used (Figure 8.2A), testing H_2O_2 100µM for 6 hours resulting in 70% of SH-SY5Y cell death (p=0.0125, Figure 8.2B,C) and in 80% of NSC-34 cell death p=0.0005, Figure 8.2D,E).

Then, the potential neuroprotective effect of ASC-EVs was investigated. Concerning the experiment on SH-SY5Y cells, the treatment with 10µg/ml ASC-EVs through the RPMI 2650 cells layer rescued cells from death, with a median value of 60% of cell viability (p=0.0204, Figure 8.2B,C).

Otherwise, regarding the experiment on NSC-34 cells, the treatment with ASC-EVs through the RPMI 2650 layer showed no significant increase in cell viability: indeed, only 29% of NSC-34 cell viability was observed compared to the control counterpart (p=0.2482, Figure 8.2D,E). Thus, ASC-EVs at the used concentration and through the RPMI 2650 cell barrier, resulted to be not efficient to induce neuroprotection on NSC-34 cells.
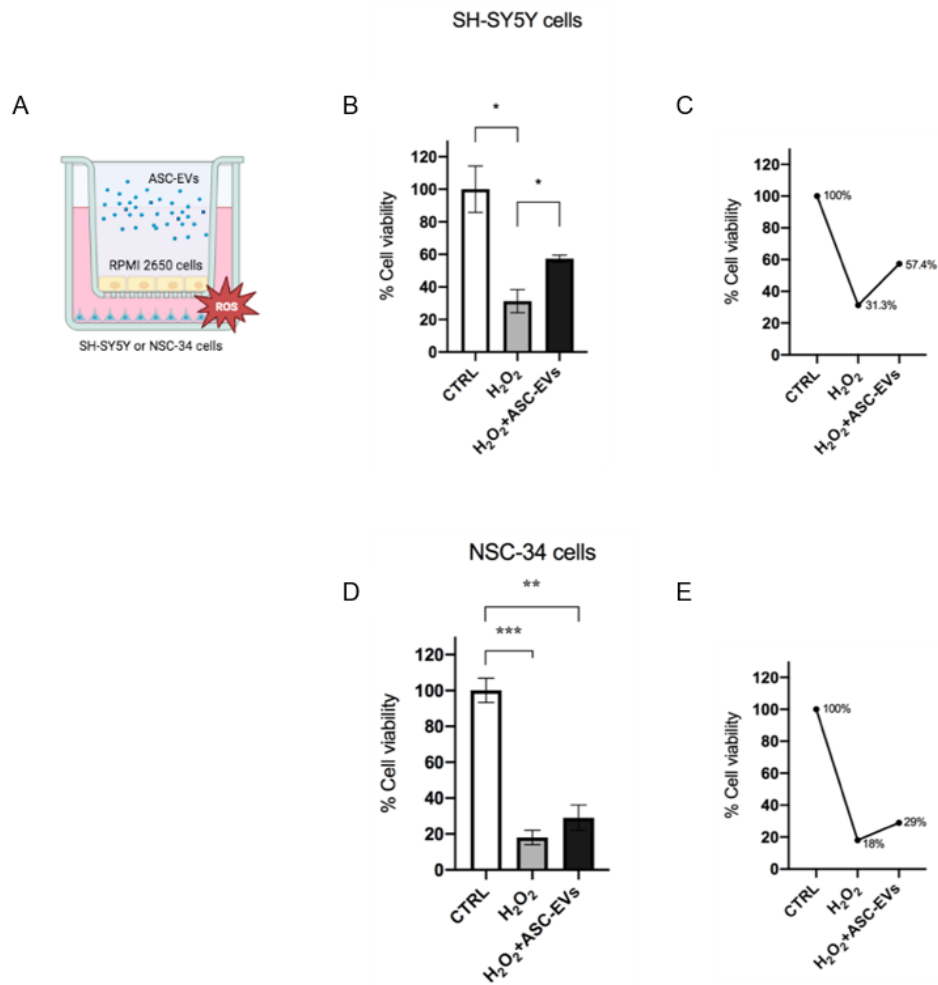
Figure 8.2. ASC-EVs neuroprotection on neuronal cells. Schematic representation of the transwell system used to culture RPMI 2650 and SH-SY5Y or NSC-34 cell lines with the treatment with H2O2 (A). Percentage of cell viability of SH-SY5Y cells after the treatment with H2O2 and ASC-EVs (B,C). Percentage of cell viability of NSC-34 cells after the treatment with H2O2 and ASC-EVs (D,E). Data are shown as mean±SEM. *p<0.05, **p<0.01 ***p<0.001.

8.3.4. *Fluorescent ASC-EVs labelling*

To assess ASC-EVs labelling with Vybrant™ DiO Cell-labelling solution have been evaluated by NTA to consider the incorporation or self-assembling by DiO dye and the changing of ASC-EVs in size. The size of ASC-EVs without DiO (139.0±2.3nm) results to be in line with measurements reported in literature [289] (Figure 8.3A). The incorporation of the DiO dye on the ASC-EVs membrane demonstrates a small shift in their size (173.9±7.1nm) (Figure 8.3B). No signal of self-assemble were observed as shown from the peaks of DiO dye alone in PBS buffer (31.2±26.2 nm) (Figure

8.3C). The results indicate that DiO dye label specifically EVs. All the data from NTA analysis are reported in table 8.1.

To confirm the specificity of DiO-labelling on ASC-EVs, injured NSC-34 motor neurons cells were treated for 6h. After treatment ASC-EVs labelled with DiO seems to be located inside NSC-34 cells, in particular in the H_2O_2-treated condition (Figure 8.4A,B). Appropriate negative controls showed no unspecific signals for DiO-labelling (Figure 8.4C, D).
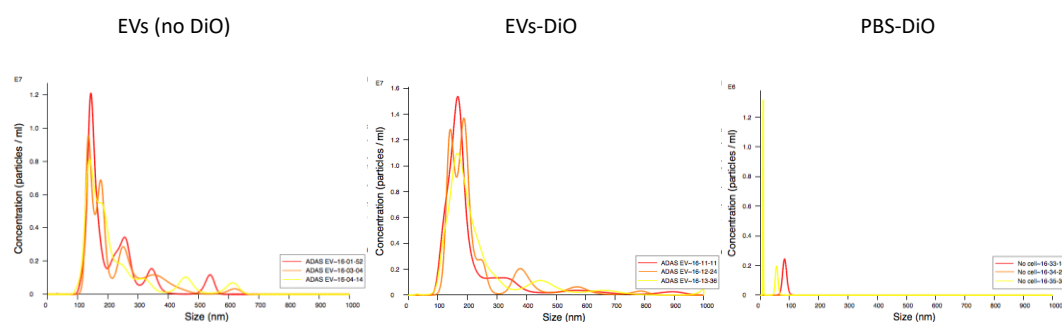
Figure 8.3. NTA analysis of ASC-EVs. ASC-EVs not labelled (A). ASC-EVs labelled with DiO dye (B). DiO dye in PBS buffer (C). Graph reported the average of three different measurements.

	Mean	Mode	Particle/ml
EVs (no DiO)	221.6 ± 3.1 nm	139.0 ± 2.3 nm	$8.18 \times 10^8 \pm 9.99 \times 10^6$
EVs-DiO	230.0 ± 5.0 nm	173.9 ± 7.1 nm	$1.37 \times 10^9 \pm 5.57 \times 10^6$
PBS-DiO	38.1 ± 24.5 nm	31.2 ± 26.2 nm	$3.28 \times 10^6 \pm 1.37 \times 10^6$

Table 8.1. NTA data output which reports mean and mode of ASC-EVs size and particle concentration with relative SD for the three different conditions.
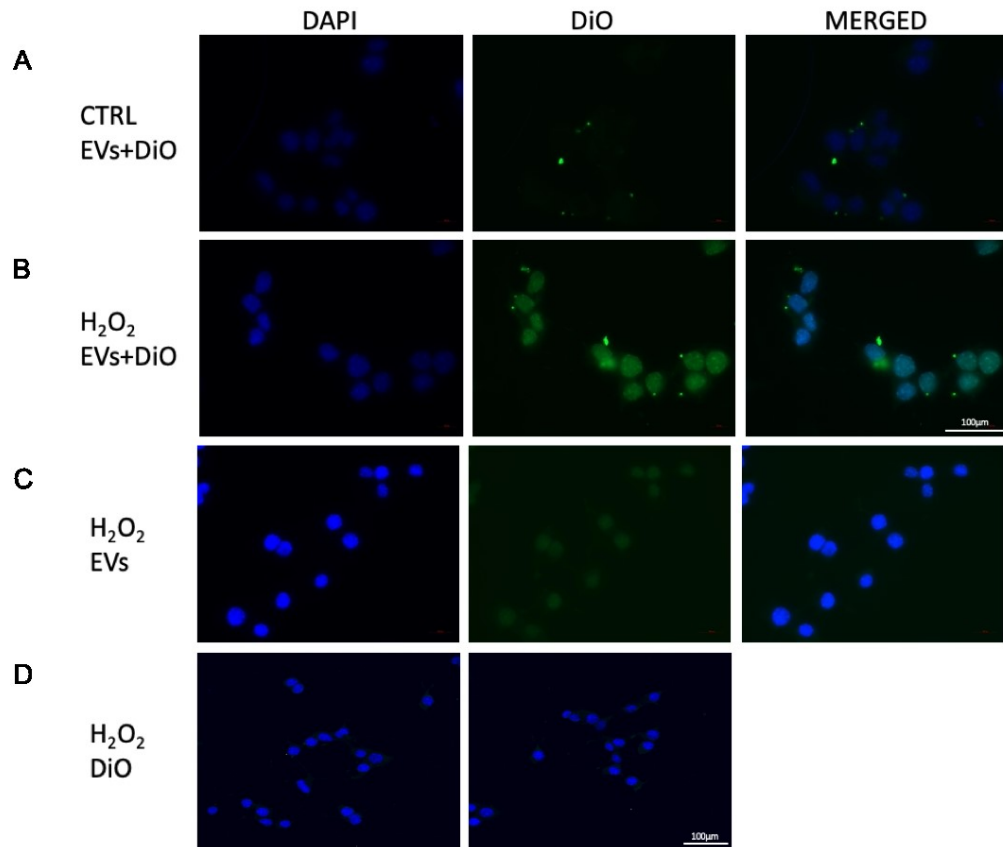
Figure 8.4. Specificity of DiO-labelling on ASC-EVs. ASC-EVs stained with DiO dye on control NSC-34 cells (A). ASC-EVs labelled with DiO on NSC-34 cells treated with H_2O_2 (B). ASC-EVs not stained with DiO dye on NSC-34 treated with H_2O_2 (C). DiO dye on NSC-34 treated with H_2O_2 (D). Cell nuclei were stained with DAPI and DiO dye fluorescence is displayed in green. Scale bar=100uM. Magnification 63X.

8.4. _DISCUSSION_

In neurodegenerative diseases one of the most prominent approaches is the use of stem cells-derived EVs. Indeed, the beneficial roles of stem cells have been demonstrated to belong to their paracrine activity, which involves the release of EVs that contain molecules able to counteract neurodegeneration [149]. Among different stem cells, MSCs seems to stand out for the release of several neuroprotective and immunomodulating molecules, as well as their ease collection from adipose tissues to obtain ASCs [197].

One of the challenge of delivering molecules to the CNS is to pass the BBB; to overcome this issue the intranasal delivery route is a very attractive and non-invasive strategy. The first transport mechanism of molecules from the nasal cavity to the brain is the intracellular one: it starts with the internalization of the molecules by olfactory neurons, whose soma reside in the epithelial layer of the olfactory region and that project their axons to the olfactory bulb. After the internalization of molecule, the endocytic vesicles are transported along the axons and finally released via exocytosis toward the olfactory bulb (reviewed in [290]). The second transport mechanism of intranasal drug delivery is the extracellular pathway: in this pathway, molecules cross the nasal epithelium, that is composed of different cell types interconnected via tight junctions, to reach the lamina propria. From the lamina propria, the drug can be absorbed by the systemic circulation [291]. For this reason, the evaluation of the mechanisms used by ASC-EVs to overcome biological barriers (like epithelia and endothelia), using an _in vitro_ cell model is useful to mimic as closely as possible the barrier properties of the human epithelia that influences drug and EVs pharmacokinetics [292]. With this purpose, using RPMI 2650 cells we set up an _in vitro_ model of human epithelium that accomplished different morphological and functional requirements, as reported in literature [287].

One of the most important risk factors in neurodegenerative diseases involves the role of ROS, which can lead to an excessive oxidative stress responsible of neuronal death [1]. Based on the injured brain/spinal cord region, different types of neurons can be involved: in motor dysfunction diseases, like ALS or SMA, the affected cells are normally MNs, while in non-motor dysfunction diseases, like AD, the affected cells are neurons. The use of ASC-EVs, containing molecules such as neurotrophic

and neuroprotective factors, chemokine and anti-inflammatory cytokine and other important modulator molecules [149], may be an efficient solution for both motor and non-motor dysfunction neurodegenerative diseases. In our settled neuroprotective system, we have used both motor neurons (NSC-34) and neurons (SH-SY5Y) cells injured with an oxidative-stress, in order to evaluate the neuroprotective role of ASC-EVs. Regarding SH-SY5Y cells, neurons achieve the statistically relevant rescue of 26.1%, while for what concerns NSC-34 cells, the motor neurons rescue is 11% showing a trend that is not statistically relevant. Previous published studies by our group have demonstrated that ASC-EVs counteract the oxidative stress on NSC-34 cells in a statistically significant manner when ASC-EVs are added directly to the injured cells without passing through the RPMI 2650 epithelial layer [196]. Therefore, a double explanation can be hypothesize: 1) the selected concentration of H_2O_2 may be an over concentration considering that ASC-EVs needs time to cross the RPMI 2650 epithelium before reaching the injured cells, compared to a system in which they are directly administered; 2) the amount of ASC-EVs could have to be increased because some of them could be trapped by epithelial cells.

An EVs labelling need arises to allow their detection, discrimination from other EVs normally released by all cells types and confirming their role in migration and internalization by injured cells. With this purpose we used a fluorescent labelling protocol [288] on ASCs to isolate fluorescent ASC-EVs, confirming that the use of a lipophilic dye did not alter the morphological characteristic of ASC-EVs and no artefacts formed by dye auto-assembling were present. Having settled the ASC-EVs labelling protocol will help in future studies that will aim to discriminate ASC-EVs diffused through the RPMI 2650 epithelium and to fix the concentration of ASC-EVs able to reach oxidative injured cells, as well as to further study the mechanisms of ASC-EVs transport and cellular uptake.

9. CONCLUSIONS

Several evidence suggest that EVs isolated from MSCs can be used for the treatment of neurodegenerative disease. Our aim is to develop a novel cell-free therapeutic approach to translate to neurodegenerative disease patients based on the use of ASC-EVs that will avoid all the limitations and risks associated to stem cell transplantation.

The experimental paradigms 1 and 2 were aimed at verifying whether ASC-EVs may exert a therapeutic effect in two different pathological animal models of SMA and ALS. To this purpose, SMNΔ7 and SOD1(G93A) mice were used as *in vivo* models of these two diseases, respectively. In both studies, the protective effect of ASC-EVs was confirmed, in particular at the central level and in terms of rescue of motor performances.

Furthermore, when using EVs-based therapy it is crucial to clarify the mechanisms used to pass through biological barriers in order to ameliorate their biodistribution. In view of this, in experiment 3 we set up an *in vitro* model to investigate the passage of ASC-EVs through an epithelial barrier and to confirm their neuroprotective effect on an oxidative stress-induced model of both motor neuron and neuron cells after their passage through the epithelium. This let us set the conditions for future studies concerning the transport and the cellular uptake of ASC-EVs by the target sites.

Altogether, the results reported in this doctoral thesis highlighted the therapeutic relevance of ASC-EVs, supporting the hypothesis that EVs can recapitulate the neuroprotective effect of their MSCs parental cells and their potential use in neurodegenerative disorders as a cell-free therapeutic approach.

10. LIMITATIONS AND FUTURE PERPECTIVES

Despite the promising results obtained in the different experimental paradigms reported in this thesis that highlighted the therapeutic relevance of ASC-EVs and their potential use in neurodegenerative disorders as a cell-free therapeutic approach, some limitations could be pointed out.

In particular, the transition from the preclinical research to the clinic has to overcome several issues; for example, the results obtained from the *in vivo* models used in our experiments to evaluate the effect of ASC-EVs, could predict the therapeutic dose and outcome for a possible treatment in humans, but they could not be exhaustive or sufficient due to implicit limitations of the animal models. Similarly, the *in vitro* model, used in the experimental paradigm 3 to deepen the knowledge about the intranasal delivery, could not be exhaustive to study the olfactory epithelium because it limits the complexity of the tissue excluding the presence of other cell types, like for example the olfactory sensory neurons. To overcome this issue, our purpose for future studies will be to use more complex models: for example, isolating cells from the nasal cavity using nasal brushes directly from patients or culturing *in vitro* tissue sections of the nasal cavity from patients biopsy or from animal models.

Furthermore, the complexity of ASC-EVs makes it difficult to identify their mechanism of action, since the neuroprotective and immunomodulatory effects we observed could be due to several and different molecules present in the ASC-EVs. To couple with this issue, future proteomic analysis or mechanism-correlated studies will help us to clarify the mechanism of action of ASC-EVs in neurodegenerative disorders. Besides, it will be useful to understand the mechanisms by which ASC-EVs can cross the biological barriers before reaching their targets and how cells targets (like motor neurons and glial cells) can uptake ASC-EVs.

Finally, some technical problems such as the lack of standardized methods of extraction and characterization of ASC-EVs, together with other issues that can affect the large scale development and manufacturing (GMP production, storage and stability of EVs…) could impact on the clinical translation of ASC-EVs-based therapy. For this reason, the efforts from the scientific community involved in the study and use of EVs will be precious to solve these limitations.

11. REFERENCES

1. Sheikh, S., et al., *Neurodegenerative Diseases: Multifactorial Conformational Diseases and Their Therapeutic Interventions.* J Neurodegener Dis, 2013. **2013**: p. 563481.
2. Jellinger, K.A., *General aspects of neurodegeneration.* J Neural Transm Suppl, 2003(65): p. 101-44.
3. Zahra, W., et al., *The Global Economic Impact of Neurodegenerative Diseases: Opportunities and Challenges*, in *Bioeconomy for Sustainable Development*, C. Keswani, Editor. 2020, Springer Singapore: Singapore. p. 333-345.
4. Duraes, F., M. Pinto, and E. Sousa, *Old Drugs as New Treatments for Neurodegenerative Diseases.* Pharmaceuticals (Basel), 2018. **11**(2).
5. Lunn, M.R. and C.H. Wang, *Spinal muscular atrophy.* Lancet, 2008. **371**(9630): p. 2120-33.
6. Wirth, B., L. Brichta, and E. Hahnen, *Spinal muscular atrophy: from gene to therapy.* Semin Pediatr Neurol, 2006. **13**(2): p. 121-31.
7. Ogino, S., et al., *Genetic risk assessment in carrier testing for spinal muscular atrophy.* Am J Med Genet, 2002. **110**(4): p. 301-7.
8. Pearn, J., *Classification of spinal muscular atrophies.* Lancet, 1980. **1**(8174): p. 919-22.
9. Czeizel, A. and J. Hamula, *A hungarian study on Werdnig-Hoffmann disease.* J Med Genet, 1989. **26**(12): p. 761-3.
10. Pearn, J., *Incidence, prevalence, and gene frequency studies of chronic childhood spinal muscular atrophy.* J Med Genet, 1978. **15**(6): p. 409-13.
11. Simone, C., et al., *Is spinal muscular atrophy a disease of the motor neurons only: pathogenesis and therapeutic implications?* Cell Mol Life Sci, 2016. **73**(5): p. 1003-20.
12. Wirth, B., et al., *Twenty-Five Years of Spinal Muscular Atrophy Research: From Phenotype to Genotype to Therapy, and What Comes Next.* Annu Rev Genomics Hum Genet, 2020. **21**: p. 231-261.
13. Dubowitz, V., *Very severe spinal muscular atrophy (SMA type 0): an expanding clinical phenotype.* Eur J Paediatr Neurol, 1999. **3**(2): p. 49-51.
14. Markowitz, J.A., M.B. Tinkle, and K.H. Fischbeck, *Spinal muscular atrophy in the neonate.* J Obstet Gynecol Neonatal Nurs, 2004. **33**(1): p. 12-20.
15. Lefebvre, S., et al., *Identification and characterization of a spinal muscular atrophy-determining gene.* Cell, 1995. **80**(1): p. 155-65.
16. Kolb, S.J. and J.T. Kissel, *Spinal Muscular Atrophy.* Neurol Clin, 2015. **33**(4): p. 831-46.
17. Zerres, K., et al., *Genetic basis of adult-onset spinal muscular atrophy.* Lancet, 1995. **346**(8983): p. 1162.
18. Ionasescu, V., J. Christensen, and M. Hart, *Intestinal pseudo-obstruction in adult spinal muscular atrophy.* Muscle Nerve, 1994. **17**(8): p. 946-8.
19. Karasick, D., S. Karasick, and E. Mapp, *Gastrointestinal radiologic manifestations of proximal spinal muscular atrophy (Kugelberg-Welander syndrome).* J Natl Med Assoc, 1982. **74**(5): p. 475-8.
20. Iannaccone, S.T., *Modern management of spinal muscular atrophy.* J Child Neurol, 2007. **22**(8): p. 974-8.
21. Bach, J.R., *Medical considerations of long-term survival of Werdnig-Hoffmann disease.* Am J Phys Med Rehabil, 2007. **86**(5): p. 349-55.
22. Tanaka, H., et al., *Cardiac involvement in the Kugelbert-Welander syndrome.* Am J Cardiol, 1976. **38**(4): p. 528-32.
23. Araujo, A., M. Araujo, and K.J. Swoboda, *Vascular perfusion abnormalities in infants with spinal muscular atrophy.* J Pediatr, 2009. **155**(2): p. 292-4.
24. Takahashi, N., et al., *Cardiac involvement in Kugelberg-Welander disease: a case report and review.* Am J Med Sci, 2006. **332**(6): p. 354-6.
25. Finsterer, J. and C. Stollberger, *Cardiac involvement in Werdnig-Hoffmann's spinal muscular atrophy.* Cardiology, 1999. **92**(3): p. 178-82.
26. Heier, C.R., et al., *Arrhythmia and cardiac defects are a feature of spinal muscular atrophy model mice.* Hum Mol Genet, 2010. **19**(20): p. 3906-18.

27. Haaker, G. and A. Fujak, *Proximal spinal muscular atrophy: current orthopedic perspective.* Appl Clin Genet, 2013. **6**(11): p. 113-20.

28. Fujak, A., et al., *Contractures of the lower extremities in spinal muscular atrophy type II. Descriptive clinical study with retrospective data collection.* Ortop Traumatol Rehabil, 2011. **13**(1): p. 27-36.

29. Felderhoff-Mueser, U., et al., *Severe spinal muscular atrophy variant associated with congenital bone fractures.* J Child Neurol, 2002. **17**(9): p. 718-21.

30. von Gontard, A., et al., *Intelligence and cognitive function in children and adolescents with spinal muscular atrophy.* Neuromuscul Disord, 2002. **12**(2): p. 130-6.

31. Zerres, K., et al., *A collaborative study on the natural history of childhood and juvenile onset proximal spinal muscular atrophy (type II and III SMA): 569 patients.* J Neurol Sci, 1997. **146**(1): p. 67-72.

32. Farrar, M.A., et al., *Emerging therapies and challenges in spinal muscular atrophy.* Ann Neurol, 2017. **81**(3): p. 355-368.

33. Lorson, C.L. and E.J. Androphy, *An exonic enhancer is required for inclusion of an essential exon in the SMA-determining gene SMN.* Hum Mol Genet, 2000. **9**(2): p. 259-65.

34. Lorson, C.L., et al., *A single nucleotide in the SMN gene regulates splicing and is responsible for spinal muscular atrophy.* Proc Natl Acad Sci U S A, 1999. **96**(11): p. 6307-11.

35. Chang, H.C., et al., *Degradation of survival motor neuron (SMN) protein is mediated via the ubiquitin/proteasome pathway.* Neurochem Int, 2004. **45**(7): p. 1107-12.

36. Vitte, J., et al., *Refined characterization of the expression and stability of the SMN gene products.* Am J Pathol, 2007. **171**(4): p. 1269-80.

37. Hahnen, E., et al., *Molecular analysis of candidate genes on chromosome 5q13 in autosomal recessive spinal muscular atrophy: evidence of homozygous deletions of the SMN gene in unaffected individuals.* Hum Mol Genet, 1995. **4**(10): p. 1927-33.

38. Wirth, B., et al., *Mildly affected patients with spinal muscular atrophy are partially protected by an increased SMN2 copy number.* Hum Genet, 2006. **119**(4): p. 422-8.

39. Miguel-Aliaga, I., et al., *The Caenorhabditis elegans orthologue of the human gene responsible for spinal muscular atrophy is a maternal product critical for germline maturation and embryonic viability.* Hum Mol Genet, 1999. **8**(12): p. 2133-43.

40. Schrank, B., et al., *Inactivation of the survival motor neuron gene, a candidate gene for human spinal muscular atrophy, leads to massive cell death in early mouse embryos.* Proc Natl Acad Sci U S A, 1997. **94**(18): p. 9920-5.

41. Rodriguez-Muela, N., et al., *Single-Cell Analysis of SMN Reveals Its Broader Role in Neuromuscular Disease.* Cell Rep, 2017. **18**(6): p. 1484-1498.

42. Chaytow, H., et al., *The role of survival motor neuron protein (SMN) in protein homeostasis.* Cell Mol Life Sci, 2018. **75**(21): p. 3877-3894.

43. Liu, Q., et al., *The spinal muscular atrophy disease gene product, SMN, and its associated protein SIP1 are in a complex with spliceosomal snRNP proteins.* Cell, 1997. **90**(6): p. 1013-21.

44. Will, C.L. and R. Lührmann, *Spliceosomal UsnRNP biogenesis, structure and function.* Curr Opin Cell Biol, 2001. **13**(3): p. 290-301.

45. Setola, V., et al., *Axonal-SMN (a-SMN), a protein isoform of the survival motor neuron gene, is specifically involved in axonogenesis.* Proc Natl Acad Sci U S A, 2007. **104**(6): p. 1959-64.

46. Giavazzi, A., et al., *Neuronal-specific roles of the survival motor neuron protein: evidence from survival motor neuron expression patterns in the developing human central nervous system.* J Neuropathol Exp Neurol, 2006. **65**(3): p. 267-77.

47. Li, H., et al., *α-COP binding to the survival motor neuron protein SMN is required for neuronal process outgrowth.* Hum Mol Genet, 2015. **24**(25): p. 7295-307.

48. McWhorter, M.L., et al., *Knockdown of the survival motor neuron (Smn) protein in zebrafish causes defects in motor axon outgrowth and pathfinding.* J Cell Biol, 2003. **162**(5): p. 919-31.

49. Le, T.T., et al., *SMNDelta7, the major product of the centromeric survival motor neuron (SMN2) gene, extends survival in mice with spinal muscular atrophy and associates with full-length SMN.* Hum Mol Genet, 2005. **14**(6): p. 845-57.

50. Genabai, N.K., et al., *Genetic inhibition of JNK3 ameliorates spinal muscular atrophy.* Hum Mol Genet, 2015. **24**(24): p. 6986-7004.

51. Schellino, R., et al., *Pharmacological c-Jun NH(2)-Terminal Kinase (JNK) Pathway Inhibition Reduces Severity of Spinal Muscular Atrophy Disease in Mice.* Front Mol Neurosci, 2018. **11**: p. 308.

52. Zheng, D., et al., *Dysregulation of the PI3K/Akt signaling pathway affects cell cycle and apoptosis of side population cells in nasopharyngeal carcinoma.* Oncol Lett, 2015. **10**(1): p. 182-188.

53. Datta, S.R., et al., *Akt phosphorylation of BAD couples survival signals to the cell-intrinsic death machinery.* Cell, 1997. **91**(2): p. 231-41.

54. Godena, V.K. and K. Ning, *Phosphatase and tensin homologue: a therapeutic target for SMA.* Signal Transduct Target Ther, 2017. **2**: p. 17038.

55. Papadimitriou, D., et al., *Inflammation in ALS and SMA: sorting out the good from the evil.* Neurobiol Dis, 2010. **37**(3): p. 493-502.

56. Przedborski, S., *Neuroinflammation and Parkinson's disease.* Handb Clin Neurol, 2007. **83**: p. 535-51.

57. Wang, D.D. and A. Bordey, *The astrocyte odyssey.* Prog Neurobiol, 2008. **86**(4): p. 342-67.

58. Ullian, E.M., et al., *Control of synapse number by glia.* Science, 2001. **291**(5504): p. 657-61.

59. Rudge, J.S., et al., *Expression of Ciliary Neurotrophic Factor and the Neurotrophins-Nerve Growth Factor, Brain-Derived Neurotrophic Factor and Neurotrophin 3-in Cultured Rat Hippocampal Astrocytes.* Eur J Neurosci, 1992. **4**(6): p. 459-471.

60. Ojeda, S.R., et al., *Glia-to-neuron signaling and the neuroendocrine control of female puberty.* Recent Prog Horm Res, 2000. **55**: p. 197-223; discussion 223-4.

61. Pehar, M., et al., *Complexity of astrocyte-motor neuron interactions in amyotrophic lateral sclerosis.* Neurodegener Dis, 2005. **2**(3-4): p. 139-46.

62. McGivern, J.V., et al., *Spinal muscular atrophy astrocytes exhibit abnormal calcium regulation and reduced growth factor production.* Glia, 2013. **61**(9): p. 1418-1428.

63. Rindt, H., et al., *Astrocytes influence the severity of spinal muscular atrophy.* Hum Mol Genet, 2015. **24**(14): p. 4094-102.

64. Kreutzberg, G.W., *Microglia: a sensor for pathological events in the CNS.* Trends Neurosci, 1996. **19**(8): p. 312-8.

65. Moisse, K. and M.J. Strong, *Innate immunity in amyotrophic lateral sclerosis.* Biochim Biophys Acta, 2006. **1762**(11-12): p. 1083-93.

66. Tarabal, O., et al., *Mechanisms involved in spinal cord central synapse loss in a mouse model of spinal muscular atrophy.* J Neuropathol Exp Neurol, 2014. **73**(6): p. 519-35.

67. Shababi, M., C.L. Lorson, and S.S. Rudnik-Schoneborn, *Spinal muscular atrophy: a motor neuron disorder or a multi-organ disease?* J Anat, 2014. **224**(1): p. 15-28.

68. Kariya, S., et al., *Reduced SMN protein impairs maturation of the neuromuscular junctions in mouse models of spinal muscular atrophy.* Hum Mol Genet, 2008. **17**(16): p. 2552-69.

69. Lee, Y.I., et al., *Muscles in a mouse model of spinal muscular atrophy show profound defects in neuromuscular development even in the absence of failure in neuromuscular transmission or loss of motor neurons.* Dev Biol, 2011. **356**(2): p. 432-44.

70. Boido, M. and A. Vercelli, *Neuromuscular Junctions as Key Contributors and Therapeutic Targets in Spinal Muscular Atrophy.* Front Neuroanat, 2016. **10**: p. 6.

71. Witzemann, V., *Development of the neuromuscular junction.* Cell Tissue Res, 2006. **326**(2): p. 263-71.

72. Marques, M.J., J.A. Conchello, and J.W. Lichtman, *From plaque to pretzel: fold formation and acetylcholine receptor loss at the developing neuromuscular junction.* J Neurosci, 2000. **20**(10): p. 3663-75.

73. Walsh, M.K. and J.W. Lichtman, *In vivo time-lapse imaging of synaptic takeover associated with naturally occurring synapse elimination.* Neuron, 2003. **37**(1): p. 67-73.

74. Valsecchi, V., et al., *Expression of Muscle-Specific MiRNA 206 in the Progression of Disease in a Murine SMA Model.* PLoS One, 2015. **10**(6): p. e0128560.

75. Ling, K.K., et al., *Severe neuromuscular denervation of clinically relevant muscles in a mouse model of spinal muscular atrophy.* Hum Mol Genet, 2012. **21**(1): p. 185-95.

76. Torres-Benito, L., R. Ruiz, and L. Tabares, *Synaptic defects in spinal muscular atrophy animal models.* Dev Neurobiol, 2012. **72**(1): p. 126-33.

77. Hua, Y., et al., *Enhancement of SMN2 exon 7 inclusion by antisense oligonucleotides targeting the exon.* PLoS Biol, 2007. **5**(4): p. e73.

78. Skordis, L.A., et al., *Bifunctional antisense oligonucleotides provide a trans-acting splicing enhancer that stimulates SMN2 gene expression in patient fibroblasts.* Proc Natl Acad Sci U S A, 2003. **100**(7): p. 4114-9.

79. Hua, Y., et al., *Antisense masking of an hnRNP A1/A2 intronic splicing silencer corrects SMN2 splicing in transgenic mice.* Am J Hum Genet, 2008. **82**(4): p. 834-48.

80. Finkel, R.S., et al., *Treatment of infantile-onset spinal muscular atrophy with nusinersen: a phase 2, open-label, dose-escalation study.* Lancet, 2016. **388**(10063): p. 3017-3026.

81. Corey, D.R., *Nusinersen, an antisense oligonucleotide drug for spinal muscular atrophy.* Nat Neurosci, 2017. **20**(4): p. 497-499.

82. Naryshkin, N.A., et al., *Motor neuron disease. SMN2 splicing modifiers improve motor function and longevity in mice with spinal muscular atrophy.* Science, 2014. **345**(6197): p. 688-93.

83. Palacino, J., et al., *SMN2 splice modulators enhance U1-pre-mRNA association and rescue SMA mice.* Nat Chem Biol, 2015. **11**(7): p. 511-7.

84. Baranello, G., et al., *Risdiplam in Type 1 Spinal Muscular Atrophy.* N Engl J Med, 2021. **384**(10): p. 915-923.

85. Scoto, M., et al., *Therapeutic approaches for spinal muscular atrophy (SMA).* Gene Ther, 2017. **24**(9): p. 514-519.

86. Martinez, T.L., et al., *Survival motor neuron protein in motor neurons determines synaptic integrity in spinal muscular atrophy.* J Neurosci, 2012. **32**(25): p. 8703-15.

87. Paez-Colasante, X., et al., *Improvement of neuromuscular synaptic phenotypes without enhanced survival and motor function in severe spinal muscular atrophy mice selectively rescued in motor neurons.* PLoS One, 2013. **8**(9): p. e75866.

88. Dominguez, E., et al., *Intravenous scAAV9 delivery of a codon-optimized SMN1 sequence rescues SMA mice.* Hum Mol Genet, 2011. **20**(4): p. 681-93.

89. Valori, C.F., et al., *Systemic delivery of scAAV9 expressing SMN prolongs survival in a model of spinal muscular atrophy.* Sci Transl Med, 2010. **2**(35): p. 35ra42.

90. Hoy, S.M., *Onasemnogene Abeparvovec: First Global Approval.* Drugs, 2019. **79**(11): p. 1255-1262.

91. Chaytow, H., et al., *Spinal muscular atrophy: From approved therapies to future therapeutic targets for personalized medicine.* Cell Rep Med, 2021. **2**(7): p. 100346.

92. Rowland, L.P., *How amyotrophic lateral sclerosis got its name: the clinical-pathologic genius of Jean-Martin Charcot.* Arch Neurol, 2001. **58**(3): p. 512-5.

93. Talbott, E.O., A.M. Malek, and D. Lacomis, *The epidemiology of amyotrophic lateral sclerosis.* Handb Clin Neurol, 2016. **138**: p. 225-38.

94. Mulder, D.W., et al., *Familial adult motor neuron disease: amyotrophic lateral sclerosis.* Neurology, 1986. **36**(4): p. 511-7.

95. Swinnen, B. and W. Robberecht, *The phenotypic variability of amyotrophic lateral sclerosis.* Nat Rev Neurol, 2014. **10**(11): p. 661-70.

96. Rowland, L.P. and N.A. Shneider, *Amyotrophic lateral sclerosis.* N Engl J Med, 2001. **344**(22): p. 1688-700.

97. van der Kleij, L.A., et al., *Regionality of disease progression predicts prognosis in amyotrophic lateral sclerosis.* Amyotroph Lateral Scler Frontotemporal Degener, 2015. **16**(7-8): p. 442-7.

98. D'Amico, E., et al., *Clinical evolution of pure upper motor neuron disease/dysfunction (PUMMD).* Muscle Nerve, 2013. **47**(1): p. 28-32.

99. Strong, M.J., et al., *Amyotrophic lateral sclerosis - frontotemporal spectrum disorder (ALS-FTSD): Revised diagnostic criteria.* Amyotroph Lateral Scler Frontotemporal Degener, 2017. **18**(3-4): p. 153-174.

100. Picher-Martel, V., et al., *From animal models to human disease: a genetic approach for personalized medicine in ALS.* Acta Neuropathologica Communications, 2016. **4**.

101. Armon, C., *An evidence-based medicine approach to the evaluation of the role of exogenous risk factors in sporadic amyotrophic lateral sclerosis.* Neuroepidemiology, 2003. **22**(4): p. 217-28.

102.   Malek, A.M., et al., *Exposure to hazardous air pollutants and the risk of amyotrophic lateral sclerosis.* Environ Pollut, 2015. **197**: p. 181-186.

103.   Rosen, D.R., et al., *Mutations in Cu/Zn superoxide dismutase gene are associated with familial amyotrophic lateral sclerosis.* Nature, 1993. **362**(6415): p. 59-62.

104.   Fukai, T. and M. Ushio-Fukai, *Superoxide dismutases: role in redox signaling, vascular function, and diseases.* Antioxid Redox Signal, 2011. **15**(6): p. 1583-606.

105.   Kaur, S.J., S.R. McKeown, and S. Rashid, *Mutant SOD1 mediated pathogenesis of Amyotrophic Lateral Sclerosis.* Gene, 2016. **577**(2): p. 109-18.

106.   Borchelt, D.R., et al., *Superoxide dismutase 1 with mutations linked to familial amyotrophic lateral sclerosis possesses significant activity.* Proc Natl Acad Sci U S A, 1994. **91**(17): p. 8292-6.

107.   Bruijn, L.I., et al., *ALS-linked SOD1 mutant G85R mediates damage to astrocytes and promotes rapidly progressive disease with SOD1-containing inclusions.* Neuron, 1997. **18**(2): p. 327-38.

108.   Rosen, D.R., et al., *A frequent ala 4 to val superoxide dismutase-1 mutation is associated with a rapidly progressive familial amyotrophic lateral sclerosis.* Hum Mol Genet, 1994. **3**(6): p. 981-7.

109.   Gurney, M.E., et al., *Motor neuron degeneration in mice that express a human Cu,Zn superoxide dismutase mutation.* Science, 1994. **264**(5166): p. 1772-5.

110.   Chen, Q., et al., *Temporal Expression of Mutant TDP-43 Correlates with Early Amyotrophic Lateral Sclerosis Phenotype and Motor Weakness.* Curr Neurovasc Res, 2018. **15**(1): p. 3-9.

111.   Alami, N.H., et al., *Axonal transport of TDP-43 mRNA granules is impaired by ALS-causing mutations.* Neuron, 2014. **81**(3): p. 536-543.

112.   Kwiatkowski, T.J., Jr., et al., *Mutations in the FUS/TLS gene on chromosome 16 cause familial amyotrophic lateral sclerosis.* Science, 2009. **323**(5918): p. 1205-8.

113.   Zou, Z.Y., et al., *Genetic epidemiology of amyotrophic lateral sclerosis: a systematic review and meta-analysis.* J Neurol Neurosurg Psychiatry, 2017. **88**(7): p. 540-549.

114.   Farg, M.A., et al., *C9ORF72, implicated in amytrophic lateral sclerosis and frontotemporal dementia, regulates endosomal trafficking.* Hum Mol Genet, 2014. **23**(13): p. 3579-95.

115.   Bonafede, R. and R. Mariotti, *ALS Pathogenesis and Therapeutic Approaches: The Role of Mesenchymal Stem Cells and Extracellular Vesicles.* Front Cell Neurosci, 2017. **11**: p. 80.

116.   Heath, P.R. and P.J. Shaw, *Update on the glutamatergic neurotransmitter system and the role of excitotoxicity in amyotrophic lateral sclerosis.* Muscle Nerve, 2002. **26**(4): p. 438-58.

117.   Hensley, K., et al., *On the relation of oxidative stress to neuroinflammation: lessons learned from the G93A-SOD1 mouse model of amyotrophic lateral sclerosis.* Antioxid Redox Signal, 2006. **8**(11-12): p. 2075-87.

118.   Spreux-Varoquaux, O., et al., *Glutamate levels in cerebrospinal fluid in amyotrophic lateral sclerosis: a reappraisal using a new HPLC method with coulometric detection in a large cohort of patients.* J Neurol Sci, 2002. **193**(2): p. 73-8.

119.   Muyderman, H. and T. Chen, *Mitochondrial dysfunction in amyotrophic lateral sclerosis - a valid pharmacological target?* Br J Pharmacol, 2014. **171**(8): p. 2191-205.

120.   Pickles, S., et al., *ALS-linked misfolded SOD1 species have divergent impacts on mitochondria.* Acta Neuropathol Commun, 2016. **4**(1): p. 43.

121.   Julien, J.P., *Amyotrophic lateral sclerosis. unfolding the toxicity of the misfolded.* Cell, 2001. **104**(4): p. 581-91.

122.   Boillée, S., C. Vande Velde, and D.W. Cleveland, *ALS: a disease of motor neurons and their nonneuronal neighbors.* Neuron, 2006. **52**(1): p. 39-59.

123.   Xiao, S., J. McLean, and J. Robertson, *Neuronal intermediate filaments and ALS: a new look at an old question.* Biochim Biophys Acta, 2006. **1762**(11-12): p. 1001-12.

124.   Haidet-Phillips, A.M., et al., *Astrocytes from familial and sporadic ALS patients are toxic to motor neurons.* Nat Biotechnol, 2011. **29**(9): p. 824-8.

125.   Clement, A.M., et al., *Wild-type nonneuronal cells extend survival of SOD1 mutant motor neurons in ALS mice.* Science, 2003. **302**(5642): p. 113-7.

126. Lacomblez, L., et al., *A confirmatory dose-ranging study of riluzole in ALS. ALS/Riluzole Study Group-II.* Neurology, 1996. **47**(6 Suppl 4): p. S242-50.

127. Wang, S.J., K.Y. Wang, and W.C. Wang, *Mechanisms underlying the riluzole inhibition of glutamate release from rat cerebral cortex nerve terminals (synaptosomes).* Neuroscience, 2004. **125**(1): p. 191-201.

128. Andrews, J.A., et al., *Real-world evidence of riluzole effectiveness in treating amyotrophic lateral sclerosis.* Amyotroph Lateral Scler Frontotemporal Degener, 2020. **21**(7-8): p. 509-518.

129. Ito, H., et al., *Treatment with edaravone, initiated at symptom onset, slows motor decline and decreases SOD1 deposition in ALS mice.* Exp Neurol, 2008. **213**(2): p. 448-55.

130. *Safety and efficacy of edaravone in well defined patients with amyotrophic lateral sclerosis: a randomised, double-blind, placebo-controlled trial.* Lancet Neurol, 2017. **16**(7): p. 505-512.

131. Paganoni, S., et al., *Trial of Sodium Phenylbutyrate-Taurursodiol for Amyotrophic Lateral Sclerosis.* N Engl J Med, 2020. **383**(10): p. 919-930.

132. Blair, H.A., *Tofersen: First Approval.* Drugs, 2023.

133. Hipp, J. and A. Atala, *Sources of stem cells for regenerative medicine.* Stem Cell Rev, 2008. **4**(1): p. 3-11.

134. Wobus, A.M., *Potential of embryonic stem cells.* Mol Aspects Med, 2001. **22**(3): p. 149-64.

135. Li, M., et al., *Generation of purified neural precursors from embryonic stem cells by lineage selection.* Curr Biol, 1998. **8**(17): p. 971-4.

136. Benninger, F., et al., *Functional integration of embryonic stem cell-derived neurons in hippocampal slice cultures.* J Neurosci, 2003. **23**(18): p. 7075-83.

137. Bjorklund, L.M., et al., *Embryonic stem cells develop into functional dopaminergic neurons after transplantation in a Parkinson rat model.* Proc Natl Acad Sci U S A, 2002. **99**(4): p. 2344-9.

138. Carson, C.T., S. Aigner, and F.H. Gage, *Stem cells: the good, bad and barely in control.* Nat Med, 2006. **12**(11): p. 1237-8.

139. Li, J.Y., et al., *Critical issues of clinical human embryonic stem cell therapy for brain repair.* Trends Neurosci, 2008. **31**(3): p. 146-53.

140. Hsu, Y.C., D.C. Lee, and I.M. Chiu, *Neural stem cells, neural progenitors, and neurotrophic factors.* Cell Transplant, 2007. **16**(2): p. 133-50.

141. Takahashi, K. and S. Yamanaka, *Induction of pluripotent stem cells from mouse embryonic and adult fibroblast cultures by defined factors.* Cell, 2006. **126**(4): p. 663-76.

142. Baglio, S.R., D.M. Pegtel, and N. Baldini, *Mesenchymal stem cell secreted vesicles provide novel opportunities in (stem) cell-free therapy.* Front Physiol, 2012. **3**: p. 359.

143. Gugliandolo, A., P. Bramanti, and E. Mazzon, *Mesenchymal Stem Cells: A Potential Therapeutic Approach for Amyotrophic Lateral Sclerosis?* Stem Cells Int, 2019. **2019**: p. 3675627.

144. Bajek, A., et al., *Adipose-Derived Stem Cells as a Tool in Cell-Based Therapies.* Arch Immunol Ther Exp (Warsz), 2016. **64**(6): p. 443-454.

145. Gir, P., et al., *Human adipose stem cells: current clinical applications.* Plast Reconstr Surg, 2012. **129**(6): p. 1277-1290.

146. Dominici, M., et al., *Minimal criteria for defining multipotent mesenchymal stromal cells. The International Society for Cellular Therapy position statement.* Cytotherapy, 2006. **8**(4): p. 315-7.

147. Joyce, N., et al., *Mesenchymal stem cells for the treatment of neurodegenerative disease.* Regen Med, 2010. **5**(6): p. 933-46.

148. Garbossa, D., et al., *Recent therapeutic strategies for spinal cord injury treatment: possible role of stem cells.* Neurosurg Rev, 2012. **35**(3): p. 293-311; discussion 311.

149. Mazzini, L., et al., *Stem cells in amyotrophic lateral sclerosis: state of the art.* Expert Opin Biol Ther, 2009. **9**(10): p. 1245-58.

150. Wyatt, T.J. and H.S. Keirstead, *Stem cell-derived neurotrophic support for the neuromuscular junction in spinal muscular atrophy.* Expert Opin Biol Ther, 2010. **10**(11): p. 1587-94.

151. Giunti, D., et al., *Mesenchymal stem cells shape microglia effector functions through the release of CX3CL1.* Stem Cells, 2012. **30**(9): p. 2044-53.

152. Devine, S.M., et al., *Mesenchymal stem cells distribute to a wide range of tissues following systemic infusion into nonhuman primates.* Blood, 2003. **101**(8): p. 2999-3001.

153. Marconi, S., et al., *Systemic treatment with adipose-derived mesenchymal stem cells ameliorates clinical and pathological features in the amyotrophic lateral sclerosis murine model.* Neuroscience, 2013. **248**: p. 333-43.

154. Lai, R.C., R.W. Yeo, and S.K. Lim, *Mesenchymal stem cell exosomes.* Semin Cell Dev Biol, 2015. **40**: p. 82-8.

155. Phinney, D.G. and D.J. Prockop, *Concise review: mesenchymal stem/multipotent stromal cells: the state of transdifferentiation and modes of tissue repair--current views.* Stem Cells, 2007. **25**(11): p. 2896-902.

156. Maacha, S., et al., *Paracrine Mechanisms of Mesenchymal Stromal Cells in Angiogenesis.* Stem Cells Int, 2020. **2020**: p. 4356359.

157. Teixeira, F.G., et al., *Mesenchymal stem cells secretome: a new paradigm for central nervous system regeneration?* Cell Mol Life Sci, 2013. **70**(20): p. 3871-82.

158. Kourembanas, S., *Exosomes: vehicles of intercellular signaling, biomarkers, and vectors of cell therapy.* Annu Rev Physiol, 2015. **77**: p. 13-27.

159. Colombo, M., G. Raposo, and C. Théry, *Biogenesis, secretion, and intercellular interactions of exosomes and other extracellular vesicles.* Annu Rev Cell Dev Biol, 2014. **30**: p. 255-89.

160. Doyle, L.M. and M.Z. Wang, *Overview of Extracellular Vesicles, Their Origin, Composition, Purpose, and Methods for Exosome Isolation and Analysis.* Cells, 2019. **8**(7).

161. Zhang, X., et al., *The Biology and Function of Extracellular Vesicles in Cancer Development.* Front Cell Dev Biol, 2021. **9**: p. 777441.

162. Raposo, G. and W. Stoorvogel, *Extracellular vesicles: exosomes, microvesicles, and friends.* J Cell Biol, 2013. **200**(4): p. 373-83.

163. Deatherage, B.L. and B.T. Cookson, *Membrane vesicle release in bacteria, eukaryotes, and archaea: a conserved yet underappreciated aspect of microbial life.* Infect Immun, 2012. **80**(6): p. 1948-57.

164. Gho, Y.S. and C. Lee, *Emergent properties of extracellular vesicles: a holistic approach to decode the complexity of intercellular communication networks.* Mol Biosyst, 2017. **13**(7): p. 1291-1296.

165. Valadi, H., et al., *Exosome-mediated transfer of mRNAs and microRNAs is a novel mechanism of genetic exchange between cells.* Nat Cell Biol, 2007. **9**(6): p. 654-9.

166. van Niel, G., G. D'Angelo, and G. Raposo, *Shedding light on the cell biology of extracellular vesicles.* Nat Rev Mol Cell Biol, 2018. **19**(4): p. 213-228.

167. Théry, C., et al., *Minimal information for studies of extracellular vesicles 2018 (MISEV2018): a position statement of the International Society for Extracellular Vesicles and update of the MISEV2014 guidelines.* J Extracell Vesicles, 2018. **7**(1): p. 1535750.

168. Witwer, K.W. and C. Théry, *Extracellular vesicles or exosomes? On primacy, precision, and popularity influencing a choice of nomenclature.* J Extracell Vesicles, 2019. **8**(1): p. 1648167.

169. Yáñez-Mó, M., et al., *Biological properties of extracellular vesicles and their physiological functions.* J Extracell Vesicles, 2015. **4**: p. 27066.

170. Bruno, S., et al., *The Role of Extracellular Vesicles as Paracrine Effectors in Stem Cell-Based Therapies.* Adv Exp Med Biol, 2019. **1201**: p. 175-193.

171. Kalani, A., A. Tyagi, and N. Tyagi, *Exosomes: mediators of neurodegeneration, neuroprotection and therapeutics.* Mol Neurobiol, 2014. **49**(1): p. 590-600.

172. Shao, L., et al., *MiRNA-Sequence Indicates That Mesenchymal Stem Cells and Exosomes Have Similar Mechanism to Enhance Cardiac Repair.* Biomed Res Int, 2017. **2017**: p. 4150705.

173. Bagno, L., et al., *Mesenchymal Stem Cell-Based Therapy for Cardiovascular Disease: Progress and Challenges.* Mol Ther, 2018. **26**(7): p. 1610-1623.

174. Ahn, S.Y., et al., *Brain-derived neurotropic factor mediates neuroprotection of mesenchymal stem cell-derived extracellular vesicles against severe intraventricular hemorrhage in newborn rats.* Stem Cells Transl Med, 2021. **10**(3): p. 374-384.

175. Harrell, C.R., et al., *Molecular Mechanisms Responsible for Therapeutic Potential of Mesenchymal Stem Cell-Derived Secretome.* Cells, 2019. **8**(5).

176. Yari, H., et al., *Emerging role of mesenchymal stromal cells (MSCs)-derived exosome in neurodegeneration-associated conditions: a groundbreaking cell-free approach.* Stem Cell Res Ther, 2022. **13**(1): p. 423.

177. Chopp, M. and Y. Li, *Treatment of neural injury with marrow stromal cells.* Lancet Neurol, 2002. **1**(2): p. 92-100.

178. Vilaca-Faria, H., A.J. Salgado, and F.G. Teixeira, *Mesenchymal Stem Cells-derived Exosomes: A New Possible Therapeutic Strategy for Parkinson's Disease?* Cells, 2019. **8**(2).

179. Pathan, M., et al., *Vesiclepedia 2019: a compendium of RNA, proteins, lipids and metabolites in extracellular vesicles.* Nucleic Acids Res, 2019. **47**(D1): p. D516-d519.

180. Baglio, S.R., et al., *Human bone marrow- and adipose-mesenchymal stem cells secrete exosomes enriched in distinctive miRNA and tRNA species.* Stem Cell Res Ther, 2015. **6**: p. 127.

181. Lee, R.H., et al., *Intravenous hMSCs improve myocardial infarction in mice because cells embolized in lung are activated to secrete the anti-inflammatory protein TSG-6.* Cell Stem Cell, 2009. **5**(1): p. 54-63.

182. Turano, E., et al., *Extracellular Vesicles from Mesenchymal Stem Cells: Towards Novel Therapeutic Strategies for Neurodegenerative Diseases.* Int J Mol Sci, 2023. **24**(3).

183. Fischer, U.M., et al., *Pulmonary passage is a major obstacle for intravenous stem cell delivery: the pulmonary first-pass effect.* Stem Cells Dev, 2009. **18**(5): p. 683-92.

184. Katsuda, T., et al., *Human adipose tissue-derived mesenchymal stem cells secrete functional neprilysin-bound exosomes.* Sci Rep, 2013. **3**: p. 1197.

185. Ding, M., et al., *Exosomes Isolated From Human Umbilical Cord Mesenchymal Stem Cells Alleviate Neuroinflammation and Reduce Amyloid-Beta Deposition by Modulating Microglial Activation in Alzheimer's Disease.* Neurochem Res, 2018. **43**(11): p. 2165-2177.

186. de Godoy, M.A., et al., *Mesenchymal stem cells and cell-derived extracellular vesicles protect hippocampal neurons from oxidative stress and synapse damage induced by amyloid-β oligomers.* J Biol Chem, 2018. **293**(6): p. 1957-1975.

187. Cui, G.H., et al., *Exosomes derived from hypoxia-preconditioned mesenchymal stromal cells ameliorate cognitive decline by rescuing synaptic dysfunction and regulating inflammatory responses in APP/PS1 mice.* Faseb j, 2018. **32**(2): p. 654-668.

188. Bodart-Santos, V., et al., *Extracellular vesicles derived from human Wharton's jelly mesenchymal stem cells protect hippocampal neurons from oxidative stress and synapse damage induced by amyloid-β oligomers.* Stem Cell Res Ther, 2019. **10**(1): p. 332.

189. Reza-Zaldivar, E.E., et al., *Mesenchymal stem cell-derived exosomes promote neurogenesis and cognitive function recovery in a mouse model of Alzheimer's disease.* Neural Regen Res, 2019. **14**(9): p. 1626-1634.

190. Pringsheim, T., et al., *The prevalence of Parkinson's disease: a systematic review and meta-analysis.* Mov Disord, 2014. **29**(13): p. 1583-90.

191. Gómez-Benito, M., et al., *Modeling Parkinson's Disease With the Alpha-Synuclein Protein.* Front Pharmacol, 2020. **11**: p. 356.

192. Mendes-Pinheiro, B., et al., *Bone Marrow Mesenchymal Stem Cells' Secretome Exerts Neuroprotective Effects in a Parkinson's Disease Rat Model.* Front Bioeng Biotechnol, 2019. **7**: p. 294.

193. Teixeira, F.G., et al., *Impact of the Secretome of Human Mesenchymal Stem Cells on Brain Structure and Animal Behavior in a Rat Model of Parkinson's Disease.* Stem Cells Transl Med, 2017. **6**(2): p. 634-646.

194. Jarmalavičiūtė, A., et al., *Exosomes from dental pulp stem cells rescue human dopaminergic neurons from 6-hydroxy-dopamine-induced apoptosis.* Cytotherapy, 2015. **17**(7): p. 932-9.

195. Chen, H.X., et al., *Exosomes derived from mesenchymal stem cells repair a Parkinson's disease model by inducing autophagy.* Cell Death Dis, 2020. **11**(4): p. 288.

196. Bonafede, R., et al., *Exosome derived from murine adipose-derived stromal cells: Neuroprotective effect on in vitro model of amyotrophic lateral sclerosis.* Exp Cell Res, 2016. **340**(1): p. 150-8.

197.	Farinazzo, A., et al., *Murine adipose-derived mesenchymal stromal cell vesicles: in vitro clues for neuroprotective and neuroregenerative approaches.* Cytotherapy, 2015. **17**(5): p. 571-8.

198.	Lee, M., et al., *Adipose-derived stem cell exosomes alleviate pathology of amyotrophic lateral sclerosis in vitro.* Biochem Biophys Res Commun, 2016. **479**(3): p. 434-439.

199.	Calabria, E., et al., *ASCs-Exosomes Recover Coupling Efficiency and Mitochondrial Membrane Potential in an in vitro Model of ALS.* Front Neurosci, 2019. **13**: p. 1070.

200.	Kojima, R., et al., *Designer exosomes produced by implanted cells intracerebrally deliver therapeutic cargo for Parkinson's disease treatment.* Nat Commun, 2018. **9**(1): p. 1305.

201.	Pan, Q., et al., *miR-132-3p priming enhances the effects of mesenchymal stromal cell-derived exosomes on ameliorating brain ischemic injury.* Stem Cell Res Ther, 2020. **11**(1): p. 260.

202.	Zhang, Z., et al., *Mesenchymal Stem Cell-Conditioned Medium Improves Mitochondrial Dysfunction and Suppresses Apoptosis in Okadaic Acid-Treated SH-SY5Y Cells by Extracellular Vesicle Mitochondrial Transfer.* J Alzheimers Dis, 2020. **78**(3): p. 1161-1176.

203.	Chen, W.W., X. Zhang, and W.J. Huang, *Role of neuroinflammation in neurodegenerative diseases (Review).* Mol Med Rep, 2016. **13**(4): p. 3391-6.

204.	Losurdo, M., et al., *Intranasal delivery of mesenchymal stem cell-derived extracellular vesicles exerts immunomodulatory and neuroprotective effects in a 3xTg model of Alzheimer's disease.* Stem Cells Transl Med, 2020. **9**(9): p. 1068-1084.

205.	Elia, C.A., et al., *Intracerebral Injection of Extracellular Vesicles from Mesenchymal Stem Cells Exerts Reduced Abeta Plaque Burden in Early Stages of a Preclinical Model of Alzheimer's Disease.* Cells, 2019. **8**(9).

206.	Narbute, K., et al., *Intranasal Administration of Extracellular Vesicles Derived from Human Teeth Stem Cells Improves Motor Symptoms and Normalizes Tyrosine Hydroxylase Expression in the Substantia Nigra and Striatum of the 6-Hydroxydopamine-Treated Rats.* Stem Cells Transl Med, 2019. **8**(5): p. 490-499.

207.	Peng, H., et al., *Intranasal Administration of Self-Oriented Nanocarriers Based on Therapeutic Exosomes for Synergistic Treatment of Parkinson's Disease.* ACS Nano, 2022.

208.	Bonafede, R., et al., *ASC-Exosomes Ameliorate the Disease Progression in SOD1(G93A) Murine Model Underlining Their Potential Therapeutic Use in Human ALS.* Int J Mol Sci, 2020. **21**(10).

209.	Giampa, C., et al., *Conditioned medium from amniotic cells protects striatal degeneration and ameliorates motor deficits in the R6/2 mouse model of Huntington's disease.* J Cell Mol Med, 2019. **23**(2): p. 1581-1592.

210.	Fathollahi, A., et al., *Intranasal administration of small extracellular vesicles derived from mesenchymal stem cells ameliorated the experimental autoimmune encephalomyelitis.* Int Immunopharmacol, 2021. **90**: p. 107207.

211.	Clark, K., et al., *Placental Mesenchymal Stem Cell-Derived Extracellular Vesicles Promote Myelin Regeneration in an Animal Model of Multiple Sclerosis.* Cells, 2019. **8**(12).

212.	Farinazzo, A., et al., *Nanovesicles from adipose-derived mesenchymal stem cells inhibit T lymphocyte trafficking and ameliorate chronic experimental autoimmune encephalomyelitis.* Sci Rep, 2018. **8**(1): p. 7473.

213.	Gimona, M., et al., *Manufacturing of Human Extracellular Vesicle-Based Therapeutics for Clinical Use.* Int J Mol Sci, 2017. **18**(6).

214.	Mendt, M., K. Rezvani, and E. Shpall, *Mesenchymal stem cell-derived exosomes for clinical use.* Bone Marrow Transplant, 2019. **54**(Suppl 2): p. 789-792.

215.	Massa, M., et al., *Clinical Applications of Mesenchymal Stem/Stromal Cell Derived Extracellular Vesicles: Therapeutic Potential of an Acellular Product.* Diagnostics (Basel), 2020. **10**(12).

216.	Hamilton, G. and T.H. Gillingwater, *Spinal muscular atrophy: going beyond the motor neuron.* Trends Mol Med, 2013. **19**(1): p. 40-50.

217.	Park, G.H., et al., *Reduced survival of motor neuron (SMN) protein in motor neuronal progenitors functions cell autonomously to cause spinal muscular atrophy in model mice expressing the human centromeric (SMN2) gene.* J Neurosci, 2010. **30**(36): p. 12005-19.

218. Abati, E., et al., *Glial cells involvement in spinal muscular atrophy: Could SMA be a neuroinflammatory disease?* Neurobiol Dis, 2020. **140**: p. 104870.

219. Uccelli, A., L. Moretta, and V. Pistoia, *Mesenchymal stem cells in health and disease.* Nat Rev Immunol, 2008. **8**(9): p. 726-36.

220. Filippi, M., et al., *Successful in vivo MRI tracking of MSCs labeled with Gadoteridol in a Spinal Cord Injury experimental model.* Exp Neurol, 2016. **282**: p. 66-77.

221. Boido, M., et al., *Mesenchymal stem cell transplantation reduces glial cyst and improves functional outcome after spinal cord compression.* World Neurosurg, 2014. **81**(1): p. 183-90.

222. Constantin, G., et al., *Adipose-derived mesenchymal stem cells ameliorate chronic experimental autoimmune encephalomyelitis.* Stem Cells, 2009. **27**(10): p. 2624-35.

223. Uccelli, A., et al., *Intravenous mesenchymal stem cells improve survival and motor function in experimental amyotrophic lateral sclerosis.* Mol Med, 2012. **18**: p. 794-804.

224. Vercelli, A., et al., *Human mesenchymal stem cell transplantation extends survival, improves motor performance and decreases neuroinflammation in mouse model of amyotrophic lateral sclerosis.* Neurobiol Dis, 2008. **31**(3): p. 395-405.

225. Abbasi-Malati, Z., et al., *Mesenchymal Stem Cells on Horizon: A New Arsenal of Therapeutic Agents.* Stem Cell Rev Rep, 2018. **14**(4): p. 484-499.

226. Wang, H., et al., *Tail-vein injection of MSC-derived small extracellular vesicles facilitates the restoration of hippocampal neuronal morphology and function in APP / PS1 mice.* Cell Death Discov, 2021. **7**(1): p. 230.

227. Laso-Garcia, F., et al., *Therapeutic potential of extracellular vesicles derived from human mesenchymal stem cells in a model of progressive multiple sclerosis.* PLoS One, 2018. **13**(9): p. e0202590.

228. Peroni, D., et al., *Stem molecular signature of adipose-derived stromal cells.* Exp Cell Res, 2008. **314**(3): p. 603-15.

229. Piras, A., et al., *Inhibition of autophagy delays motoneuron degeneration and extends lifespan in a mouse model of spinal muscular atrophy.* Cell Death Dis, 2017. **8**(12): p. 3223.

230. El-Khodor, B.F., et al., *Identification of a battery of tests for drug candidate evaluation in the SMNDelta7 neonate model of spinal muscular atrophy.* Exp Neurol, 2008. **212**(1): p. 29-43.

231. Kowal, J., et al., *Proteomic comparison defines novel markers to characterize heterogeneous populations of extracellular vesicle subtypes.* Proc Natl Acad Sci U S A, 2016. **113**(8): p. E968-77.

232. Bonafede, R., et al., *The Anti-Apoptotic Effect of ASC-Exosomes in an In Vitro ALS Model and Their Proteomic Analysis.* Cells, 2019. **8**(9).

233. Qiu, J., et al., *History of development of the life-saving drug "Nusinersen" in spinal muscular atrophy.* Front Cell Neurosci, 2022. **16**: p. 942976.

234. Ratni, H., et al., *Discovery of Risdiplam, a Selective Survival of Motor Neuron-2 (SMN2) Gene Splicing Modifier for the Treatment of Spinal Muscular Atrophy (SMA).* J Med Chem, 2018. **61**(15): p. 6501-6517.

235. Blair, H.A., *Onasemnogene Abeparvovec: A Review in Spinal Muscular Atrophy.* CNS Drugs, 2022. **36**(9): p. 995-1005.

236. Menduti, G., et al., *Drug Screening and Drug Repositioning as Promising Therapeutic Approaches for Spinal Muscular Atrophy Treatment.* Front Pharmacol, 2020. **11**: p. 592234.

237. Phinney, D.G. and M.F. Pittenger, *Concise Review: MSC-Derived Exosomes for Cell-Free Therapy.* Stem Cells, 2017. **35**(4): p. 851-858.

238. Zhang, L., L. Mao, and H. Wang, *The Neuroprotection Effects of Exosome in Central Nervous System Injuries: a New Target for Therapeutic Intervention.* Mol Neurobiol, 2022.

239. Vincent, A.M. and E.L. Feldman, *Control of cell survival by IGF signaling pathways.* Growth Horm IGF Res, 2002. **12**(4): p. 193-7.

240. Biondi, O., et al., *IGF-1R Reduction Triggers Neuroprotective Signaling Pathways in Spinal Muscular Atrophy Mice.* J Neurosci, 2015. **35**(34): p. 12063-79.

241. Sansa, A., et al., *Intracellular pathways involved in cell survival are deregulated in mouse and human spinal muscular atrophy motoneurons.* Neurobiol Dis, 2021. **155**: p. 105366.

242. Ullah, F., et al., *The Effects of Modified Curcumin Preparations on Glial Morphology in Aging and Neuroinflammation.* Neurochem Res, 2022. **47**(4): p. 813-824.

243. Ziebell, J.M., P.D. Adelson, and J. Lifshitz, *Microglia: dismantling and rebuilding circuits after acute neurological injury.* Metab Brain Dis, 2015. **30**(2): p. 393-400.

244. Schmidt, R. and T. Voit, *Ultrasound measurement of quadriceps muscle in the first year of life. Normal values and application to spinal muscular atrophy.* Neuropediatrics, 1993. **24**(1): p. 36-42.

245. d'Errico, P., et al., *Selective vulnerability of spinal and cortical motor neuron subpopulations in delta7 SMA mice.* PLoS One, 2013. **8**(12): p. e82654.

246. Perets, N., et al., *Golden Exosomes Selectively Target Brain Pathologies in Neurodegenerative and Neurodevelopmental Disorders.* Nano Lett, 2019. **19**(6): p. 3422-3431.

247. Perets, N., et al., *Intranasal administration of exosomes derived from mesenchymal stem cells ameliorates autistic-like behaviors of BTBR mice.* Mol Autism, 2018. **9**: p. 57.

248. Shimaoka, M., et al., *Connexins and Integrins in Exosomes.* Cancers (Basel), 2019. **11**(1).

249. Herman, S., I. Fishel, and D. Offen, *Intranasal delivery of mesenchymal stem cells-derived extracellular vesicles for the treatment of neurological diseases.* Stem Cells, 2021. **39**(12): p. 1589-1600.

250. Keller, L.A., O. Merkel, and A. Popp, *Intranasal drug delivery: opportunities and toxicologic challenges during drug development.* Drug Deliv Transl Res, 2022. **12**(4): p. 735-757.

251. Zhuang, X., et al., *Treatment of brain inflammatory diseases by delivering exosome encapsulated anti-inflammatory drugs from the nasal region to the brain.* Mol Ther, 2011. **19**(10): p. 1769-79.

252. Brown, R.H. and A. Al-Chalabi, *Amyotrophic Lateral Sclerosis.* N Engl J Med, 2017. **377**(2): p. 162-172.

253. Costa, J. and M. de Carvalho, *Emerging molecular biomarker targets for amyotrophic lateral sclerosis.* Clin Chim Acta, 2016. **455**: p. 7-14.

254. Vinsant, S., et al., *Characterization of early pathogenesis in the SOD1(G93A) mouse model of ALS: part I, background and methods.* Brain Behav, 2013. **3**(4): p. 335-50.

255. Benatar, M., *Lost in translation: treatment trials in the SOD1 mouse and in human ALS.* Neurobiol Dis, 2007. **26**(1): p. 1-13.

256. Meamar, R., et al., *Stem cell therapy in amyotrophic lateral sclerosis.* J Clin Neurosci, 2013. **20**(12): p. 1659-63.

257. Boucherie, C., et al., *Chimerization of astroglial population in the lumbar spinal cord after mesenchymal stem cell transplantation prolongs survival in a rat model of amyotrophic lateral sclerosis.* J Neurosci Res, 2009. **87**(9): p. 2034-46.

258. de Munter, J., et al., *Neuro-Cells therapy improves motor outcomes and suppresses inflammation during experimental syndrome of amyotrophic lateral sclerosis in mice.* CNS Neurosci Ther, 2019.

259. Martinez-Muriana, A., et al., *Combined intramuscular and intraspinal transplant of bone marrow cells improves neuromuscular function in the SOD1(G93A) mice.* Stem Cell Res Ther, 2020. **11**(1): p. 53.

260. Zhang, Y., M. Yu, and W. Tian, *Physiological and pathological impact of exosomes of adipose tissue.* Cell Prolif, 2016. **49**(1): p. 3-13.

261. Kalani, A. and N. Tyagi, *Exosomes in neurological disease, neuroprotection, repair and therapeutics: problems and perspectives.* Neural Regen Res, 2015. **10**(10): p. 1565-7.

262. Abati, E., et al., *Advances, Challenges, and Perspectives in Translational Stem Cell Therapy for Amyotrophic Lateral Sclerosis.* Mol Neurobiol, 2019. **56**(10): p. 6703-6715.

263. Cappella, M., et al., *Gene Therapy for ALS-A Perspective.* Int J Mol Sci, 2019. **20**(18).

264. Jaiswal, M.K., *Riluzole and edaravone: A tale of two amyotrophic lateral sclerosis drugs.* Med Res Rev, 2019. **39**(2): p. 733-748.

265. Gorabi, A.M., et al., *The Therapeutic Potential of Mesenchymal Stem Cell-Derived Exosomes in Treatment of Neurodegenerative Diseases.* Mol Neurobiol, 2019. **56**(12): p. 8157-8167.

117

266.   Xin, H., et al., *Systemic administration of exosomes released from mesenchymal stromal cells promote functional recovery and neurovascular plasticity after stroke in rats.* J Cereb Blood Flow Metab, 2013. **33**(11): p. 1711-5.

267.   Zhang, Y., et al., *Effect of exosomes derived from multipluripotent mesenchymal stromal cells on functional recovery and neurovascular plasticity in rats after traumatic brain injury.* J Neurosurg, 2015. **122**(4): p. 856-67.

268.   Long, Q., et al., *Intranasal MSC-derived A1-exosomes ease inflammation, and prevent abnormal neurogenesis and memory dysfunction after status epilepticus.* Proc Natl Acad Sci U S A, 2017. **114**(17): p. E3536-E3545.

269.   Sun, X., et al., *Stem Cell-Derived Exosomes Protect Astrocyte Cultures From in vitro Ischemia and Decrease Injury as Post-stroke Intravenous Therapy.* Front Cell Neurosci, 2019. **13**: p. 394.

270.   Clark, J.A., et al., *Axonal degeneration, distal collateral branching and neuromuscular junction architecture alterations occur prior to symptom onset in the SOD1(G93A) mouse model of amyotrophic lateral sclerosis.* J Chem Neuroanat, 2016. **76**(Pt A): p. 35-47.

271.   Bian, S., et al., *Extracellular vesicles derived from human bone marrow mesenchymal stem cells promote angiogenesis in a rat myocardial infarction model.* J Mol Med (Berl), 2014. **92**(4): p. 387-97.

272.   Nojima, H., et al., *Hepatocyte exosomes mediate liver repair and regeneration via sphingosine-1-phosphate.* J Hepatol, 2016. **64**(1): p. 60-8.

273.   Xiong, Z.H., et al., *Protective effect of human umbilical cord mesenchymal stem cell exosomes on preserving the morphology and angiogenesis of placenta in rats with preeclampsia.* Biomed Pharmacother, 2018. **105**: p. 1240-1247.

274.   Dai, J., et al., *Alterations in AQP4 expression and polarization in the course of motor neuron degeneration in SOD1G93A mice.* Mol Med Rep, 2017. **16**(2): p. 1739-1746.

275.   Nagai, M., et al., *Astrocytes expressing ALS-linked mutated SOD1 release factors selectively toxic to motor neurons.* Nat Neurosci, 2007. **10**(5): p. 615-22.

276.   Yamanaka, K. and O. Komine, *The multi-dimensional roles of astrocytes in ALS.* Neurosci Res, 2018. **126**: p. 31-38.

277.   Wang, L., et al., *Mesenchymal Stem Cell-Derived Exosomes Reduce A1 Astrocytes via Downregulation of Phosphorylated NFkappaB P65 Subunit in Spinal Cord Injury.* Cell Physiol Biochem, 2018. **50**(4): p. 1535-1559.

278.   Xian, P., et al., *Mesenchymal stem cell-derived exosomes as a nanotherapeutic agent for amelioration of inflammation-induced astrocyte alterations in mice.* Theranostics, 2019. **9**(20): p. 5956-5975.

279.   Mendt, M., et al., *Generation and testing of clinical-grade exosomes for pancreatic cancer.* JCI Insight, 2018. **3**(8).

280.   Wiklander, O.P., et al., *Extracellular vesicle in vivo biodistribution is determined by cell source, route of administration and targeting.* J Extracell Vesicles, 2015. **4**: p. 26316.

281.   Ozturk, S., et al., *Therapeutic Applications of Stem Cells and Extracellular Vesicles in Emergency Care: Futuristic Perspectives.* Stem Cell Rev Rep, 2021. **17**(2): p. 390-410.

282.   Zhang, Y., et al., *Mesenchymal Stem Cell-Derived Exosomes Improve Functional Recovery in Rats After Traumatic Brain Injury: A Dose-Response and Therapeutic Window Study.* Neurorehabil Neural Repair, 2020. **34**(7): p. 616-626.

283.   Erdő, F., et al., *Evaluation of intranasal delivery route of drug administration for brain targeting.* Brain Res Bull, 2018. **143**: p. 155-170.

284.   Hanson, L.R. and W.H. Frey, 2nd, *Intranasal delivery bypasses the blood-brain barrier to target therapeutic agents to the central nervous system and treat neurodegenerative disease.* BMC Neurosci, 2008. **9 Suppl 3**(Suppl 3): p. S5.

285.   Bagheri-Mohammadi, S., et al., *Intranasal administration of endometrial mesenchymal stem cells as a suitable approach for Parkinson's disease therapy.* Mol Biol Rep, 2019. **46**(4): p. 4293-4302.

286.   Yu-Taeger, L., et al., *Intranasal Administration of Mesenchymal Stem Cells Ameliorates the Abnormal Dopamine Transmission System and Inflammatory Reaction in the R6/2 Mouse Model of Huntington Disease.* Cells, 2019. **8**(6).

287.   Gonçalves, V.S.S., et al., *Application of RPMI 2650 as a cell model to evaluate solid formulations for intranasal delivery of drugs.* Int J Pharm, 2016. **515**(1-2): p. 1-10.

288. Williams, C., et al., *Assessing the role of surface glycans of extracellular vesicles on cellular uptake.* Sci Rep, 2019. **9**(1): p. 11920.

289. Li, C., et al., *Overcoming the blood-brain barrier: Exosomes as theranostic nanocarriers for precision neuroimaging.* J Control Release, 2022. **349**: p. 902-916.

290. Crowe, T.P., et al., *Mechanism of intranasal drug delivery directly to the brain.* Life Sci, 2018. **195**: p. 44-52.

291. Brightman, M.W. and R.D. Broadwell, *The morphological approach to the study of normal and abnormal brain permeability.* Adv Exp Med Biol, 1976. **69**: p. 41-54.

292. Mercier, C., N. Perek, and X. Delavenne, *Is RPMI 2650 a Suitable In Vitro Nasal Model for Drug Transport Studies?* Eur J Drug Metab Pharmacokinet, 2018. **43**(1): p. 13-24.